CRYOPRESERVATION EFFECTS ON THE *IN VITRO* AND *IN VIVO* FUNCTION OF A MODEL PANCREATIC SUBSTITUTE

A Dissertation
Presented to
The Academic Faculty

by

Alison Noelle Lawson

In Partial Fulfillment
of the Requirements for the Degree
Doctor of Philosophy in the
School of Chemical & Biomolecular Engineering

Georgia Institute of Technology
May 2011

CRYOPRESERVATION EFFECTS ON THE *IN VITRO* AND *IN VIVO* FUNCTION OF A MODEL PANCREATIC SUBSTITUTE

Approved by:

Dr. Athanassios Sambanis, Advisor
School of Chemical & Biomolecular Engineering
Georgia Institute of Technology

Dr. Hang Lu
School of Chemical & Biomolecular Engineering
Georgia Institute of Technology

Dr. Susan Safley
School of Medicine
Emory University

Dr. Ying Song
Chief Scientific Officer
Beike Biotechnology, Co., Ltd., China

Dr. Lakeshia Taite
School of Chemical & Biomolecular Engineering
Georgia Institute of Technology

Date Approved: March 18, 2011

For in this hope we were saved. But hope that is seen is no hope at all. Who hopes for what they already have? But if we hope for what we do not yet have, we wait for it patiently. In the same way, the Spirit helps us in our weakness. We do not know what we ought to pray for, but the Spirit himself intercedes for us through wordless groans. And he who searches our hearts knows the mind of the Spirit, because the Spirit intercedes for God's people in accordance with the will of God. And we know that in all things God works for the good of those who love him, who have been called according to his purpose. For those God foreknew he also predestined to be conformed to the image of his Son, that he might be the firstborn among many brothers and sisters. And those he predestined, he also called; those he called, he also justified; those he justified, he also glorified.

Romans 8:24-30, NIV

ACKNOWLEDGEMENTS

First and foremost, I would like to thank Dr. Athanassios Sambanis who has been an incredible mentor over the last five years. Under his tutelage, I have both become a better chemical engineer and started the transition to biologist. He has displayed tremendous patience with me and has allowed me to make and learn from my own, frequent mistakes. I would also like to take this opportunity to thank my committee members for their feedback and guidance during this process. They have always given me a new perspective on my research and its broad applicability. I have also had the opportunity to use many of the core facilities at IBB and am indebted to Steve Woodard, Dr. Laura O'Farrell and Kim Benjamin for their technical assistance with microscopes and mice.

During my time here at Georgia Tech, I've had the privilege of working with some delightful people in the Sambanis Lab. At the beginning of my time here, I had the opportunity to learn lab and tissue culture techniques from Jeff Gross, Neil Mukherjee and Angie Gulino. I was able to continue working with and learning from Heather Bara through numerous hours of *in vivo* work in the Physiological Research Laboratory. Over the years I have had the privilege to work with Hajira Ahmad, Saif Al-Mamari, Candice Castellino, Stephanie Duncanson, Kiranmai Durvasula, Fernie Goh, Priya Jayachandran, Sudhaker Muthyala and Aubrey Tiernan. Their support, helpful discussions and presence in the lab has had a significant impact on my work and has made my time here much more memorable. I would especially like to thank Hajira who has spent countless hours vitrifying and troubleshooting the vitrification process with me. None of my *in vivo*

studies would have been possible without the help of Fernie and Kiranmai. Last, but not least, I would like to thank my undergraduate student, Chun Yong, who provided superb mechanical testing as well as comic relief for the lab. It has been a privilege to serve as his mentor.

Finally, I would like to thank all the folks who have provided immeasurable support outside of the laboratory. My parents, Mark and Donna Stucky, always told me to shoot for the stars but were never disappointed if my best efforts fell short. They were my stalwart supporters and never missed an opportunity to love me from afar or convince me that I would succeed. I would also like to thank my brother, Alex. We are not much for emotional words, but he has, on occasion, admitted that he is proud of me and that has made quite a difference. He and his wife, Marie, have blessed me with a delightful niece who has given me much more perspective and many hugs. Almost two years ago, I had the honor of joining the Lawson family and becoming a daughter to Becky. Even before it was official, she was there with encouraging words and love. Finally, I would like to thank the man who makes my life wildly, but delightfully, unpredictable. My husband, Richard, who caterwauls, back-seat drives and corrects my chemical engineering equations all while making me certain that I am blessed with much more than I deserve.

This work was supported by funding from the National Institutes of Health (R01DK073991) and the National Science Foundation through the Student and Teacher Enhancement Program (STEP) Fellowship. This funding is gratefully acknowledged.

TABLE OF CONTENTS

LIST OF TABLES

LIST OF FIGURES

LIST OF SYMBOLS AND ABBREVIATIONS

CPA	Cryoprotective Agent
DMSO	Dimethyl Sulfoxide
DPS	3M DMSO + 3M PD + 0.5M Sucrose
ECM	Extracellular Matrix
IDD	Insulin-Dependent Diabetes
P6	1M DMSO + 5M PD + 0.34M PEG400
PD	1,2-Propanediol
PEG400	Poly ethylene glycol (M.W. 400)
PLL	Poly-L-Lysine
T1DM	Type 1 Diabetes Mellitus
T2DM	Type 2 Diabetes Mellitus

SUMMARY

The use of encapsulated cell systems is widespread in the field of Tissue Engineering. They are primarily used to deliver cells that secrete therapeutic molecules. More specifically, encapsulated systems have shown promise in the delivery of insulin-secreting cells or cell clusters to revert diabetes. Although often overlooked, cryopreservation is critical in bringing these constructs from the laboratory to the clinic. Two main types of cryopreservation are currently being investigated for the preservation of tissue-engineered constructs: conventional freezing and vitrification. Conventional freezing is often used for preserving cell suspensions and uses low concentrations of cryoprotective agents (CPAs), slow cooling and rapid warming. Vitrification, or ice-free cryopreservation, utilizes high concentrations of CPAs paired with rapid cooling and warming to achieve a vitreous, or glassy, state. Our overall goal was to determine the effects of both types of cryopreservation on the *in vitro* and *in vivo* performance of an encapsulated cell system, a model tissue-engineered pancreatic substitute. The specific aims in this thesis were (1) to model CPA delivery and removal to encapsulated cells, and their effects on cell viability; (2) to characterize *in vitro* the effects of cryopreservation protocols on cell viability and the biomaterial structure and function of a pancreatic substitute; (3) to characterize *in vivo* the effects of cryopreservation on the biocompatibility and efficacy of a pancreatic substitute. This research addresses the systematic design of vitrification protocols and how these protocols and conventional freezing affect a tissue-engineered construct. Our results indicate that temperature of exposure is the most critical parameter for the proper design of vitrification protocols.

Overexposure is another concern as it leads to a decrease in viable cell number. The use of a mathematical model is critical for the design of addition and removal protocols to ensure CPA equilibration and minimize CPA exposure. Results from *in vitro* studies indicate that both vitrification and conventionally frozen perform comparably to fresh. However, *in vivo* studies reveal that vitrification performs worse than both conventionally frozen and fresh beads. With adjustments, it may be possible to improve the performance of the vitrified beads. Nevertheless, for this encapsulated system, conventional freezing is the better method and allows successful cryopreservation.

CHAPTER 1

INTRODUCTION

It is estimated that 23.6 million Americans have Type 1 or Type 2 diabetes mellitus although not all of these have been diagnosed (Vijan 2010). An additional 50 million Americans are estimated to have impaired fasting glucose and 25% of these will develop Type 2 diabetes, likely within the next two and a half years (Stolar 2010). Type 1 diabetics require daily exogenous insulin and were previously known as insulin-dependent diabetics. Although not all of those diagnosed with Type 2 diabetes currently require exogenous insulin, the pathogenesis of this disease indicates the eventual need for exogenous insulin for many who are diagnosed. Exogenous insulin is readily available but does not provide the tight glycemic control that is present in a healthy individual. The use of exogenous insulin is life-saving for diabetics, but it is not the ideal treatment. Currently, whole organ transplantation and transplantation of the insulin-secreting cell clusters, islets of Langerhans, are the only treatments that can achieve glycemic control mimicking that of a healthy individual. These two treatments require lifelong immunosuppression and are plagued by cell source issues. Alternatively, the use of encapsulation to deliver insulin-secreting cells or cell clusters has shown promise. The physical barrier of encapsulation provides a level of immune protection that allows the use of allogeneic and xenogeneic cell sources with reduced immunosuppression. As this technology is improved, it may become a viable treatment option for insulin-dependent diabetics.

The encapsulation and delivery of insulin-secreting cells or cell clusters to treat insulin-dependent diabetes appears promising. However, as is the case with any tissue-engineered construct, additional obstacles remain before it can achieve widespread clinical use. Due to manufacturing processes, lengthy sterility testing and quality control testing, tissue-engineered constructs will need to be successfully preserved. The preservation of these constructs is considered to be critical in providing off-the-shelf availability in a clinical setting (Karlsson and Toner 1996; Pancrazio et al. 2007; Sambanis 2000).

Conventional freezing and vitrification are the two main types of cryopreservation currently being investigated. Conventional freezing utilizes low levels of cryoprotective agents (CPAs) along with slow cooling and rapid warming. This method is termed conventional freezing because it has commonly been used to preserve cell suspensions in laboratory cell banking. Conventional freezing allows ice formation which occurs preferentially in the extracellular space or extracellular matrix (ECM) (Karlsson and Toner 1996; Pegg 2010). Extracellular ice formation may not have a significant effect on the preservation of cell suspensions. However, ice formation has been shown to cause damage to the ECM (Agudelo and Iwata 2008; Heng et al. 2004; Mukherjee et al. 2005) when used for the preservation of larger tissue-engineered constructs or natural tissues. This ice formation may be detrimental to the biomechanical function of the construct (Schenke-Layland et al. 2007). Additionally, ice damage may change the overall morphology of the construct which could result in an increased inflammatory response *in vivo* (Bunger et al. 2003; Lanza et al. 1991).

Vitrification, or ice-free cryopreservation, utilizes high concentrations of CPAs, rapid cooling and rapid warming to eliminate ice formation and achieve a vitreous, or glassy, state. Unfortunately, the use of high concentrations of CPAs also introduces the issues of osmotic excursions and CPA cytotoxicity. Exposing cells to a high concentration (6-8M) of CPA in a single step will lead to excessive osmotic excursions which will shrink the cell until the electrolyte concentration within the cell is lethal. Single-step removal of such high concentrations of CPAs would also lead to excessive osmotic excursions, resulting in cell lysis. To circumvent this issue, CPA solutions are generally added and removed in multiple steps to minimize osmotic excursions. The high concentration of CPAs is itself toxic to cells and so exposure during addition and removal must be minimized.

The use of conventional freezing and vitrification for the preservation of encapsulated cell systems has seen mixed results. Conventional freezing has been successfully used to maintain human and porcine islets (Beattie et al. 1997; Stiegler et al. 2006). The encapsulation itself may benefit the outcome as alginate encapsulation of neurospheres has been shown to improve the outcome of conventional freezing compared to free neurospheres (Malpique et al. 2010). Alternatively, conventional freezing has been shown to damage the alginate matrix (Agudelo and Iwata 2008; Heng et al. 2004; Mukherjee et al. 2005) which may be detrimental to the function of the construct.

Initial studies in our laboratory indicated that systematically designed vitrification protocols minimize cell death and maintain the integrity of the alginate bead. The tissue-engineered pancreatic substitute used in these studies consisted of a murine insulinoma cell line, βTC3 cells, encapsulated in a calcium-alginate/poly-L-lysine/alginate (APA)

bead. Conventionally frozen beads performed worse than vitrified beads in their insulin secretory function, although some vitrified groups experienced more cell death than conventionally frozen beads (Mukherjee et al. 2005). The proliferative nature of the cells may allow them to rebound from low viability. Unfortunately, these vitrification studies, done by Dr. Mukherjee, required manual manipulation to achieve appropriate cooling and warming rates and did not allow for overnight storage. In order to be more clinically relevant and consistent, a mechanical freezer equipped with an isopentane bath was used to achieve the necessary cooling and warming rate for further studies. In this new system, the better performing vitrification solution, VS55 consisting of 3.1M dimethyl sulfoxide (DMSO) + 2.2M 1,2 propanediol (PD) and 3.1M formamide, was no longer consistently vitrifiable. Another previously used solution, DP6+0.3MS consisting of 3M DMSO + 3M PD and 0.3M sucrose, was modified by raising the sucrose concentration to 0.5M to ensure consistent, successful vitrification. Additionally, preliminary studies indicated that a simpler conventional freezing protocol utilizing 10% DMSO in fully-supplemented DMEM was comparable or better for the βTC-tet cell line than the previous protocol which incorporated mannitol in removal steps. This new protocol may also be a better reflection of general laboratory practices. The use of the βTC-tet cell line replaced the use of the βTC3 cell line. The βTC-tet cell line has been engineered for growth regulation in the presence of tetracycline and has been successfully used *in vivo* (Black et al. 2006). After these modifications were made, research was initiated to determine the effects of cryopreservation, both conventional freezing and vitrification, on the *in vitro* and *in vivo* cellular and biomaterial function of the tissue-engineered construct.

In order to gain insight into the design of CPA addition and removal protocols and their effect on the success of preservation, the previously published mathematical model describing the mass transport through the matrix and cellular membrane (Mukherjee et al. 2008) was expanded to incorporate heat transport as well as cytotoxicity due to CPA exposure. CHAPTER 3 describes the experimentally determined cytotoxicity kinetics for two of the most commonly used CPAs, DMSO and PD for varying exposure times and temperatures as well as a range of concentrations. Supplemental data for these studies can be found in the APPENDIX A. The experimental results were subsequently described using a toxicity equation adapted from the field of sterilization. CHAPTER 4 utilizes this toxicity equation in the expansion of the mathematical model. The mathematical model was used to gain insight into the design of addition and removal protocols for the encapsulated system as well as a more challenging natural tissue, articular cartilage. Matlab® code for the mathematical model is given in APPENDIX B.

Simultaneous to the expansion of the mathematical model, research was initiated to examine the effects of cryopreservation on the cellular and biomaterial components of the tissue-engineered pancreatic substitute as seen in CHAPTER 5. Designed CPA addition and removal protocols for two vitrification solutions, DPS (3M DMSO + 3M PD + 0.5M Sucrose) and P6 (1M DMSO +5M PD + 0.34M polyethylene glycol), were used to vitrify APA beads containing βTC-tet cells. Samples were rapidly cooled to -100°C, then more slowly cooled through the glass-transition temperature to -130°C. For conventional freezing, beads were exposed to 10% DMSO in supplemented medium for 10 minutes before being slowly cooled to -80°C and then plunged in liquid nitrogen (LN2). Preserved samples were stored overnight before warming. The cellular

component was assessed for viable cell number as well as insulin secretory function. The biomaterial component was assessed for integrity by mechanical testing and permeability studies. Overall morphology and matrix integrity were assessed histologically.

After *in vitro* assessment, two *in vivo* studies were undertaken to determine the effects of cryopreservation on the *in vivo* inflammatory response to the beads and the overall *in vivo* efficacy of the beads in reverting an induced diabetic mouse model. The sub-therapeutic and therapeutic *in vivo* studies are described in CHAPTER 6. For the sub-therapeutic study, healthy mice were implanted with a small volume of fresh, vitrified or conventionally frozen APA beads. Mice were sacrificed on days 2, 7 and 14 and the explants were assessed for secretory function, host-cell attachment and overall morphology. Short-term therapeutic studies were carried out in streptozotocin-induced diabetic mice. Diabetic mice were implanted with a therapeutic volume of fresh, vitrified or conventionally frozen APA beads. Mice were sacrificed upon implant failure or at two weeks, whichever came first. Explants were assessed in the same way for both therapeutic and sub-therapeutic studies.

All of the aforementioned chapters contain the motivation, experimental methods, results and discussion. General information on insulin-dependent diabetes and cryopreservation are reviewed in CHAPTER 2. CHAPTER 7 discusses conclusions and future research directions.

In summary, this thesis determined the effects of a rationally designed vitrification protocol and a conventional freezing protocol on the *in vitro* and *in vivo* performance of an encapsulated system. A mathematical model, expanded to incorporate heat transfer and CPA cytotoxicity, was used to design CPA addition and removal

protocols. This mathematical model could be easily adjusted for use with a variety of natural tissues or tissue-engineered constructs. Experimental studies on the *in vitro* and *in vivo* performance of conventionally frozen or vitrified APA beads were carried out. Previous studies in this area have utilized a wide variety of techniques and solutions with varying success. Although many of these previous studies indicated successful preservation, it remained difficult to ascertain which method of preservation would be preferable for a specific system. This thesis presents one of the first systematic comparisons of the two main types of cryopreservation, conventional freezing and vitrification, and their effects on the cellular and biomaterial components and *in vivo* efficacy of a tissue-engineered pancreatic substitute. The results presented in this thesis indicate that while vitrification may be better for some tissue-engineered constructs, this encapsulated system can be successfully preserved by conventional freezing. The tissue-engineered pancreatic substitute is an encapsulated cell system, making these results broadly applicable in the field of Tissue Engineering.

CHAPTER 2

BACKGROUND

2.1 Diabetes Mellitus and Treatment Options

Diabetes currently affects approximately 23.6 million Americans (CDC 2007). Although many of the patients diagnosed with diabetes do not use exogenous insulin, 27% of those diagnosed require exogenous insulin. Diabetics may be diagnosed with Type 1 or Type 2 Diabetes. The two main types are discussed below.

2.1.1 Type 1 Diabetes Mellitus

Type 1 Diabetes Mellitus (T1DM) is an autoimmune genetic disease that normally presents during childhood. Although the molecular mechanism is not entirely understood, aberrant antigen presentation has been implicated (Todd 2010). As the disease progresses, the insulin-secreting β-cell mass decreases. This leads to compromised insulin secretory capacity. Patients diagnosed with T1DM depend upon exogenous insulin to maintain normal glycemic levels and are considered to be insulin-dependent. The incidence of this and other autoimmune diseases is on the rise which indicates that unknown environmental factors may also play a role in T1DM (Todd 2010). Temporal variations in the disease development within genetically susceptible members of the same family indicate that unknown environmental cues may trigger the autoimmune response that causes T1DM (Csorba et al. 2010). Currently, T1DM accounts for 5-10% of the diagnosed cases of diabetes in America, according to the CDC (National Diabetes Fact Sheet 2007).

2.1.2 Type 2 Diabetes Mellitus

Otherwise known as adult-onset diabetes, Type 2 diabetes mellitus (T2DM) is generally associated with obesity and a sedentary lifestyle. Specific environmental factors and genetic predisposition determine a patient's risk for T2DM (McCarthy 2010) although environmental factors appear to play a larger role in the pathogenesis of T2DM relative to T1DM. Type 2 Diabetes manifests as both insulin resistance and decreased insulin secretion. Although the exact mechanisms remain unclear, several deficiencies are well documented. The skeletal muscle consumes most of the circulating glucose in the blood of a healthy individual. Decreased insulin-stimulated glucose uptake of skeletal muscle has been implicated as one of the main causes of impaired insulin activation, or insulin resistance (Choi and Kim 2010). Insulin resistance eventually causes a decline in β-cell mass and function. Significant efforts are still being made to better understand the pathogenesis of T2DM. Unfortunately, due to the high incidence of obesity in those diagnosed with Type 2 Diabetes, it is difficult to ascertain what biochemical cues may cause the progression toward T2DM and what may be a consequence of the disease (Tripathy and Chavez 2010). Nevertheless, the pathogenesis of T2DM generally leads to the need for exogenous insulin. Insulin-dependent diabetes (IDD) is on the rise, so it is critical to not only consider its treatment but also the complications that often accompany it.

2.1.3 Current Treatment: Diet, Exercise & Medication

If diagnosed early enough, the progression of T2DM can usually be slowed through better nutrition and increased exercise (Russell-Minda et al. 2009). Additionally, patients are asked to monitor their blood glucose daily so that their physician can

determine how far the disease has progressed. When diet and exercise are insufficient to maintain appropriate glycemic levels, oral medications such as Metformin are added to the patient's regimen (Vijan 2010). Unfortunately, most Type 2 diabetics will eventually require the use of exogenous insulin as their disease progresses.

2.1.4 Current Treatment: Exogenous Insulin

The administration of exogenous insulin is critical for those with IDD, including those with T1DM and some with T2DM. This often requires the use of multiple injections or an insulin pump. An insulin pump delivers insulin continuously in response to input blood plasma glucose levels. These pumps are capable of calculating dosage and varying the profile and duration of the insulin administered. Evidence suggests that the use of an insulin pump is superior to multiple daily injections (Alsaleh et al. 2010). This may be particularly true for Type 1 diabetics who are generally diagnosed at a young age and are particularly prone to a fear of injections (Frid et al. 2010). Due to the high cost of insulin pumps, generally $4000-$5000, many diabetics rely on multiple daily injections. Unfortunately, studies focused on Type 2 diabetics indicate that only 35.8% of patients achieve their recommended glycemic control levels (Stolar 2010).

2.1.5 Current Treatment: Transplantation

Whole organ pancreas transplantation is currently the only proven way to achieve long-term insulin independence. Unfortunately, the limited availability makes pancreas transplantation an option for very few. Additionally, pancreas recipients will require lifelong immunosuppression to minimize the risk of rejection. Due to the risks of immunosuppression, pancreas transplantation is generally only done in conjunction with another organ, such as kidney or liver (Lam et al. 2010). The alternative of islet

transplantation appeared to be very promising after the publication of the Edmonton protocol which utilized low-level immunosuppression to increase the success of transplanted islets (Shapiro et al. 2000). By 2005, there were 66 patients in the Edmonton series who had received transplants. Most achieved insulin independence for some amount of time, but the median time for these patients to require insulin therapy again was just 15 months (Robertson 2010). The implantation of islets is also currently plagued with other issues, such as tissue availability, standardization of pancreas digestion and loss of islet function over time (Langer 2010).

2.1.6 Complications

The incidence of the secondary complications of diabetes generally increases with the duration of disease. On average, patients diagnosed before the age of 35 lose around 26 years of life due to secondary complications (Stolar 2010). The most prevalent complication is cardiovascular disease which was responsible for approximately 50% of the deaths caused by complications of T2DM in 2010 (Zoungas and Patel 2010). Additional complications include retinopathy which can result in loss of vision, nephropathy which can result in renal failure and neuropathy which generally includes loss of sensation in extremities as well as foot ulcers. Although the mechanisms that cause these complications are varied, evidence indicates that hyperglycemia plays a role (Nathan 1993). Utilizing intensive insulin therapy may lower the chances of experiencing these complications but also increases the possibility of hypoglycemic episodes (Tesfaye and Seaquist 2010). Hypoglycemia is of particular concern for those who require exogenous insulin because the body's usual response to hypoglycemia, a decrease in insulin secretion, is rendered ineffective.

2.2 Tissue-Engineered Pancreatic Substitute

2.2.1 Cell Source

One of the most critical issues in developing alternative, tissue engineering strategies for the treatment of IDD is the cell source. In recent years, several sources have come to the forefront for consideration in a tissue-engineered pancreatic substitute. The most prominent of these is the use of islets. Significant work has been done in this area since the Edmonton protocol was published (Shapiro and Lakey 2000). Due to the limited supply of cadaveric donor tissue, efforts have focused on the use of xenogeneic islets, most often porcine. Porcine insulin is very similar to human insulin and the use of pigs could provide a ready supply of islets. Research has been done to investigate the use of adult, neonatal and fetal porcine islets but due to the xenogeneic nature of the islets, some amount of immunosuppression or immune protection is generally used. Efforts in this field have yielded multiple porcine to non-human primate transplantations with varied success (Hering and Walawalkar 2009). The use of encapsulated islets, which exhibit a level of immune protection due to the physical barrier provided by the encapsulation, has emerged as one of the more promising technologies. Encapsulation can be done in conjunction with immunosuppression for improved performance (Safley et al. 2005). Several challenges remain before islets will be clinically relevant. Islets are somewhat fragile and difficult to isolate consistently (Ricordi et al. 1986) and are particularly prone to hypoxia-induced damage (de Groot et al. 2004). Additionally, the number of islets required by most clinical patients is approximately 10,000 islet equivalents/kg (Emamaullee and Shapiro 2007), making the necessary implant volume, and therefore the implant site, an issue.

Several other cell sources are currently being considered. Stem cells, either embryonic or induced pluripotent, have been investigated to replace the insulin-secreting β-cells present in a healthy individual. Induced pluripotent stem cell-derived β-like cells have recently been used to demonstrate glucose-responsive insulin secretion and have successfully reverted diabetes in diabetic mice for up to four months (Alipio et al. 2010). The use of embryonic stem cells is farther off due to the difficulty and low efficiency of differentiation (Guo and Hebrok 2009). Unfortunately, in both of these cases, the risk of teratoma, or tumor, formation remains, as well as concerns about the immune response to the cells.

Genetically engineered non-β cells have also shown promise. In theory, these cells could be harvested from the patient, expanded, genetically engineered and then implanted in the same patient. Most efforts have centered on the use of cells that already exhibit glucose-responsive behavior. Enteroendocrine cells have been used because their native function is to secrete incretin hormones, which help regulate insulin secretion. Studies done with these cells have shown insulin secretion (Bara and Sambanis 2009) although not enough to revert diabetes in a diabetic mouse model (Bara et al. 2009). Other groups have seen success using both enteroendocrine cells (Han et al. 2007) and genetically engineered adipocytes (Ito et al. 2005). Native hepatocytes are also sensitive to glucose. Hepatic cells have been successfully genetically engineered to release insulin in a glucose-responsive manner (Kozlowski et al. 2007; Thule et al. 2000). These technologies will still require significant work before they become viable treatment options for IDD.

The most simple cell source used in the laboratory is proliferating cell lines, usually derived from mice, rats or humans. Many of the cell lines that exist are not responsive to glucose stimulation in the physiological range or require additives to be responsive (Skelin et al. 2010). Work done in Dr. Efrat's laboratory at Albert Einstein College utilized transgenic mice to develop the βTC cell lines. Although initial cell lines developed by this group were not responsive to glucose stimulation (Efrat et al. 1988), later cell lines have been shown to have normal glucose responsiveness for up to 60 passages. Additionally, the βTC-tet cell line allows growth regulation with cell growth arrested in the presence of tetracycline (Fleischer et al. 1998). These cells have been widely studied and well characterized by several different groups (Black et al. 2006; Cheng et al. 2006; Simpson et al. 2005). Due to their robust nature and insulin secretion characteristics, these cells are particularly useful in the laboratory setting.

2.2.2 Microencapsulation

The encapsulation of cells or cell clusters is promising and has been applied to treat anemia, dwarfism, kidney and liver failure as well as pituitary and central nervous system deficiencies (de Vos et al. 2006). Microencapsulation is particularly promising due to the short diffusion lengths of beads which are comparable to the maximum diffusion length of oxygen (Mueller-Klieser et al. 1986). For encapsulated systems with a semi-permeable membrane, the overall risk of implant failure is also minimized because each microsphere has an individual membrane rather than the entire implant relying on a single membrane (Soon-Shiong 1999).

Calcium alginate/poly-L-lysine/alginate (APA) beads, as shown in Figure 2.1, have been most widely used for encapsulation (Dusseault et al. 2005), in part due to the

mild conditions of encapsulation (Gugerli et al. 2002). Alginate is derived from seaweed and is composed of mannuronic (m) and guluronic acid (g) residues. High-mannuronic acid alginates have been shown to bind more effectively with poly-L-lysine (PLL) (de Groot et al. 2004), but are not as stiff as high-guluronic acid alginates. This is due to the accepted mechanism of cross-linking, known as the egg-box model, shown in Figure 2.2 (Grant et al. 1973). Both high-m and high-g alginates have been studied and characterized for the encapsulation of β-cells (Constantinidis et al. 1999; Stabler et al. 2001). The use of PLL in conjunction with the alginate does not affect β-cell growth (Benson et al. 1997) and has been shown to play a significant role in the stability of alginate beads (de Groot et al. 2004). The alginate used for encapsulation must also be very pure with low levels of endotoxin or contaminants to minimize immune response *in vivo*.

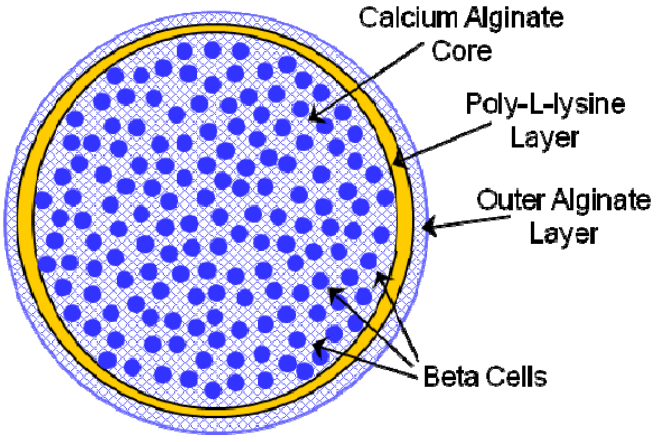

Figure 2.1 Schematic of APA bead.

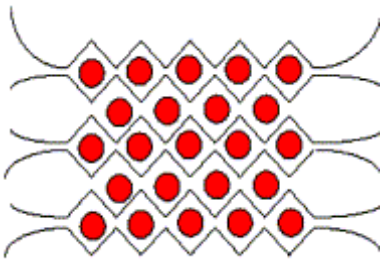

Figure 2.2 Egg-box model. Solid circles represent calcium ions positioned between "G-blocks" of consecutive guluronic acid residues. "M-blocks" of consecutive mannuronic acid residues represented by curves.
Adapted from Simpson, et al. 2004.

Concerns about APA beads are primarily due to the PLL layer. The PLL layer serves as a semi-permeable membrane that is meant to allow nutrients and oxygen in as well as therapeutic molecules, such as insulin, and waste products out. Although it does not allow immune cells, such as macrophages in, it does allow smaller signaling molecules such as TNF and IL-1β to pass through (Kulseng et al. 1997). These molecules play a role in the host reaction to the beads (Robitaille et al. 2005). Additionally, PLL is considered to be inflammatory (de Vos et al. 2006; Ponce et al. 2006). This has been noted by several groups (Safley et al. 2008; Strand et al. 2001) and may be due to incomplete coverage by the second alginate layer (de Groot et al. 2004; Juste et al. 2005).

In response to these concerns, many different materials have been suggested. Barium has been used as an alternative to calcium because barium cross-links more strongly with alginate (Zimmermann et al. 2005). Barium alginate has been used with some success either alone (Safley et al. 2008) or in conjunction with a poly-L-lysine layer

(Li et al. 2006a). Concerns still remain due to the known toxicity of barium (de Vos et al. 2006). Other materials that have been used with limited success include polyethylene glycol (Weber et al. 2006), polyanions based on poly(methyl vinyl ether-alt-maleic acid) (Gardner et al. 2010), agarose (Kumachev et al. 2011) and alginate with vinyl monomers (Wang et al. 2005) or methacrylates (Jeon et al. 2009) for polymerization.

2.2.3 Macroencapsulation

Macroencapsulation has also been investigated for the delivery of secreting cells or cell clusters. The larger dimension of these constructs makes the diffusion of oxygen a concern. Two geometries have commonly been used in an attempt to circumvent this issue: hollow fiber and disc. Studies have shown that correctly designed hollow fibers can provide sufficient oxygenation to maintain cells and even allow growth and propagation (Cornolti et al. 2009; Hoesli et al. 2009). The design of these devices is critical to their success. Increased surface area to volume will lead to increased function and growth of cells. The cell density also plays a significant role in the function of the cells. Higher cell densities have been found to significantly increase insulin secretion due to cell-cell signaling (La Flamme et al. 2007). *In vivo* studies have had varied results with reports of success in reverting diabetes in mice when using hollow fibers (Delaunay et al. 1998) and less success when comparing the hollow fiber and disc geometry to microencapsulated spheres (Yang et al. 1994). A few new technologies may help to overcome the current limitations of macroencapsulation. Fibrin ribbons can be incorporated in polyethylene glycol scaffolds to increase vascularization (Mason and Mahoney 2010). Cell sheet engineering using chondrocytes has also been used recently to deliver insulin-secreting cells. Unfortunately, this study did not see long-term

maintenance of insulin secretion (Lee et al. 2008). Designing a geometry that will accommodate the number of cells necessary for a larger animal remains problematic.

2.3 Cryopreservation

The need for preservation of tissues and tissue-engineered constructs is widely recognized (Karlsson and Toner 1996; Sambanis 2000). Several main types of preservation exist: desiccation, hypothermia and cryopreservation. Desiccation, or freeze-drying, is usually done for pharmaceuticals and proteins. This process causes an increase in solute concentration due to drying that allows the formation of a vitreous, or glassy, state. Although desiccation can provide long-term storage, most research has focused on the process of drying and ignored the issue of rehydration. This method may one day be viable for more than pharmaceuticals and proteins but significant work regarding rehydration remains to be done. Additionally, it is not clear that desiccation would adequately preserve three-dimensional constructs, especially hydrogels which are commonly used as biomaterials.

Hypothermia and cryopreservation both take advantage of the relationship between temperature and cell metabolism. Most enzymes exhibit a two-fold decrease in activity for every 10°C decrease in temperature (Belzer and Southard 1988). Therefore, a decrease from 37°C to 0°C will result in enzyme activity that is 8% of the original activity. Hypothermic storage occurs around 4°C and significantly slows the metabolism of cells. These cells still require nutrients and oxygen to survive despite their depressed metabolism. Hypothermic perfusion preservation can provide the necessary oxygen, but also introduces the possibility of pressure-driven shear stress damage (Fuller and Lee 2007). Unfortunately, the length of storage possible with hypothermic storage is only on

the order of hours to days (Van Buskirk et al. 2004). Due to this, hypothermic storage is primarily used for tissues that have not yet been successfully cryopreserved. Cryopreservation utilizes cryoprotective agents (CPAs) to replace a portion of water within the cell or construct. Cryopreserved constructs and tissues are held at temperatures ranging from -80 to -196°C and the storage time can extend from months to years (Van Buskirk et al. 2004). At sufficiently low temperatures, all rotational and translational molecular motion ceases and cells achieve a state of stasis (Brockbank et al. 2003). Although there are difficulties associated with the cryopreservation of tissues or tissue-engineered constructs, this method of preservation currently appears to be the most promising.

2.3.1 Cryoprotective Agents (CPAs)

The definition of a CPA is functional. A CPA is classified as such because experiments have shown that it will yield higher post-thaw survival than could be achieved without it (Fuller 2004). Commonly, CPAs are divided into two categories: permeating and non-permeating. Permeating CPAs, such as dimethyl sulfoxide (DMSO) or propanediol (PD), have low molecular weights and can pass through the cell membrane (Karlsson and Toner 1996). These serve to displace water within the cell and protect against intracellular ice formation (Brockbank and Taylor 2007). Polymers and sugars are often used as non-permeating CPAs. Due to their high molecular weight, they cannot pass through the cell membrane. The most commonly used non-permeating CPAs are trehalose, sucrose, polyethylene glycol (PEG) and polyvinylpyrrolidone. These solutes serve different purposes depending on the type of cryopreservation. As they cannot permeate into the cells, they can serve to draw more water out of the cells or they

may be used to affect the extracellular solution properties (Fuller 2004). Although CPAs are used to improve the overall outcome of cryopreservation, they can also be toxic to cells. Toxicity is a function of the temperature of exposure, time of exposure, CPA identity and CPA concentration (Elmoazzen et al. 2007) and will be discussed further in the context of the two main types of cryopreservation: conventional freezing and vitrification.

2.3.2 Conventional Freezing

Conventional freezing utilizes low concentrations of CPAs which are generally coupled with slow cooling and rapid warming. This approach has been most successfully used to preserve cell suspensions. The most commonly used CPA in conventional freezing is DMSO.

2.3.2.1 Basic Operating Procedures

Two main types of damage can occur to cells during conventional freezing: solution effects and intracellular ice formation. Both of these phenomena occur during the cooling step and are determined by the rate of cooling, as seen in Figure 2.3. During cooling, ice forms preferentially in the extracellular space or matrix (Li and Liu 2010; Pegg 2010) and causes a decrease in the concentration of water outside of the cells. Extracellular ice does not incorporate solutes and so the concentration of the CPA and other solutes outside of the cell increases (Szarko et al. 2010). This creates a concentration gradient across the cell membrane which generally causes water to move out of the cell. If the rate of cooling is too slow, too much water will exit the cell and the intracellular electrolyte concentration will increase. This can cause cell death and is denoted “Solution Effects” in Figure 2.3. Alternatively, if the rate of cooling is too rapid,

the rate of extracellular ice formation will exceed the rate of water permeating out of the cell. As the sample is cooled, the temperature will eventually be low enough to cause the cell membrane to be virtually impermeable (Karlsson and Toner 1996). At some point, the cell will become supercooled and intracellular ice will form, denoted "Intracellular Ice Formation" in Figure 2.3. Any amount of intracellular ice formation (IIF) is lethal to most cell types. Optimally, the cooling rate should be sufficient to allow some intracellular water to escape so that, as the cell is cooled, the intracellular environment will become highly viscous and achieve a vitreous, or glassy, state that will not allow ice formation. The use of CPAs in conventional freezing is primarily to replace water within the cell. This decreases the chances of IIF and the CPA acts as a solvent to reduce the electrolyte concentration within the cell during freezing (Karlsson and Toner 2000).

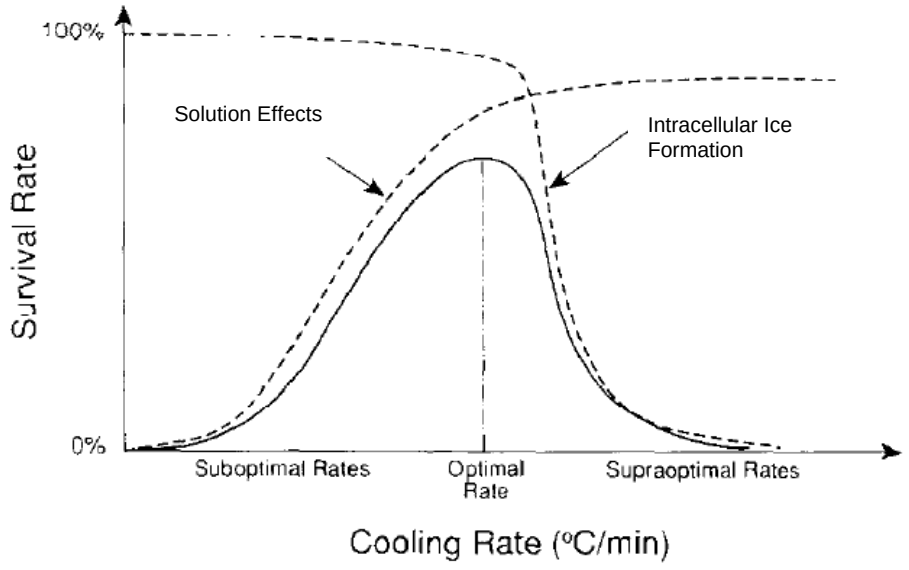

Figure 2.3 Survival curve indicating mechanisms of cell death during cooling in conventional freezing.
(Karlsson and Toner 1996)

The warming step is also important to the outcome of conventional freezing. Generally, the warming rate should be equivalent to or faster than the cooling rate used. If the rate is equivalent, the cell will undergo the same osmotic excursions that were experienced upon cooling. Faster warming allows more rapid melting of ice. However, if the rate of warming for a slowly cooled sample occurs too rapidly, excessive osmotic excursions may occur as the cell is rehydrated.

2.3.2.2 Challenges

Although the use of conventional freezing is sufficient for the cryopreservation of cell suspensions, the occurrence of extracellular ice may be detrimental to tissues or constructs. A prominent cryobiology investigator, Dr. David Pegg, recently stated, "It seems to be inescapable that the formation of ice, whether intracellular or extracellular, in tissues and organs is severely damaging (Pegg 2010)." This is particularly true for tissues that primarily serve a mechanical purpose (Schenke-Layland et al. 2007). Additionally, the occurrence of ice is generally random and heterogeneous (Brockbank et al. 2003). Impurities or particulates serve as nucleation sites and contribute to the random nature of ice formation. Some proponents of conventional freezing have recommended the seeding of ice at a particular temperature to eliminate the random nature of ice formation. Even in this situation, ice may be damaging.

2.3.3 Vitrification

Vitrification utilizes high concentrations of CPAs, rapid cooling and rapid warming to achieve ice-free cryopreservation. Although vitrification generally occurs intracellularly in conventional freezing, the term vitrification refers to an ice-free state throughout the system.

2.3.3.1 Operating Procedures

Ice formation is usually governed by thermodynamics. However, in vitrification, ice nucleation becomes governed by kinetics. The high concentrations of CPAs slow the formation of ice crystals and rapid cooling brings the sample to the glass-transition temperature, T_g, before ice crystals can form. At T_g, the solution is so viscous that molecular diffusion stops. This stops the growth of any ice nuclei that may have formed. Although called ice-free cryopreservation, vitrification is defined as having a total crystallized fraction of less than 10E-6 (Karlsson and Toner 1996). This can be determined using thermal analysis, such as differential scanning calorimetry, but is often confirmed by macroscopic observation (Weiss et al. 2010).

To achieve the vitrified state, a sample must be cooled very quickly. The critical cooling rate is the rate at which ice formation will be suppressed. It varies depending on CPA or CPA cocktail used and the concentration of solutes present in the solution. The addition of non-permeating CPAs is especially useful for vitrification and can increase the stability of the glassy state or decrease the critical cooling rate. Warming is also critical as devitrification and recrystallization are common problems. It is very likely that a vitreous state will still contain ice nuclei. If the warming rate isn't fast enough, ice crystals will form, denoted as devitrification, and grow, denoted as recrystallization. This formation of ice will occur very rapidly and may be more detrimental to cells than the ice formation that occurs in conventional freezing. The critical warming rate is the rate above which there is insufficient time for crystallization to occur before the system reaches the melting point (Brockbank et al. 2003). The CPAs or CPA cocktails that are

used to vitrify dictate the critical cooling and warming rates necessary to successfully achieve vitrification.

2.3.3.2 Challenges

Although consistently achieving the critical cooling and warming rates is important for successful vitrification, these rates can be manipulated to within experimentally achievable parameters by using different or higher concentrations of CPAs. The more difficult challenge is incorporating the higher concentrations of CPAs without damaging the cells. Two types of damage generally occur when using such high concentrations of CPAs: excessive osmotic excursions and cytotoxicity.

In order to maintain osmotic excursions within a tolerable range, high concentrations of CPAs must be added in a step-wise manner. This is particularly true for constructs where mass transfer through the construct must also be included. Appropriate CPA addition and removal protocols can be designed using mathematical modeling (Mukherjee et al. 2008). These protocols will maintain cells within tolerable cellular volumes during the addition and removal procedures.

The issue of CPA cytotoxicity specifically arises due to the high concentrations necessary to achieve vitrification. The low concentrations of CPAs used for conventional freezing are usually in the range of 10-20%. Cells do not experience significant toxicity at these levels (Heng et al. 2004; Judas et al. 2007; Stiegler et al. 2006). CPA toxicity is dependent upon time and temperature of exposure as well as CPA identity and concentration. Cytotoxicity has been noted as being the limiting factor for successful cryopreservation (Fahy 2010). For the preservation of larger constructs or tissues, mass transfer limitations may require longer exposure to CPAs. In response to this, novel

CPAs or CPA carrier solutions have been proposed (Matsumura et al. 2010; Wusteman et al. 2008a). Additionally, the idea of CPA Toxicity Neutralization has led to the use of CPA cocktails to achieve the necessary concentrations (Fahy 2010). Non-permeating solutes are also being used by some to replace permeating solutes (Grondin et al. 2009; Katenz et al. 2007; Petrenko et al. 2008) as toxicity has been shown to depend more heavily on permeating than non-permeating CPAs (Fahy et al. 2004). In spite of this work, CPA toxicity continues to be a challenge in the vitrification of cells, constructs and tissues.

2.4 Cryopreservation of Tissue-Engineered Constructs & Tissues

While the cryopreservation of cell suspensions has been shown to be relatively simple, this is not the case for larger systems. More specifically, the preservation of natural tissues or tissue-engineered constructs is much more complex. Although the field of Tissue Engineering is relatively new with the flagship journal being launched in 1995, significant work has already been done to investigate the preservation of tissue-engineered constructs. Microencapsulation is of particular interest for delivery of secreting cells or cell clusters. Cryopreservation of an encapsulated cell system has yielded highly variable results. Conventional freezing has been successful for maintaining encapsulated islets (Schneider and Klein 2011; Stiegler et al. 2006) and myoblasts (Murua et al. 2009) as well as their *in vivo* function. Studies have also shown that the success of conventional freezing is improved by the alginate encapsulation (Malpique et al. 2010). However, other groups have reported that conventional freezing leads to damage in the matrix of an encapsulated system (Agudelo and Iwata 2008; Hang et al. 2010; Heng et al. 2004; Mukherjee et al. 2005). Encapsulated cells and islets have

also been successfully preserved using vitrification, although none have compared the performance of the two methods within the context of *in vivo* efficacy (Agudelo et al. 2009; Wu et al. 2007). Additionally, alginate encapsulation appears to improve the success of vitrification (Zhang et al. 2010).

Ice damage to the extracellular matrix is clearly detrimental for constructs that serve a biomechanical function (Schenke-Layland et al. 2007). Vitrification has been shown to maintain the viscoelastic properties of human vascular grafts better than conventional freezing (Thakrar et al. 2006). Other studies have shown that the ice formation that occurs during the conventional freezing of tissue-engineered blood vessels significantly decreases the tissue's ability to contract (Dahl et al. 2006). Vitrification may also be preferable for adherent cells. There is evidence that suggests that conventional freezing downregulates the β1 integrin that is critical to attachment for hepatocytes (Terry et al. 2007).

2.5 Mathematical Modeling of Cryopreservation Processes

Significant amounts of modeling efforts have focused on the understanding of different processes in cryopreservation. Many of these reflect the challenges associated with the CPAs themselves and predicting their behavior. These range from the synthesis of phase diagrams (Han et al. 2010; Kleinhans and Mazur 2007) and mixing of CPAs (Kyrychenko and Dyubko 2008) to the prediction of critical cooling rates for different CPAs (Fan et al. 2007). Several studies have sought to understand the process of conventional freezing (Cui et al. 2002), or more specifically the issue of intracellular ice formation (Li and Liu 2010; Ross-Rodriguez et al. 2010). However, few have attempted to use simulations to gain insight into the vitrification process. In order to minimize the

CPA cytotoxicity experienced by cells, it is critical to address the addition and removal protocols. Cell membrane permeability is an important component of this and has been reviewed in the context of cryobiology by Kleinhans (Kleinhans 1998). More recently, this has been incorporated into a model describing the mass transfer and membrane permeation of CPAs for the vitrification of articular cartilage (Mukherjee et al. 2008). Mathematical models such as these allow for systematic design of protocols that minimize cell death due to excessive osmotic excursions.

2.6 Animal Model of Diabetes

There are many different animal models, although most *in vivo* studies begin with a small animal model. For the study of diabetes, this can be one of several commonly used models. Previous studies using βTC-tet cells, a murine insulinoma cell line, have shown success in an allogeneic host (Black et al. 2006). Therefore, it is desirable, when comparing methods of preservation for a tissue-engineered pancreatic substitute, to focus on a mouse model. Two main models have been used throughout literature to investigate diabetes: a streptozotocin (stz)-induced mouse model and a non-obese diabetic (NOD) mouse model. Streptozotocin is an alkylating drug that specifically targets and destroys the insulin-secreting β cells in the mouse. As stz is metabolized, it produces reactive oxygen species. Beta cells are particularly susceptible to oxidative changes. Oxidative stress has also been implicated in the mechanism of β-cell death in NOD mice (Morimoto et al. 2005). Rather than being induced, the NOD mouse exhibits a spontaneous occurrence of diabetes with 90% of female and 60% of male mice achieving a diabetic state between 12-30 weeks of age. This strain of mouse was developed by inbreeding and selecting for hyperglycemia. Due to this, the NOD mouse may also have specific

genes and phenotypes that may not be relevant to diabetes (Rees and Alcolado 2005). Additionally, NOD mice may not reflect human IDD as they can survive for weeks without the use of exogenous insulin.

CHAPTER 3

CYTOTOXICITY EFFECTS OF CRYOPROTECTANTS AS SINGLE-COMPONENT AND COCKTAIL VITRIFICATION SOLUTIONS[1]

Cryoprotectant (CPA) cytotoxicity constitutes a challenge in developing cryopreservation protocols, specifically in vitrification where high CPA concentrations are necessary to achieve the ice-free, vitreous state. Few cytotoxicity studies have investigated vitrification-relevant concentrations of CPAs, and the benefits and disadvantages of cocktail solutions and of incorporating non-permeating solutes have not been fully evaluated. In this study, we address these issues by determining the cytotoxicity kinetics for dimethylsulfoxide (DMSO) and 1,2-propanediol (PD) on alginate-encapsulated βTC-tet mouse insulinomas for a range of concentrations and temperatures. Cytotoxicity kinetics were also determined for two cocktails, DPS (3M DMSO + 3M PD + 0.5M sucrose) and P6 (1M DMSO + 5M PD + 0.34 M polyethylene glycol with M.W. of 400). PD was found to be more cytotoxic than DMSO at higher concentrations and temperatures. This was reflected in P6 being more cytotoxic at room temperature than P6 at 4^{o}C or DPS at either temperature. Addition of non-permeating solutes increased the cytotoxicity of cocktails. Furthermore, results indicate that CPA cytotoxicity may not be additive and that combining CPAs may increase cytotoxicity synergistically. Finally, when comparing cytotoxic effects towards encapsulated HepG2 and βTC-tet cells, and towards βTC-tet cells in capsules and in monolayers, CPAs appear more cytotoxic towards cells with higher metabolic activity. The incorporation of these

[1] This work is in press: Lawson, Ahmad & Sambanis (2011).Cryobiology. 10.1016/j.cryobiol.2011.01.012

results in the rational design of CPA addition/removal processes in vitrification is discussed.

3.1 Introduction

Within the field of Cryobiology, much work has been done to determine the cytotoxic effects of the cryoprotectant agents (CPAs) necessary for preservation. The cytotoxicity of CPAs has been shown to increase with time, temperature and concentration (Wang et al. 2007b). Cytotoxicity is especially critical for vitrification, which requires much higher concentrations of CPAs. Recently, vitrification has been touted by some to be the most promising method of preservation for tissues (Fahy et al. 2006) as well as tissue-engineered constructs (Kuleshova et al. 2007; Yin et al. 2009) due to the need to minimize or eliminate ice formation during preservation. Very few of the cytotoxicity studies available achieve the high concentrations of cryoprotectants necessary for successful vitrification (Wang et al. 2007b; Wusteman et al. 2002). To improve the vitrification process, several investigators have chosen to use cocktail solutions combining CPAs to achieve the necessary concentrations. These cocktails have gained widespread use for two reasons. The combination of different permeating and non-permeating CPAs has been shown to decrease the total concentration necessary to achieve successful vitrification (Petrenko et al. 2008; Sutton 1992). Also, the addition of non-permeating CPAs may improve the viability and function of the cells or tissues that are preserved (Beattie et al. 1997; Kuleshova et al. 1999; Li et al. 2006b). Some studies have focused on determining the predictability of vitrification (Shaw et al. 1997) and vitrification solution toxicity (Fahy et al. 2006; Fahy et al. 2004). However, few of these studies have directly compared the cocktail solutions to their individual CPA components

to determine if cytotoxicity may be additive or have synergistic effects to either reduce or increase cytotoxicity. Most that have investigated this have focused on the addition of additives that do not contribute to the overall glass-forming ability of the solution, such as amides (Fahy 2010; Fahy et al. 1987).

Additional questions that remain on the use of CPAs in cryopreservation include variations on CPA cytotoxicity towards different cell types or even the same cell in different types of culture. Evidence for these differences can be seen in a review of studies which range from the preservation of embryos (Kuleshova et al. 1999; Mukaida et al. 1998) to tissues (Elmoazzen et al. 2007; Wang et al. 2007b) or cells (Wusteman et al. 2002; Wusteman et al. 2008b). To our knowledge, although cytotoxicity studies have been carried out for many of these, no studies have investigated differences in cytotoxicity towards cells cultured in monolayers and cells in tissue constructs or a tissue itself.

In this study, we address these critical issues concerning the cytotoxicity of CPAs. Alginate-encapsulated mouse insulinoma βTC-tet cells were chosen for the majority of the experiments due to their use as a pancreatic substitute (Gross et al. 2007; Simpson et al. 2005). Cytotoxicity measurements were performed in a systematic way so as to investigate the effects of temperature, concentration and exposure time. Initial studies focused on single-component CPAs applied at concentrations of 2M to 6M in order to be relevant for both conventional freezing and vitrification. The cytotoxicity of cocktail CPAs with and without non-permeating solutes was compared to single-component CPAs. To address the effects of culturing method on cytotoxicity, the cytotoxic effects of CPAs towards βTC-tet cells in monolayers and in capsules were evaluated and compared.

Lastly, variations of CPA cytotoxicity towards different cell types were studied by comparing CPA effects on encapsulated HepG2 cells and βTC-tet insulinomas. Conclusions regarding fundamental issues of CPA cytotoxicity and the use of such systematic studies in designing optimized cryopreservation protocols are discussed.

3.2 Materials and Methods

3.2.1 Cell Culture

Mouse insulinoma βTC-tet cells were obtained from Dr. Efrat, Albert Einstein College of Medicine, Bronx, NY (Fleischer et al. 1998). Monolayer cultures were initiated from frozen stocks and propagated in T-flasks in complete growth medium consisting of Dulbecco's Modified Eagle's Medium (DMEM) (Sigma-Aldrich, St. Louis, MO) supplemented with 10% fetal bovine serum (Gemini Bioproducts, West Sacramento, CA), 1 % L-glutamine (Mediatech, Inc., Manassas, VA) and 1 % penicillin/streptomycin (Mediatech, Inc.). Monolayer human liver carcinoma HepG2 cells (American Type Culture Collection, Manassas, VA) were cultured in DMEM (Cellgro by Mediatech, Inc.) supplemented with 10% fetal bovine serum and 1% penicillin/streptomycin as above. Cells were incubated in a humidified incubator at 37°C and 5% CO_2 and were split at a ratio of 1:5 (βTC-tet) or 1:10 (HepG2) when 90% confluent. Experiments were performed with βTC-tet cells of passage 38-44 and with HepG2 cells of passage 18-23. For monolayer studies, βTC-tet cells were plated at a density of 500,000 cells/well in 24-well cell-culture treated plates (Corning Inc., Corning, NY). The cells were cultured as above for two days before cytotoxicity studies were performed.

3.2.2 Alginate Encapsulation

Encapsulation of βTC-tet and HepG2 cells was carried out using previously published protocols (Stabler et al. 2001), briefly as follows. Cells were detached from monolayer cultures by trypsinization (0.25% Trypsin-EDTA, Mediatech Cellgro) and suspended at a density of $3.0x10^7$ cells/ml of 2% sodium alginate (Pronova Ultra Pure LVM alginate NovaMatrix of FMC BioPolymer AS, Norway). An electrostatic droplet generator (Nisco Engineering AG, Zurich, Switzerland) was used to generate droplets which fell into a well-stirred 1.1% $CaCl_2$ bath, forming beads of gel containing entrapped cells. Complete growth medium was used to wash and store the beads. Beads were cultured overnight in a non-tissue culture treated T-flask on a rocker plate in a 37°C and 5% CO_2, humidified incubator. For cytotoxicity studies, beads were transferred to a 100 μm cell strainer (Becton-Dickinson, Franklin Lakes, NJ) and exposed to CPA solutions in a non-treated 6-well plates (Corning). Beads were agitated throughout CPA addition and removal except for the final addition step where they were agitated for 4 minutes regardless of incubation time.

3.2.3 CPA Solutions

Solutions for cytotoxicity studies were prepared using a concentrated and modified version of the EuroCollins carrier solution containing 174.76 g/L dextrose, 5.6 g/L KCl, 4.2 g/L $NaHCO_3$ and 8.2 g/L NaCl. This concentrated EuroCollins solution was diluted in the final solution volume at a ratio of 1:5. The cocktail solutions were DP6 (3M DMSO + 3M PD), DPS (3M DMSO + 3M PD + 0.5M Sucrose), P6 (1M DMSO + 5M PD + 0.34M polyethylene glycol with M.W. 400) and 5/1 (1M DMSO + 5M PD). All chemicals were purchased from Sigma-Aldrich except sucrose and $NaHCO_3$ (Fisher).

DP6 was compared to the complete solution, DPS, and 5/1 compared to the complete solution, P6, in order to investigate the effect of the non-permeating solutes. CPAs were added in a step-wise fashion. Protocols for addition and removal were designed using a previously established model (Mukherjee et al. 2007). Cells were incubated in the final solution for different times to determine the kinetics of cytotoxicity. Incubation times for other addition and removal steps remained constant for all solutions. The addition/removal protocols for cocktails and high concentration single-component CPA solutions are shown in Table 3.1. All addition steps were carried out at the indicated temperature (4°C or room temperature) and all removal steps were carried out at room temperature. Room temperature was 25°C ± 1°C, while 4°C was achieved by keeping solutions in an ice/water bath.

Table 3.1. Addition and removal protocols for 6M PD, 6M DMSO, DPS, PEG400, DP6 and 5/1. Sucrose is denoted S. Lower concentration single component CPAs were added and removed in the same manner: 2M was added in one step (A2) and removed in one step (R4), 4M was added in two steps (A2, A3) and removed in two steps (R3, R4). *Incubation in final addition step was changed to determine cytotoxicity kinetics.

Solution (M)	6M PD PD/S	6M DMSO DMSO/S	DPS DMSO/PD/S	P6 DMSO/PD/PEG	DP6 DMSO/PD/S	5/1 DMSO/PD/S	Time (min)
A1	--	--	--	0.25/1/0	--	--	4
A2	2/0	2/0	1/1/0.15	0.5/2/0.1	1/1/0	0.33/1.67/0	4
A3	4/0	4/0	2/2/0.3	0.75/3.5/0.2	2/2/0	0.67/3.33/0	4
A4	6/0	6/0	3/3/0.5	1/5/0.3384	3/3/0	1/5/0	15*
R1	--	--	2.25/2.25/0.3	0.75/4/0.2	--	--	2
R2	4/0.5	4/0.6	1.5/1.5/0.2	0.5/2/0.2	2/2/0.5	0.67/3.33/0.5	2
R3	2/0.25	2/0.35	0.75/0.75/0.1	0.25/1/0	1/1/0.25	0.33/1.67/0.3	2
R4	0/0	0/0	0/0/0	0/0/0	0/0/0	0/0/0	4

3.2.4 Metabolic Activity and Viability

To determine the metabolic activity of cells, 100 µL alginate beads or a cell monolayer were incubated with a solution of alamarBlue™ consisting of 100 µL alamarBlue™ and 1 mL complete growth medium in a 12 well plate for 3 hours (encapsulated βTC-tet cells), 4 hours (monolayer βTC-tet cells) or 1.5 hours (encapsulated HepG2 cells) in a 37°C and 5% CO_2, humidified incubator. Incubation times for alamarBlue™ were varied due to different cell number (encapsulated βTC-tet cells vs. monolayer βTC-tet cells) or metabolic activity of the cells (βTC-tet cells vs. HepG2 cells). With the selected incubation times, all assays fell within range wherein fluorescence was proportional to metabolic activity. A control consisting of 100 µL of alamarBlue™ and 1 mL medium was incubated for the same length of time. After this incubation, 100 µL supernatant from each well was transferred to a black 96 well plate and the fluorescence read using a SPECTRAMAX Gemini Fluorescent plate reader (Molecular Devices, Sunnyvale, CA) using an excitation wavelength of 544 nm and an emission wavelength of 590 nm. The data obtained from treated encapsulated cells using this assay were normalized to the data from untreated beads. For monolayers, the untreated control was subjected to the same number of washes as the test groups but was washed with complete growth medium. This was done to account for any detachment due simply to washing.

Cell viability was assessed using the dye exclusion stain Trypan Blue (0.4% Sigma). Beads were dissolved using 2% sodium citrate (Fisher). The resulting cell suspension was added to Trypan Blue in a 1:1 ratio and stained cells with compromised

membranes and non-stained cells were counted. Trypan blue-linked viability, henceforth referred to simply as viability, was normalized to the data from untreated beads.

3.2.5 Statistical Analysis

Although regression analysis is often used when considering time as a variable, the time points investigated were discrete and the data were collected from independent test groups. Therefore, statistical calculations were performed using a one-way ANOVA and Tukey's test to determine differences due to exposure time, temperature and concentration of CPA. For the comparison of single-component CPAs to cocktails, test groups were only compared to other test groups at the same temperature and exposure time. For comparisons of βTC-tet vs. HepG2 cells and of encapsulated cells vs. monolayers, statistical differences were evaluated only between cell type or culture method keeping all other variables the same. A p value of less than 0.05 was considered to indicate statistical difference.

3.3 Results and Discussion

CPA cytotoxicity is of particular concern in vitrification, which, to achieve the vitreous state, requires much higher CPA concentrations than conventional freezing. The chemical identity of the CPA used, the exposure time, temperature and concentration all play a role in the survival of cells during addition and removal procedures. Single-component CPAs and CPA cocktails were investigated to determine the role that these parameters play in the overall cytotoxicity of the solution. These studies were carried out with encapsulated βTC-tet cells. The same system was used to address the question of additivity of cytotoxicity in cocktail solutions relative to single-component CPAs. To

determine the effect of the mode of cell culture on CPA cytotoxicity, experiments were carried out with βTC-tet cells cultured in monolayers and in capsules. Finally, cytotoxicity studies were performed with encapsulated βTC-tet cells and encapsulated HepG2 cells to investigate the extent to which cytotoxic effects vary between cell types. Results are described and discussed below.

3.3.1 Single-Component CPAs

Results on the viability of encapsulated βTC-tet cells exposed to DMSO or PD for various times, at different concentrations, and at two temperatures, are shown in Figures 3.1 and 3.2. Pairwise comparisons were done for all groups and the results are shown in Table 3.2.

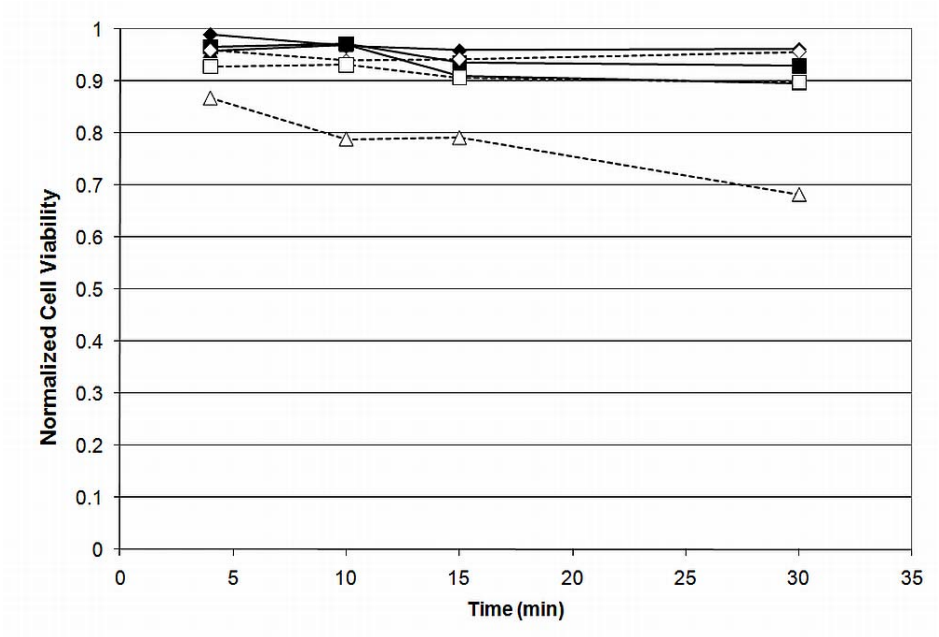

Figure 3.1. Cell viability vs. time for DMSO for 2M (—◆—), 4M (—■—) and 6M (—▲—) at 4°C or room temperature (empty) for encapsulated βTC-tet cells. Cell viability normalized to untreated control.

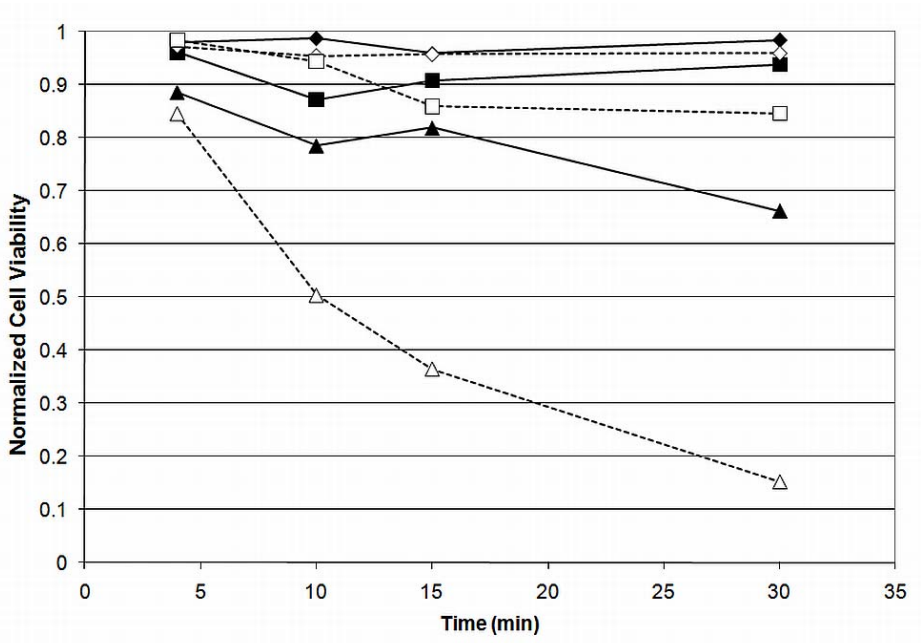

Figure 3.2. Cell viability vs. time for PD for 2M (—◆—), 4M (—■—) and 6M (—▲—) at 4°C or room temperature (empty) for encapsulated βTC-tet cells. Cell viability normalized to untreated control. Error bars not shown for clarity. Statistical significance shown in Table 2, *n=3*.

Table 3.2. Pairwise comparisons of single-component cytotoxicity kinetics. $p<0.05$ for corresponding letters (e.g. $p<0.05$ when comparing 2M and 6M DMSO at 30 minutes at room temperature, letter A)

Trypan blue-linked viability	Incubation at 4°C				Incubation at Room Temperature			
	4 min	10 min	15 min	30 min	4 min	10 min	15 min	30 min
2M DMSO	-	-	-	-	-	-	-	A
4M DMSO	-	-	-	-	-	-	-	-
6M DMSO	-	-	-	-	-	-	-	A
2M PD	-	-	-	S	L	J	G	D,E
4M PD	-	-	-	T	M	K	H	D,F
6M PD	U	V	B	C,S,T,U	L,M,N,O,P	V,J,K,N,Q	B,G,H,O,R	C,E,F,P,Q,R

As expected, cell viability generally decreased with an increase in time, temperature or concentration for either CPA. Viability decreased only slightly when cells were exposed to DMSO with the only significant decrease occurring at room temperature as concentration was increased from 2M to 6M with an incubation time of 30 minutes. The relatively high viabilities remaining after incubation in 6M DMSO at shorter incubation times also indicate that cell death due to osmotic excursions has been minimized. PD resulted in lower cell viabilities than DMSO at higher concentrations and temperature. Although cell viability did not decrease significantly over a change in temperature or time for incubation in 2M or 4M PD, incubation in 6M PD caused a significantly higher loss of viability, which increased with time and temperature. This is an indication that temperature control is much more important for PD than for DMSO. These results corroborate several previous studies which have shown that PD is more cytotoxic (Tsai et al. 2008; Wusteman et al. 2008b). It has been shown that temperature control during CPA addition and removal is critical for maintaining cell viability during vitrification (Pegg et al. 2006; Wang et al. 2007a). However, the importance of temperature control may vary with the identity of CPAs, alone or in cocktails. To our knowledge, these data are the first to show that PD cytotoxicity is more dependent on temperature than that of DMSO.

The metabolically active cell number measured by alamarBlue™ exhibited the same trends although it was consistently lower than viability and appeared to be more susceptible to the CPA cytotoxicity as concentration, time or temperature increased (results not shown). There are several possible reasons for this difference, the most likely being that exposure to CPAs lowers the metabolism of cells before compromising the

integrity of cell membranes. Indeed, studies with human hepatocytes (Stephenne et al. 2007) and other cell types (He and Woods 2004) indicate that cryopreservation reduces cellular metabolism, although it is unclear if this occurred because of the CPA exposure, the cooling/warming process, or both, as these studies investigated the aggregate effect. Another possibility for the difference in the assays is that exposure to the CPAs may activate apoptotic pathways, as demonstrated in porcine embryos (Rajaei et al. 2005). This may become evident in metabolic activity assays before causing a loss in membrane integrity. Additionally, the processes of vitrification (Rahimi et al. 2009) and conventional freezing (Baust et al. 2000; Heng et al. 2006) have both been shown to activate apoptosis, although again these studies evaluated the aggregate CPA addition/removal and cooling/warming effects. In our studies, direct apoptosis measurements were not performed. In several of the experiments, encapsulated cells subjected to CPA addition/removal were cultured for another day and the viability measured. This indirect measure indicated that no significant apoptosis occurred (APPENDIX). We chose to present Trypan blue-linked viability, rather than total metabolic activity, for the majority of the figures, as this is a more direct measure of cellular necrosis. Additionally, a depression in cellular metabolism may be reversible while the loss of membrane integrity necessary for Trypan blue to enter the cell is not.

3.3.2 CPA Cocktails

The toxicity kinetics for DPS and P6 were studied and compared (Figure 3.3). The toxicity of P6 was comparable to DPS at 4°C; however, P6 exhibited a much higher increase in toxicity as temperature was increased. In this case, statistical comparisons were made between P6 at room temperature and DPS at both temperatures as well as P6

at 4°C. Encapsulated cells exposed to P6 at room temperature had a statistically lower viability at each time point relative to P6 at 4°C or DPS at either temperature. These results indicate that temperature control is much more important for P6 than for DPS; they are also compatible with the single-component cytotoxicity results, as the concentration of PD is higher in P6 than DPS, resulting in the viability being more temperature-dependent for the P6 cocktail. On the other hand, the loss of cell viability caused by CPA cocktails was higher than the sum of cell viability loss caused by the pure CPAs at the concentrations found in the cocktail, with the latter obtained or estimated from Figures 3.1 and 3.2. Therefore, further experiments were carried out to directly compare the cytotoxicity of the single components to those of the cocktails without the non-permeating CPAs (DP6 and 5/1) and finally, to those of the full cocktails (DPS and P6). These studies were performed at a single incubation time (15 minutes) for the individual permeating CPAs as well as the cocktails.

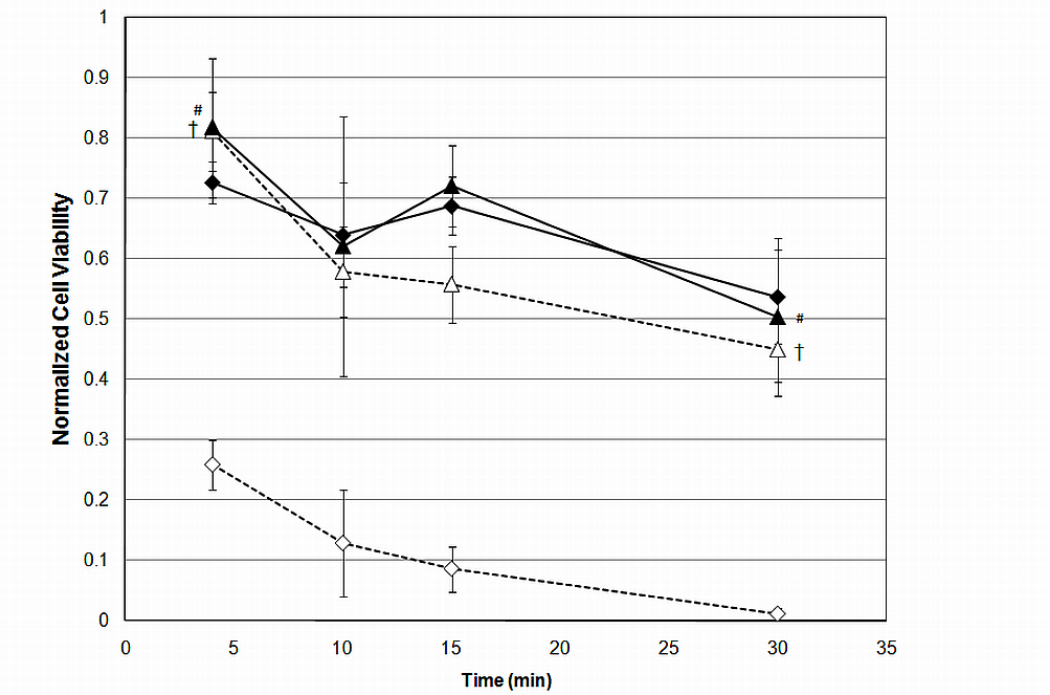

Figure 3.3. Cell viability vs. time for P6 (—◆—) and DPS (—▲—) at 4°C or room temperature (empty) for encapsulated βTC-tet cells. Cell viability normalized to untreated control. Error bars indicate standard deviations, *n=3*. #, † indicate $p<0.05$ when comparing groups. Additionally, $p<0.05$ when comparing P6 at RT to all other groups at each time point (not indicated for clarity).

Results from these studies are shown in Figures 3.4 and 3.5. These figures also show the "cumulative viability" values calculated as shown below using average viabilities at the corresponding temperature and concentration of each CPA in the cocktail (e.g., 3M PD and 3M DMSO viabilities used to determine "cumulative viability" for DP6). These values have no error bars and statistical significance is not indicated.

$$\text{Cumulative viability} = 1 - (1 - \text{viability}_{CPA1}) - (1 - \text{viability}_{CPA2})$$

It should also be noted that, in our hands, 6M PD, 6M DMSO, 5/1 and DP6 are not vitrifiable (as evidenced by macroscopic observation) and in order to consistently achieve

vitrification, non-permeating solutes need to be added. Addition of non-permeating solutes may allow for a reduction in the concentration of permeating CPA necessary to achieve vitrification (Kuleshova et al. 1999; Sutton 1992) and may inhibit ice formation during vitrification (Wang et al. 2009). Currently, non-permeating CPAs are considered to have little effect on or be beneficial for the overall solution cytotoxicity (Katenz et al. 2007; Petrenko et al. 2008; Rodrigues et al. 2008) and may stabilize cell membranes (Rudolph and Crowe 1985). However, those results were obtained with low concentrations of CPAs which may not be significantly toxic to cells. Our results show that the viabilities of cells exposed to complete cocktails were lower than those of cells exposed to incomplete cocktails, consisting only of the permeating CPAs, and the latter were closer to the cumulative viabilities. Although the introduction of a non-permeating solute may improve the consistency of solution vitrification, it resulted in an increase in cytotoxicity, the only exception being 5/1 relative to P6 at 4°C (Figure 3.5). A possible reason for this is that the addition of non-permeating CPAs results in an increase in the intracellular concentrations of permeating CPAs, as also predicted by membrane permeability models (Kleinhans 1998). Overall, it is important that the possibility of significantly increasing cytotoxicity be considered when adding non-permeating CPAs to solutions of permeating CPAs.

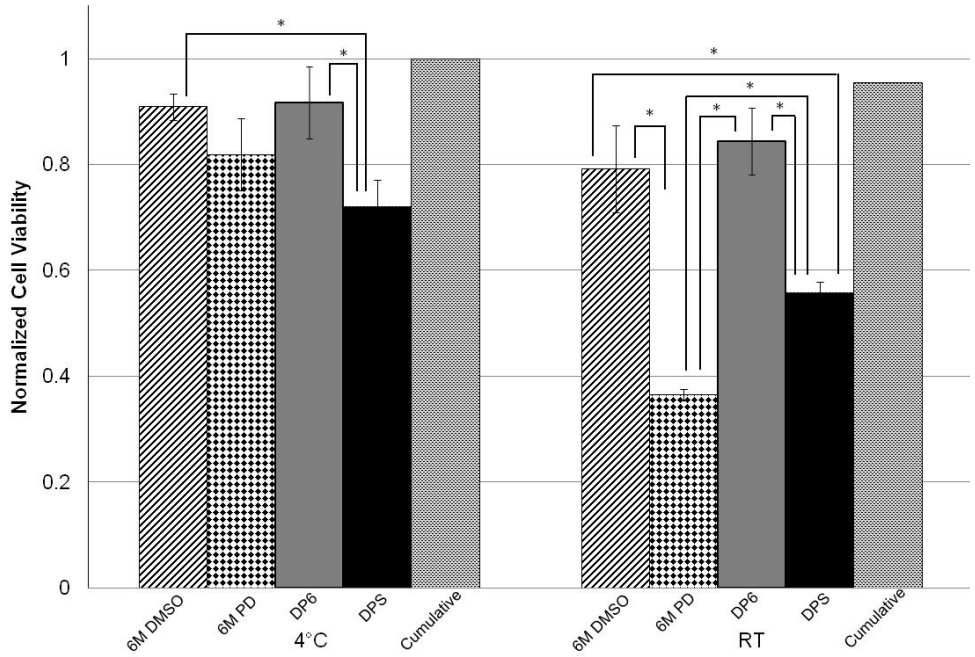

Figure 3.4. Cell viability for 6M DMSO, 6M PD, DP6 and DPS compared to "cumulative viability" for an incubation period of 15 minutes for encapsulated βTC-tet cells. Cell viability normalized to untreated control. Error bars indicate standard deviations, no error bars for cumulative viability, *n=3*. * indicates $p<0.05$

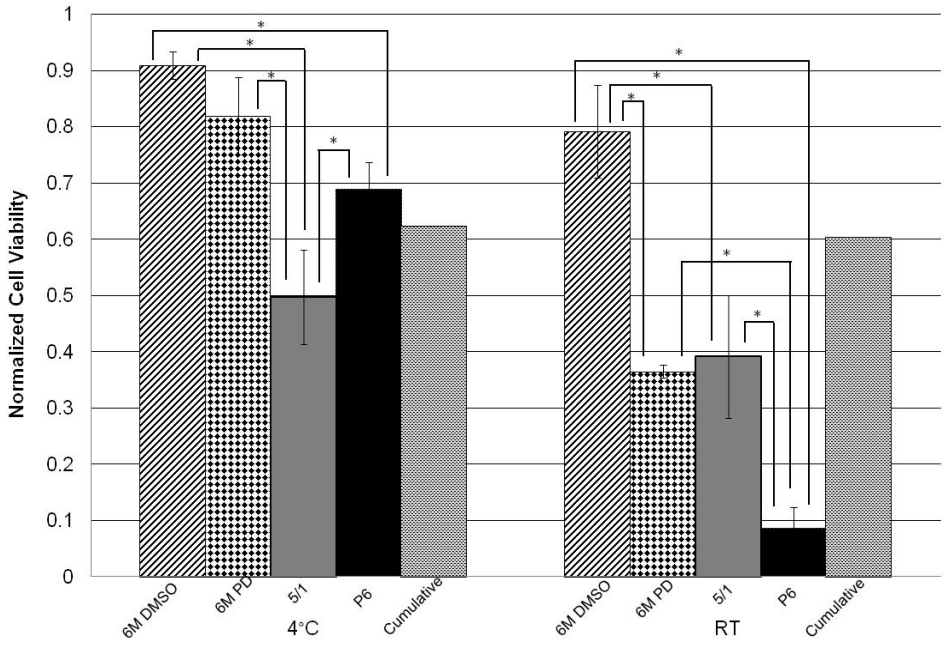

Figure 3.5. Cell viability for 6M DMSO, 6M PD, 5/1 and P6 compared to "cumulative viability" for an incubation period of 15 minutes for encapsulated βTC-tet cells. Cell viability normalized to untreated control. Error bars indicate standard deviations, no error bars for cumulative viability, *n=3*. * indicates $p<0.05$

Some interesting comments can also be made in comparing single-component cytotoxicity to that of cocktails. The less cytotoxic CPA, DMSO at 6M concentration, resulted in comparable or higher viabilities relative to cocktail solutions at either temperature. This was also the case for 6M PD at 4°C. However, at room temperature 6M PD performed worse than DP6 and DPS and was comparable to 5/1, as expected given that 5/1 is mostly PD. However, addition of the non-permeating PEG in forming P6 significantly increased the cytotoxicity of the latter relative to 6M PD and 5/1. These results suggest that the presence of PD at a high concentration in a cocktail affects the temperature dependence significantly.

Notably, P6 and 5/1 performed differently at the two temperatures, with P6 being less cytotoxic than 5/1 at 4°C but more cytotoxic at room temperature. The increase in cytotoxicity at room temperature is likely due to the decreased intracellular water content as discussed above. The difference at 4°C might be due to the protective effect of non-permeating solutes cited in several publications (Katenz et al. 2007; Petrenko et al. 2008; Rodrigues et al. 2008; Rudolph and Crowe 1985). These results therefore suggest that the protective effect of non-permeating CPAs is present at low temperatures, but it is outweighed by the negative osmotic effects at higher temperatures.

As seen in Figures 3.4 and 3.5, the cumulative viabilities appear higher than those obtained with the incomplete cocktails. This suggests that CPA cocktail cytotoxicity may not be additive and that combining CPAs may have a synergistic effect, causing increased cytotoxicity.

3.3.3 Comparison of Culturing Method

Figure 3.6 shows the normalized number of metabolically active cells, measured by alamarBlue™ for βTC-tet cells in suspension within an alginate matrix and in monolayers exposed to different CPAs at 4°C and room temperature for 15 min. It appears that the cells in a monolayer fare better than encapsulated cells at low temperatures and concentrations while they experience more cytotoxicity at higher CPA concentrations (DP6) and higher temperature.

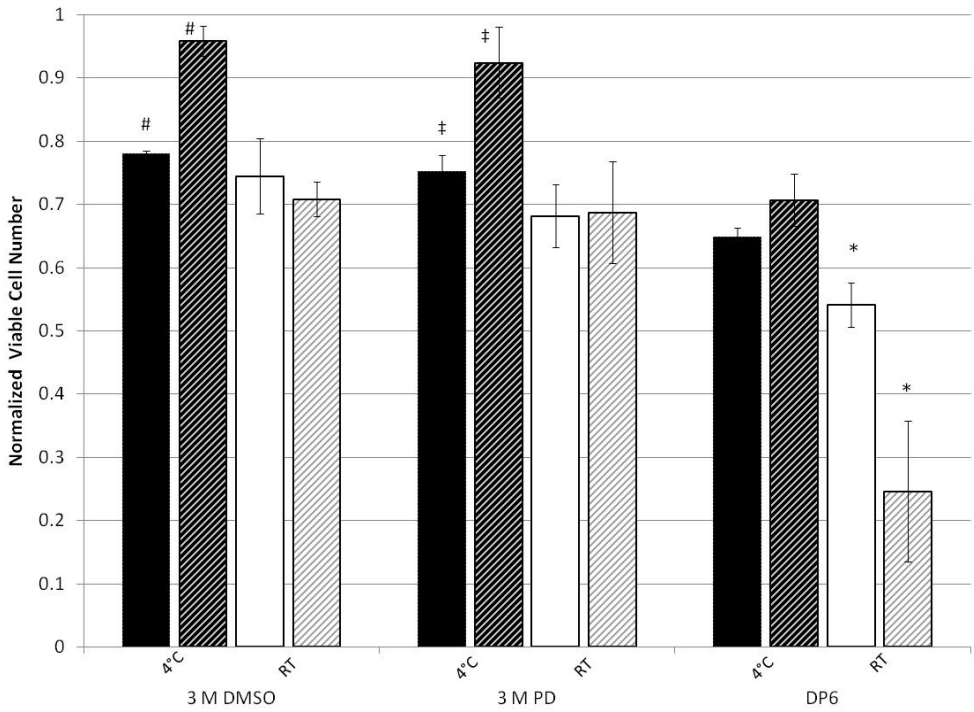

Figure 3.6. Viable cell number for 3M DMSO, 3M PD and DP6 for monolayer βTC-tet cells (stripes) compared to encapsulated βTC-tet cells (solids) for an incubation period of 15 minutes. Viable cell number determined by alamarBlue™, normalized to untreated control. Error bars indicate standard deviations, *n=3*. *, # indicates $p<0.05$.

There are several differences between the two systems that may explain these results. The most obvious difference is that there is a short period of time necessary for diffusion of the CPAs towards the center of the alginate bead. Previous studies (Mukherjee 2008) investigated the diffusion of different CPAs into and out of alginate beads at room temperature. Those results, also temperature-corrected for diffusion at 4°C, indicate that equilibration is essentially reached within two to three minutes at either temperature, which is negligible given the exposure time of 15 minutes. Hence, diffusional resistance is an unlikely cause of the observed difference. Additionally, the cytotoxicity experienced by the encapsulated cells is not consistently lower due to a shorter exposure time. Another difference between the two systems is the culture itself. βTC-tet cells encapsulated in alginate are suspended whereas those in a monolayer are adhered to the tissue culture surface. This difference is the most likely cause for the results as studies investigating the metabolism of a similar cell line, βTC3 murine insulinomas, have shown that the metabolism of monolayers is significantly higher than encapsulated cells (Simpson et al. 2006). This increase in metabolism would cause an increase in the cytotoxic effects at room temperature and higher concentrations. At the lower temperature, the effects of higher metabolism are tempered as metabolism is significantly depressed (Belzer 1988). These effects would also be less noticeable at lower concentrations where the CPAs are less cytotoxic. The reason for the differences at lower temperatures is less clear. It might be that the results showing that monolayers experience less cytotoxicity when exposed to a lower concentration of CPAs at a lower temperature is actually a reflection of the control group that was used for normalization. The control monolayer group was subjected to the maximum number of washes,

corresponding to the number of washes used in the addition and removal for DP6, albeit with supplemented DMEM. These extra washes may have caused some detachment of living cells which then resulted in artificially high normalized viability. This difference would not be seen at room temperature where the metabolism, and possibly attachment, is higher. These data indicate that monolayer cytotoxicity studies may not be directly applicable to the same cells in suspension, seeded in a construct, or present in a natural tissue.

3.3.4 Comparison of Cell Type

The cytotoxic effects of DMSO, PD and DP6 on encapsulated βTC-tet and HepG2 cells were determined for an incubation period of 15 minutes at 4°C and room temperature. Results on the normalized cell viability measured by Trypan Blue are shown in Figure 3.7. The cytotoxicity of the single-components is very similar between the two cell types. However, the cocktail solution DP6 had a much higher cytotoxicity towards HepG2 than βTC-tet cells at room temperature. This is likely due to the difference in metabolism and the rate of cell growth between the two cell lines. βTC-tet cells encapsulated in 2% LVM alginate double in approximately two weeks (Simpson et al. 2005) while HepG2s encapsulated in 1% LVM alginate triple in ten days (Chin et al. 2008). Despite the small differences in alginate concentration, it is expected that the HepG2 cells are more metabolically active than βTC-tet cells. This is similar to what was observed when comparing monolayers and encapsulated cells and indicates that cytotoxicity likely increases as the metabolism of the cells is higher.

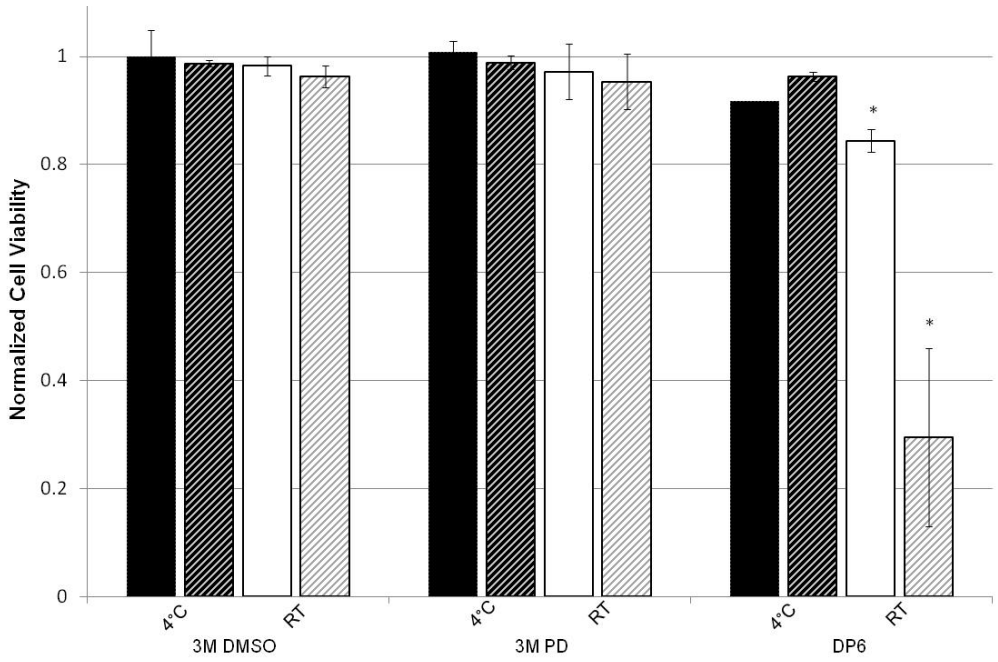

Figure 3.7. Cell viability for 3M DMSO, 3M PD and DP6 for encapsulated βTC-tet cells (solids) compared to encapsulated HepG2 cells (stripes) for an incubation period of 15 minutes. Cell viability normalized to untreated control. Error bars indicate standard deviations, *n=3*. * indicates $p<0.05$

3.4 Summary

Our studies determined the cytotoxicity kinetics on encapsulated βTC-tet cells of two commonly used CPAs, DMSO and PD, at different concentrations and two temperatures. Studies were extended to investigate the additivity of CPA cytotoxicity in cocktail solutions. Results generally agree with the literature but allow insight into the importance of temperature control and the use of CPA cocktails. Although it may be beneficial to add non-permeating solutes to cocktails to improve their ability to vitrify, this addition may not be as innocuous as previously thought. The importance of temperature control varies between CPAs and CPA cocktails and is more critical for cells with higher metabolism, either due to cell type or culturing method.

CHAPTER 4

MATHEMATICAL MODELING OF CRYOPROTECTANT ADDITION AND REMOVAL FOR THE CRYOPRESERVATION OF ENGINEERED OR NATURAL TISSUES

Long-term storage of natural tissues or tissue-engineered constructs is critical to allow off-the-shelf availability. Vitrification is a method of cryopreservation that eliminates ice formation, which may be detrimental to the function of the tissue or construct. In order to achieve the vitreous, or glassy, state, high concentrations of CPAs must be added and later removed. Such high concentrations of CPAs may be deleterious to cells as the CPAs are cytotoxic and single-step addition or removal will result in excessive osmotic excursions and cell death. A previously described mathematical model accounting for the mass transfer of CPAs through the sample matrix and cell membrane was expanded to incorporate heat transfer and CPA cytotoxicity. Simulations were performed for two systems, an encapsulated system of insulin-secreting cells and articular cartilage, each with different transport properties, geometry and size. Both cytotoxicity and mass transfer are highly dependent upon temperature, with increased temperature allowing more rapid mass transfer but also causing an increase in cytotoxicity. The effects of temperature are exacerbated for articular cartilage, which has a larger dimension and slower mass transport through the matrix. Simulations indicate that addition and removal at 4°C is preferable to 25°C, as cell death is higher at the latter temperature due to the increased cytotoxicity in spite of the faster mass transport. Additionally, the model indicates that less cytotoxic CPAs, especially at high

temperature, would significantly improve the cryopreservation outcome. Overall, the mathematical model allows the design of addition and removal protocols that ensure CPA equilibration throughout the sample while still minimizing CPA exposure and maximizing cell survival.

4.1 Introduction

Significant progress has been made in the field of Tissue Engineering to develop and design novel constructs for the repair, replacement or regeneration of certain tissues or organs. However, cryopreservation technologies are often overlooked until a construct is very close to being clinically available. The preservation of these constructs during manufacturing processes and transport is critical in bringing these constructs to off-the-shelf, clinical use (Karlsson and Toner 1996; Sambanis 2000). The need for preservation also extends to natural tissues which are in limited supply. Cryopreservation may be relatively simple for cells in suspension, but the addition of a three dimensional matrix, as in a construct or natural tissue, introduces resistance to heat and mass transport (Karlsson and Toner 1996). Therefore, cryopreservation of tissue-engineered constructs or natural tissues is rarely straight-forward and often requires significant experimental work to achieve success. Ice formation is also a critical issue as it has been shown to be detrimental to the mechanical properties of both tissue-engineered constructs (Dahl et al. 2006) and natural tissues (Thakrar et al. 2006). Vitrification, or ice-free cryopreservation appears to be the most promising method of preservation (Kuleshova et al. 2007). Vitrification requires high concentrations of cryoprotective agents (CPAs) and rapid cooling and warming to achieve a vitreous, or glassy, state. This method eliminates the problem of ice formation both within the cell and in the extracellular matrix (Brockbank

et al. 2003). Generally, the high concentrations of CPAs in vitrification are achieved using a CPA cocktail solution which is added and removed using multi-step protocols to minimize cellular osmotic excursions. Samples are rapidly cooled and stored in the vitreous state before warming and eventual use.

A significant amount of theoretical work has been done to better understand cryopreservation. Many of the previous studies have focused on the understanding of the cooling and warming of the sample during conventional freezing. More specifically, these efforts cover important issues such as intracellular ice formation (Li and Liu 2010; Ross-Rodriguez et al. 2010), solute interactions (Kyrychenko and Dyubko 2008), effects of temperature on cell membrane function (Dragomir and Pausescu 1974) and synthetic phase diagrams (Han et al. 2010). While theoretical studies are important in gaining fundamental understanding, very little work has been done to investigate the methods of vitrification. Vitrification requires rapid cooling and warming, but these rates are primarily dictated by the critical cooling and warming rates necessary for the solution to achieve a glassy state. There is therefore little room for improvement. Little theoretical work has been done to address the other critical issue of vitrification, which is the addition and removal of CPAs and their effect on cells, constructs or natural tissues. A review of current vitrification literature reveals different CPAs and CPA cocktails being used to varying effect. Without better understanding of the addition and removal protocol, the preservation of tissue-engineered constructs or natural tissues will remain difficult. A successful protocol will achieve full equilibration of the CPA or CPA cocktail throughout the sample to ensure successful vitrification, while minimizing osmotic excursions and CPA-induced cytotoxicity; the latter is dependent on the CPA

identity and concentration as well as the exposure time and temperature (Lawson et al. 2011).

To address all of these complexities, a previously published mathematical model (Mukherjee et al. 2008) of mass transfer through the extracellular matrix and cellular membrane was expanded to incorporate heat transfer and CPA cytotoxicity. This model describes the CPA addition followed by immediate removal and does not consider the rapid cooling, storage or warming that would occur during vitrification. Addition and removal protocols were designed to maintain osmotic excursions of the cells within tolerable limits and achieve CPA equilibrium throughout the entire construct. The temperature and duration of addition and removal steps were varied to determine their effects on cytotoxicity. In order to gain additional insight, these simulations were carried out for two systems with different transport properties, geometry and size. The first system modeled was an encapsulated cell system of spherical geometry that is small in size (500 μm in diameter) and in which the matrix poses little resistance to mass transfer, exhibiting CPA diffusivities equal to approximately 80% of those in water (Mukherjee et al. 2007). The second system was based on articular cartilage of slab geometry, a tissue that is notoriously difficult to cryopreserve (Brockbank et al. 2010; Jomha et al. 2002; Pegg et al. 2006). This system had larger dimensions with a clinically relevant overall thickness of 2 mm and significantly higher resistance to mass transfer with CPA diffusivities close to 30% of those in water (Mukherjee et al. 2008). These two systems were chosen to cover a broad range of tissues and tissue-engineered constructs and the results provide insight into the design of CPA addition and removal protocols.

4.2 Mathematical Modeling

A two-compartment mathematical model, previously described for articular cartilage, (Mukherjee et al. 2008) was used to characterize the transport of CPAs through a hydrogel matrix in spherical geometry (shown in Figure 4.1) and across the cell membrane of βTC-tet cells in an encapsulated system. MATLAB software (MathWorks, Natick, MA) was used to couple the two compartments. Heat transfer and an additional equation describing the cytotoxicity kinetics of the βTC-tet cells in the presence of CPAs were incorporated into the mathematical model. The same model structure was also used to describe another system: articular cartilage of slab geometry. The parameters used for simulations are shown in Table 4.1. Chondrocytes, as would be present in articular cartilage, were assumed to have the same parameters as βTC-tet cells. Additionally, the dependence of diffusivity and cell permeability on temperature were assumed to follow the Arrhenius relationship (similar to equation 15).

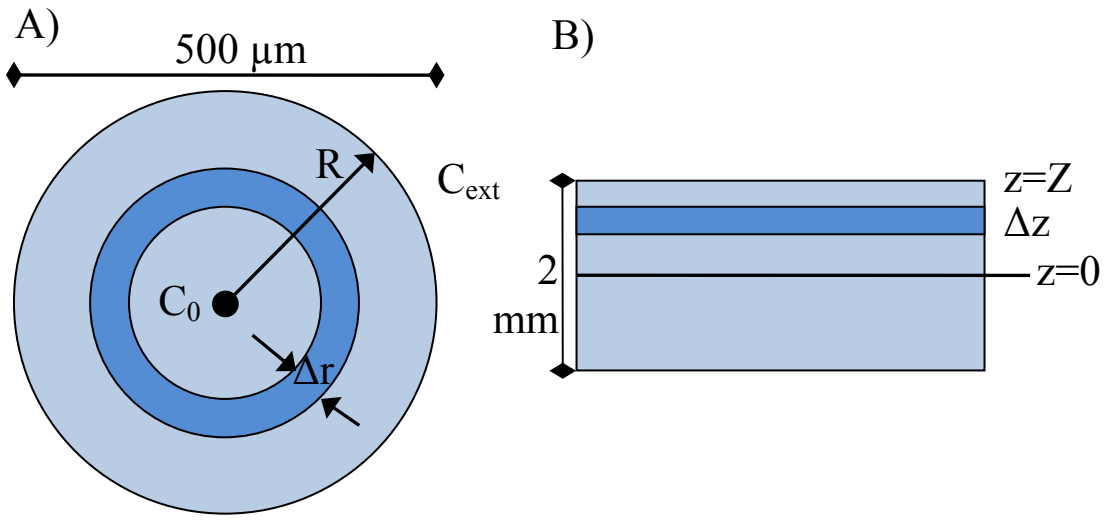

Figure 4.1. Schematic for A) alginate bead and B) articular cartilage.

Table 4.1 Values of model parameters used in this study for mass and heat transfer, permeability & cytotoxicity. Cell permeability parameters and cytotoxicity parameters were the same for both cell types. Water permeability values (L_p) were higher for DMSO than for PD and were used for all simulations.

	D_{eff}/D_{bulk}	α ($\mu m^2/s$)	L_p (A) (μm/min atm)	L_p (E_a) (cal/mol)	P_s (A) (μm/s)	P_s (E_a) (cal/mol)	B $(mol/kg)^{-1}$	b (L/mol min)	d (K)	f (L/mol)
Alginate	0.8	1.46E11	--	--	--	--	--	--	--	--
Cartilage	0.3	1.32E5	--	--	--	--	--	--	--	--
DMSO	--	--	6.67E-4	15400	4.73E-2	14100	0.0843	2.0E4	4270	0.08
PD	--	--	--	--	5.81E-2	14600	0.0576	1.2E5	4930	0.17

4.2.1 CPA Transport and Heat Transfer through Matrix

Effective diffusivities were previously determined for CPAs through 2% calcium-alginate beads (Mukherjee 2008) and through articular cartilage (Mukherjee et al. 2008). These values are given in Table 4.1. Thermal diffusivity for 2% calcium-alginate beads was assumed to be that of water (Bird et al. 2002). A value from literature for the thermal diffusivity of nasal septal cartilage was used to approximate this parameter value for articular cartilage. Although these tissues are different, the thermal properties for biological tissues, ranging from skeletal muscle to cardiac tissue, are of the same order of magnitude as the approximate thermal diffusivity used in this study for cartilage and it is therefore an acceptable approximation (Youn et al. 2000). The values for both of these parameters are also given in Table 4.1.

4.2.2 Model Assumptions

The following assumptions were incorporated in developing the model equations for the two types of tissue considered.

1) No CPA reaction or consumption by the cells or matrix.
2) Homogenous cell distribution throughout matrix. This is a good assumption for freshly encapsulated cells and immature cartilage which are both relatively homogenous (Jadin et al. 2005)
3) Effective diffusivities and thermal diffusivities are isotropic.
4) Cell membrane permeability values are only affected by a change in temperature and are independent of CPA concentration.
5) No solute-solute interactions for multi-solute CPA transport across cell membrane or in matrix.

Mass transport through the spherical alginate matrix is described in equation 1 below. In this equation, C = CPA concentration (mol/L), r = radial position (μm) and D_{eff} = effective diffusivity (μm^2/s).

$$\frac{\partial C}{\partial t} = D_{eff}\left[\frac{1}{r^2}\frac{\partial}{\partial r}\left(r^2\frac{\partial C}{\partial r}\right)\right] \quad (1)$$

The initial and boundary conditions used to solve equation 1 are as follows:

$C(r, t=0) = 0$ (no CPA initially present in the matrix) (2)

$C(r=R, t) = C_{external}$ (CPA concentration at the bead radius, R, is equal to the external concentration in the bulk liquid, i.e. no boundary layer and partition coefficient of 1) (3)

$\frac{\partial C}{\partial r}(r=0,t) = 0$ (symmetry at the center of the bead) (4)

Mass transport through the slab geometry of articular cartilage is described in equation 5. Initial and boundary conditions are similar to equations 2-4.

$$\frac{\partial C}{\partial t} = D_{eff}\left[\frac{\partial^2 C}{\partial z^2}\right] \tag{5}$$

Heat transfer through the spherical alginate matrix is analogous to mass transport as described in equation 1 and is shown in equation 6. Equation 7 describes heat transfer through the slab geometry. In both equations, α = thermal diffusivity (μm^2/s) and T = temperature (K).

$$\frac{\partial T}{\partial t} = \alpha\left[\frac{1}{r^2}\frac{\partial}{\partial r}\left(r^2\frac{\partial T}{\partial r}\right)\right] \tag{6}$$

$$\frac{\partial T}{\partial t} = \alpha\left[\frac{\partial^2 T}{\partial z^2}\right] \tag{7}$$

Initial and boundary conditions for the heat transfer equations (equation 6 & 7) are similar to those for mass transport and are shown for the slab geometry (equation 7).

$T(z, t=0) = T_0$ (articular cartilage at initial temperature, T_0) (8)

$T(z=Z, t) = T_{external}$ (temperature at the slab edge, Z, (9)

is equal to the external temperature in the bulk liquid)

$\frac{\partial T}{\partial z}(z=0,t) = 0$ (symmetry at the center of the slab) (10)

4.2.3 CPA Transport across Cell Membrane

Parameters for βTC-tet cell membrane permeabilities were previously determined (Mukherjee et al. 2007). A two-parameter formalism with modifications was used to

describe solute transport across the cell membrane (Kleinhans 1998). This is described in equations 11 and 12.

$$\frac{dV_w}{dt} = -L_p ART\left(M^e - M^i\right) \tag{11}$$

$$\frac{dN_{si}}{dt} = P_s A\left(M_{si}^e - M_{si}^i\right) \tag{12}$$

Equation 11 describes the water flux through the cell membrane while equation 12 describes the solute flux. In these equations, V_w (μm^3) is the volume of water inside the cell, L_p ($\mu m/s \cdot atm$) is the water permeability, A(μm^2) is the cell surface area, R ($\mu m^3 \cdot atm/mol \cdot K$) is the gas constant, T (K) is the absolute temperature, M^e and M^i (osmoles/μm^3) are the total external and internal osmotic concentrations, respectively, P_s ($\mu m/s$) is the i^{th} solute permeability, N_{si} (osmoles) is the intracellular amount of the i^{th} solute and M_{si}^e and M_{si}^i (osmoles/μm^3) are the external and internal osmotic concentrations for the i^{th} solute, respectively. M^e and M^i were determined using the osmotic virial equation (Eqn 13) and parameters published by Prickett (Prickett et al. 2010) (shown in Table 4.1). In equation 13, π is the osmolality of the solution (osmole/kg solvent), m_i is the molal concentration (moles solute/ kg solvent), and B is the osmotic virial coefficient (kg solvent/moles solute). Osmolality was then converted to osmolarity for use in the permeability equations.

$$\pi = m_i + B_i m_i^2 \tag{13}$$

4.2.4 Cytotoxicity Kinetics

CPA cytotoxicity is governed by the time and temperature of exposure, CPA identity and concentration. Chemical and thermal cytotoxicity experienced by cells has been well characterized in the field of sterilization. First-order kinetics are often used

(shown in equation 14), although these kinetics indicate that the reaction rate constant is independent of time which may not be the case in a biological system.

$$\frac{dn}{dt} = -k_d n \tag{14}$$

If the cells within the system are not homogenous, some being more robust than others, this should be reflected in the cytotoxicity kinetics. These states of varying resistance to CPA toxicity could be described as a continuous distribution of states in the cell population. In order to appropriately reflect this in a system, the subpopulations would need to be isolated and the rate constant determined for each. Alternatively, work done by Peleg, et al. suggests that the reaction rate constant could be made dependent on time (Peleg and Normand 2004). This method is shown in equations 15 and 16. If the exponent *m* is greater than 1, this indicates that cells are progressively weakened due to exposure. Based on previous experimental work (Lawson et al. 2011), the exponent for encapsulated βTC-tet cells is less than 1, indicating that cells that are more susceptible to cytotoxicity are killed first, leaving more robust cells. Although this is not a mechanistic model, it was chosen for the sake of simplicity. The reaction rate constant also is dependent on temperature (Arrhenius relationship) as seen in equation 16.

$$\frac{n}{n_o} = \exp\left(-\frac{1}{m}k_d t\right) \tag{15}$$

$$k_d = A\exp\left(-E/RT\right)t^{m-1} \tag{16}$$

Work done by Char (Char et al. 2010) on sterilization that combines temperature and chemical cytotoxicity indicates that the concentration of the chemical affects the parameter *A*, as well as the exponent *m*. Therefore, the pre-exponential factor in equation 16, *A,* was replaced by *bmC,* where *b* is an experimentally fit parameter and *C* is CPA

concentration. Additionally, *E/R* is replaced by an experimentally fit parameter, *d*. Finally, the exponent *m* is replaced by *fC* where *f* is an experimentally fit parameter. Equation 17 is the result. This equation was fit to previously published experimental cytotoxicity data to determine all parameters (Lawson et al. 2011).

$$\frac{n}{n_o} = \exp\left(-b * C * \exp\left(-d / T\right)\ t^{fC}\right) \tag{17}$$

In this equation, n is viable cell number, n_o is initial viable cell number, resulting in a survival curve in terms of normalized viable cell number. Additionally, C is concentration in mol/L, T is temperature in Kelvin, t is time in minutes and b, d and f have units of L/(mol*min), K, and L/mol, respectively. Figure 4.2 shows experimental data in comparison to the fitted cytotoxicity equation. Parameters were determined by least squares fit using Microsoft® Excel® Solver and parameter values are shown in Table 4.1.

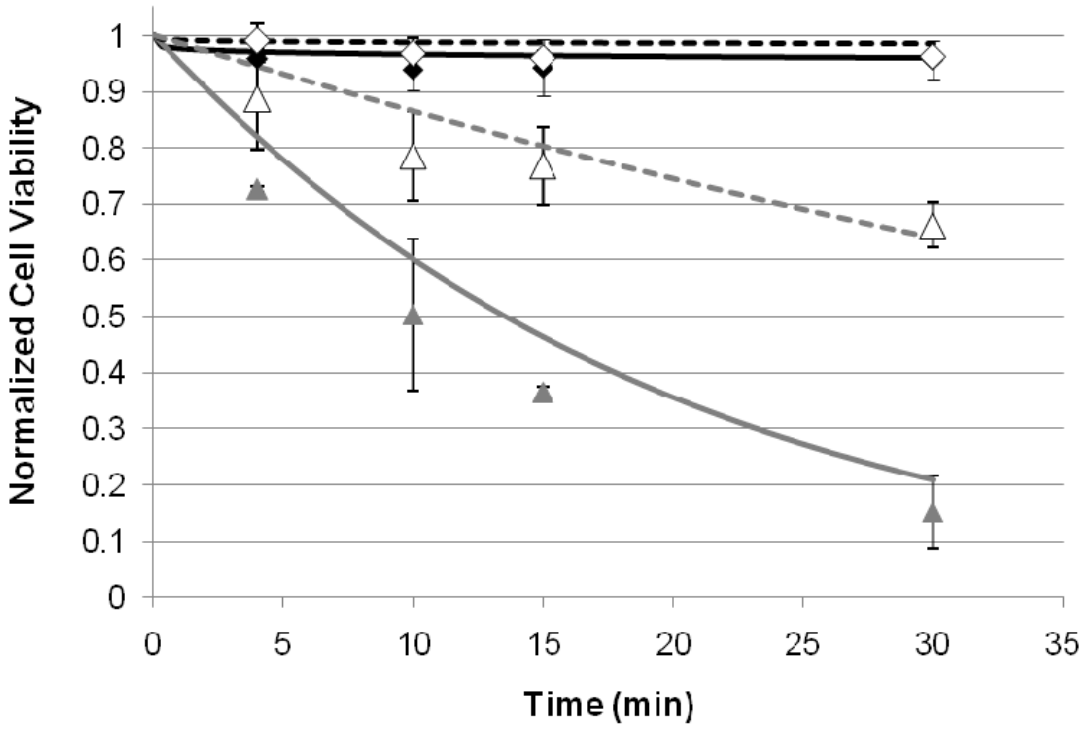

Figure 4.2. Comparison of cytotoxicity equation, equation 17, (lines) with experimentally determined normalized cell viability (n/n_0) (data points) for 2M DMSO (black, diamond) or 6M PD (gray, triangle) with addition steps carried out at 25°C (solid) or 4°C (empty points, dashed line).

4.3. Results

4.3.1 Heat Transfer

Heat transfer was incorporated into the mathematical model for two reasons. Previously, the assumption was made that heat transfer would be very rapid compared to mass transfer (Mukherjee et al. 2008). It was necessary to confirm this. If not, then it might have been beneficial to add CPAs as the sample was cooled to minimize cytotoxicity. Figure 4.3 shows the temperature profile for different positions throughout the articular cartilage slab in response to step changes in temperature at the edge of the slab. The slab geometry of articular cartilage was chosen as a "worst-case" scenario due

to the large dimension and slower thermal diffusivity. Step changes were simulated from 37°C (physiological) to 25°C (approximate room temperature), 25°C to 4°C (ice water bath) and 4°C to -20°C (freezer). Even for the largest of these step changes, 4°C to -20°C, the target temperature is achieved throughout the slab within approximately 10 seconds. The time necessary for heat transfer is therefore negligible compared to the time necessary for mass transfer which is 40-80 minutes (see Figure 4.6). Hence, all other simulations were performed isothermally.

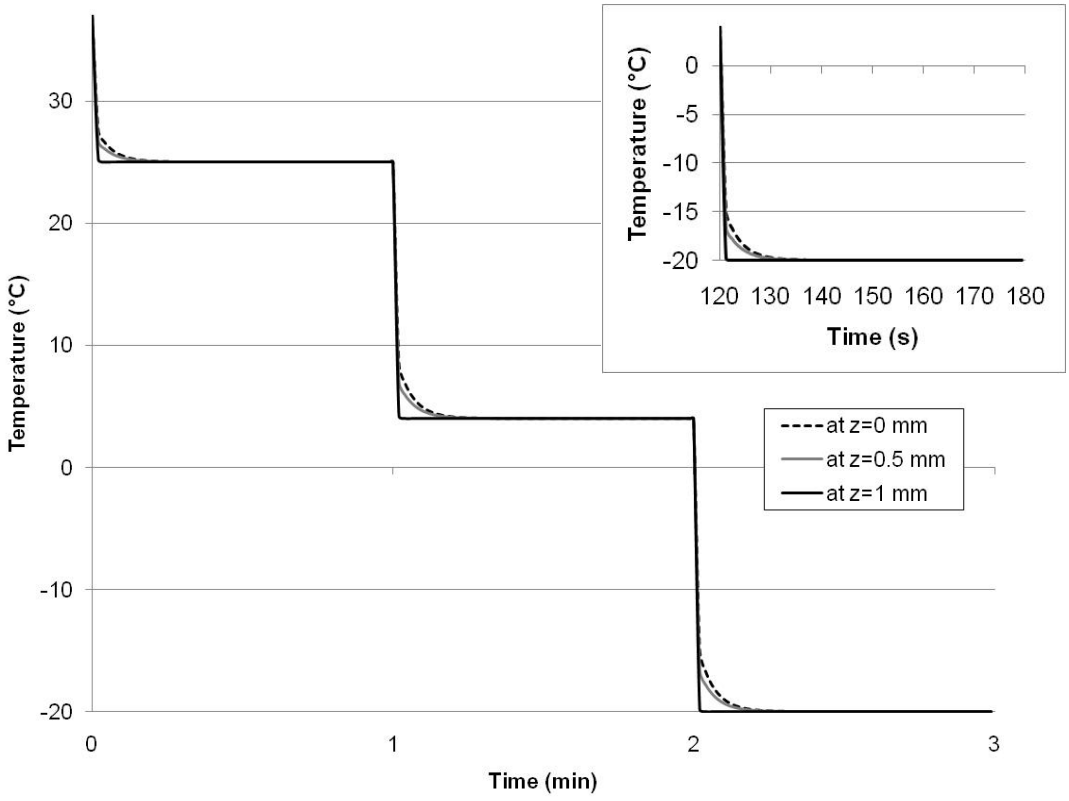

Figure 4.3. Temperature profile at center of slab (z=0), midway through slab (z=0.5mm), and at edge of slab (z=1) in response to temperature step changes at the edge of the slab.

4.3.2 Mass Transfer through Alginate Bead

The case of the alginate bead presents little resistance to mass or heat transfer. To be vitrification-relevant, a vitrification solution consisting of dimethyl sulfoxide (DMSO), propanediol (PD) and polyethylene glycol was used. The standard addition and removal protocol is given in Table 4.2. This protocol was designed to ensure that the osmotic excursions experienced by the cells within the matrix remained within the tolerable range as determined for βTC-tet cells previously (Mukherjee et al. 2007).

Table 4.2. Simulated addition and removal protocol for alginate beads. All removal steps were carried out at 25°C. Addition and removal exposure times were lengthened for simulations of articular cartilage.

	Components (M)			Time (min)	Temperature (°C)
Step	PEG400	PD	DMSO		
A1	0	1	0.5	3	4 or 25
A2	0	2	1	3	4 or 25
A3	0	4	1	3	4 or 25
A4	0.3384	5	1	3	4 or 25
R1	0.2	4	0.75	2	25
R2	0.2	2	0.5	2	25
R3	0	1	0.25	2	25
R4	0	0	0	5	25

Figure 4.4A shows results for 4°C or 25°C addition with all removal steps occurring at 25°C. The viable cell number at the edge of the bead is shown because cells at the edge are exposed to the CPAs longer than those at the center. This position serves as a "worst-case" scenario although viable cell number varies little (~2%) over the radius of the bead due to the small dimension (diameter of 500 μm) and high diffusivity. These results indicate that temperature has a significant effect on the CPA cytotoxicity experienced by βTC-tet cells at relatively short timescales. These short timescales are well within the experimental timescales used to determine the cytotoxicity equation parameters. As such, they are a direct reflection of experiment and are interpolated rather than extrapolated from experimental data. Additionally, removal at room temperature causes a greater loss in viable cell number (~3%) when addition occurred at 4°C than when addition occurred at room temperature (<1%) as shown in Figure 4.4. This difference is relatively small and indicates that the temperature of removal may not be as critical for constructs that exhibit rapid mass transfer. The minimal loss in viable cell number that occurs during removal when all exposure is carried out at 25°C indicates that the more susceptible cells die during the addition steps leaving more robust cells behind. Figure 4.4B shows the concentration of CPA at the center of the bead during addition and removal. Achieving or approaching equilibration of CPAs is critical to the success of vitrification. The temperature of addition and removal significantly affects the amount of time necessary to achieve full equilibration. At a higher temperature, equilibration occurs much more quickly, allowing shorter incubation times and decreasing the cell's exposure to CPAs during addition and removal. Cell viability at the edge of the bead for different exposure times is shown in Figure 4.5. Due to faster mass transport at 25°C,

equilibration through the bead occurs within 1.5 minutes/step as opposed to 3 minutes/step at 4°C. A direct comparison of the results of properly designed protocols at 4°C (Figure 4.4A, 3 minutes/step) and at 25°C (Figure 4.5, 1.5 minutes/step) still indicate more cell loss at the higher temperature with a resulting normalized viable cell number for exposure at 25°C of 89.6% compared to 93.3% at 4°C. Overexposure to CPAs, as seen for 3 or 10 minute steps at 25°C (Figure 4.5), further decreases the cell viability in the bead after addition and removal.

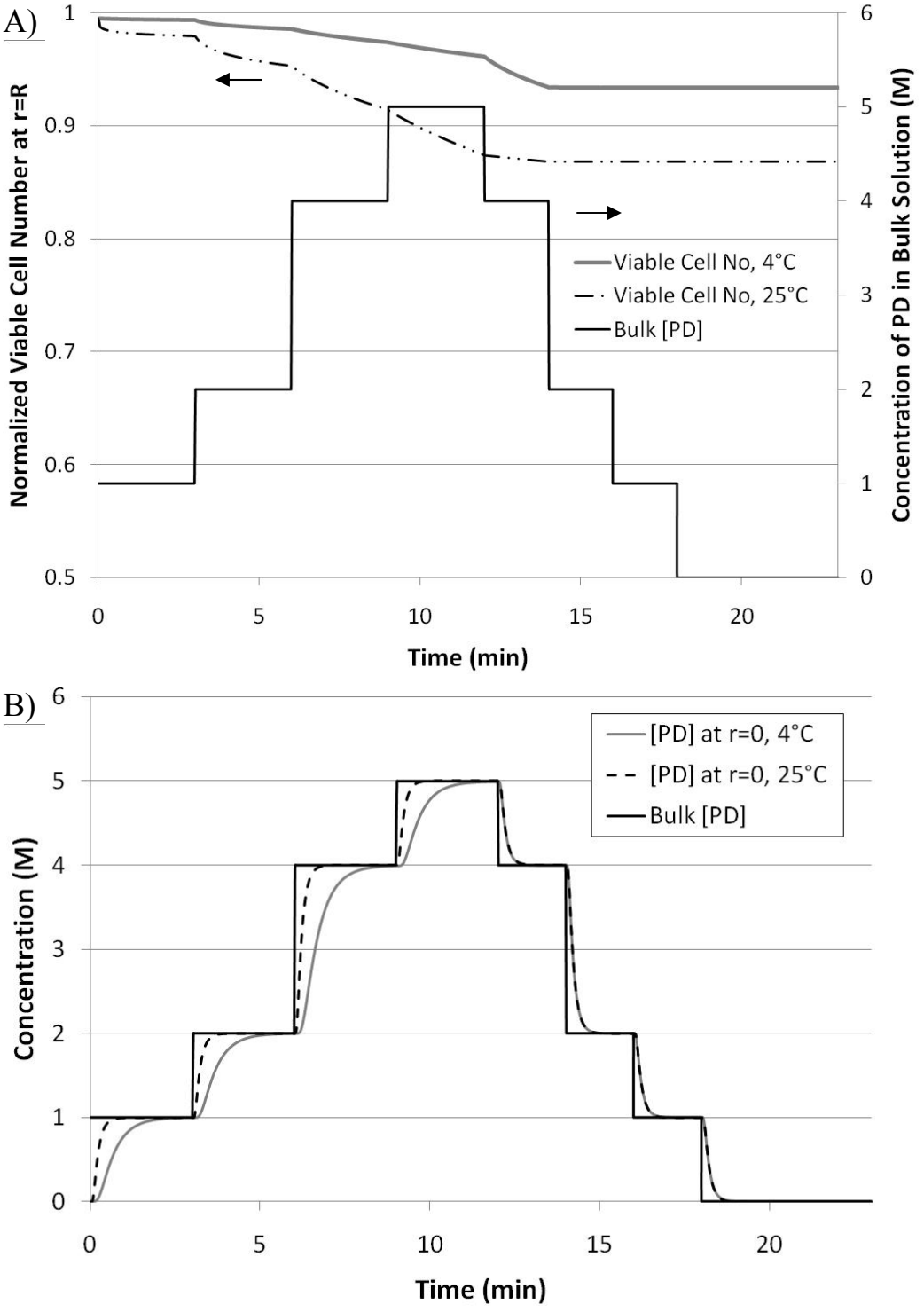

Figure 4.4. A) Normalized viable cell number (n/n_0) at edge of bead and B) concentration profile for predominant CPA, PD, at center of bead for 4°C (solid gray) and 25°C (dashed black) addition and concentration in bulk solution (solid black) for 3 min/addition step. All removal steps carried out at 25°C.

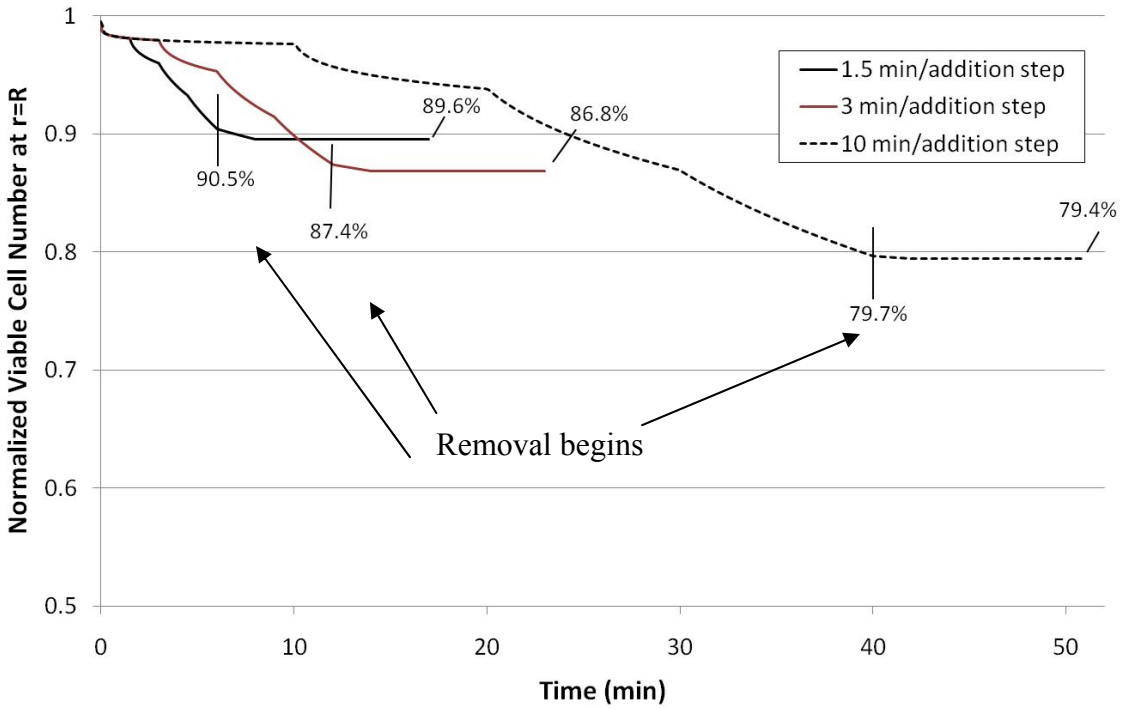

Figure 4.5. Normalized viable cell number (n/n_0) at edge of bead for different exposure times at 25°C. At this temperature, 1.5 min/addition step is sufficient to achieve equilibrium. 3 min/addition step and 10 min/addition step are overexposures.

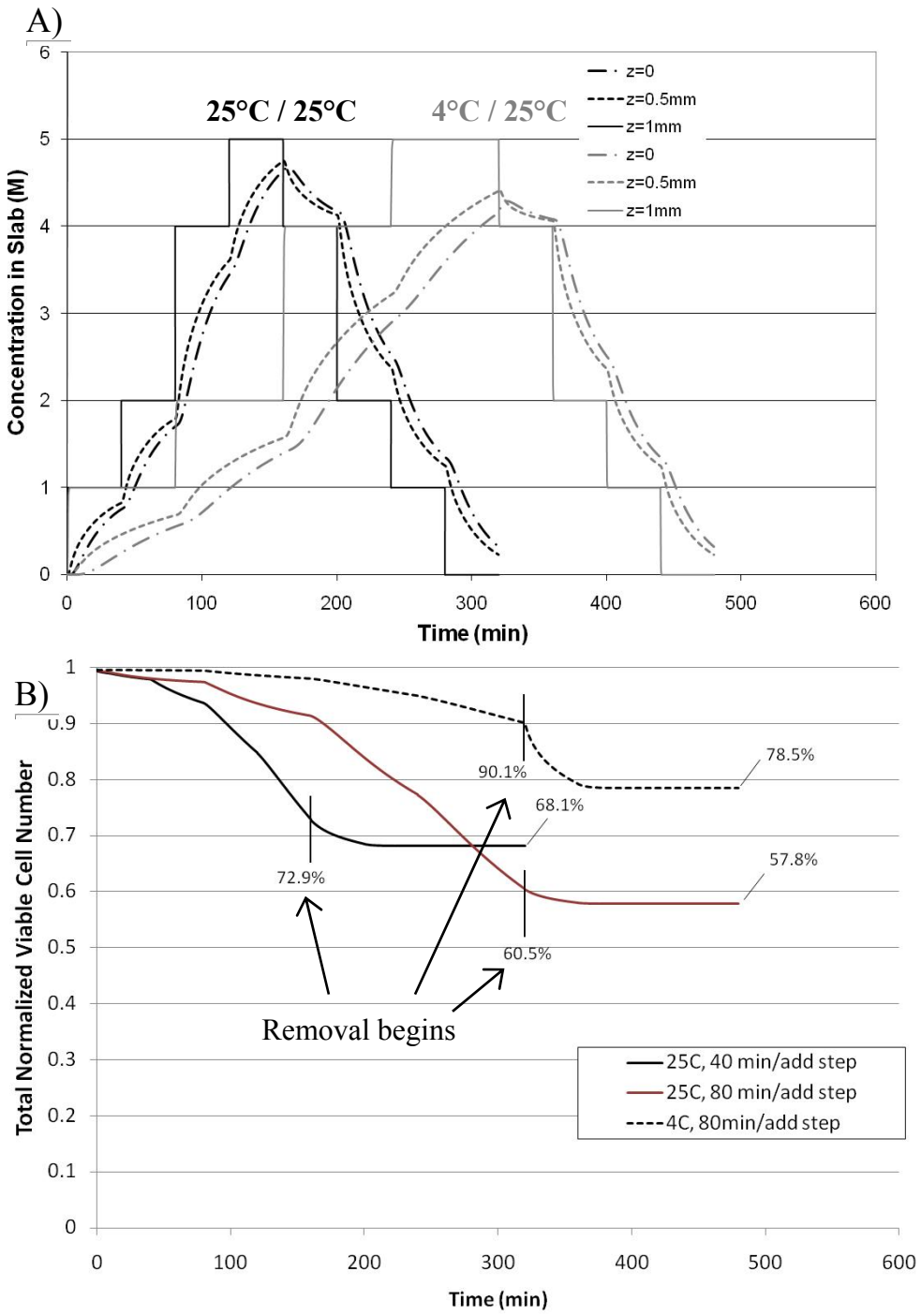

Figure 4.6. A) Concentration profiles of predominant CPA, PD, throughout slab for two temperatures and B) total normalized viable cell number (n/n_0) in slab for different exposure times and temperatures. All removal steps occurred at 25°C (40 minutes/step).

4.3.3 Mass Transfer through Articular Cartilage

Mass transfer through articular cartilage is hindered due to the dense nature of the tissue. The composition of each addition and removal step for articular cartilage was the same as for alginate beads. To address the mass transfer issues, the duration of the addition and removal steps was adjusted. The duration of all addition and removal steps were equal to each other, and this time was adjusted to ensure approximately 90% equilibration at the center of the slab by the end of all addition steps. Concentration profiles throughout the slab for exposure at both temperatures are shown in Figure 4.6A. The temperature effects on mass transfer are exacerbated for articular cartilage due to the reduced diffusivity and increased sample dimension. Simulations indicate that addition steps must be twice as long when carried out at 4°C (80 min/step) than 25°C (40 min/step).

Figure 4.6B shows the effects of temperature and overexposure on cytotoxicity by comparing three scenarios. In the first scenario, addition steps occurred at 4°C and required 80 min/step to achieve approximately 90% equilibration. Addition steps for the second scenario occurred at 25°C and required only 40 min/step. These two scenarios were compared to overexposure: addition steps carried out at 25°C for 80 min/step. All removal steps were carried out at 25^{o}C and at 40 min/step. The total normalized viable cell number was calculated by integrating the viable cell number over the entire slab using the trapezoidal rule. Results indicate that while overexposure increases cell death, temperature also plays a significant role. Additionally, more cell death is seen during removal at 25°C when addition was carried out at a lower temperature (4°C). These effects can be seen more clearly in Figure 4.7, where the normalized viable cell number

at the center and edge of the slab is shown for two scenarios: addition and removal at 4°C (80 min/step) or addition at 4°C (80 min/step) and removal at 25°C (40 min/step). These results clearly indicate that temperature is critical, even for removal steps. In the second scenario, where addition occurs at 4°C and removal occurs at 25°C, there is a significant loss in viable cell number during removal. The steep decrease in normalized viability at the center of the slab during removal at 25°C reflects two distinct phenomena. The high viable cell number present at the beginning of removal indicates the presence of many cells that are still quite susceptible to CPA toxicity. These cells will rapidly die when exposed to the higher temperature during removal. The edge of the slab experiences this phenomenon to a lesser extent as the edge of the slab equilibrates with the bulk solution concentration almost instantaneously which decreases the CPA concentration and time of exposure that occurs during removal. At the center of the slab, this issue is compounded by the slow mass transfer. Even at the higher temperature, Figure 4.6A clearly shows that the center of the slab, as well as the half way inner point, experience prolonged exposure to the CPAs during removal when compared to the outer edge of the slab. This is the most likely cause for the lower final viable cell number at the center of the slab as compared to the edge. This prolonged exposure also occurs for removal at 4°C although the cytotoxicity at this temperature causes the decrease in viable cell number to be much less dramatic. Overall, removal at 4°C causes an additional viable cell loss of 3.7% at the center of the slab compared to 0.6% at the edge the slab. These simulations indicate that temperature is even more critical for larger constructs.

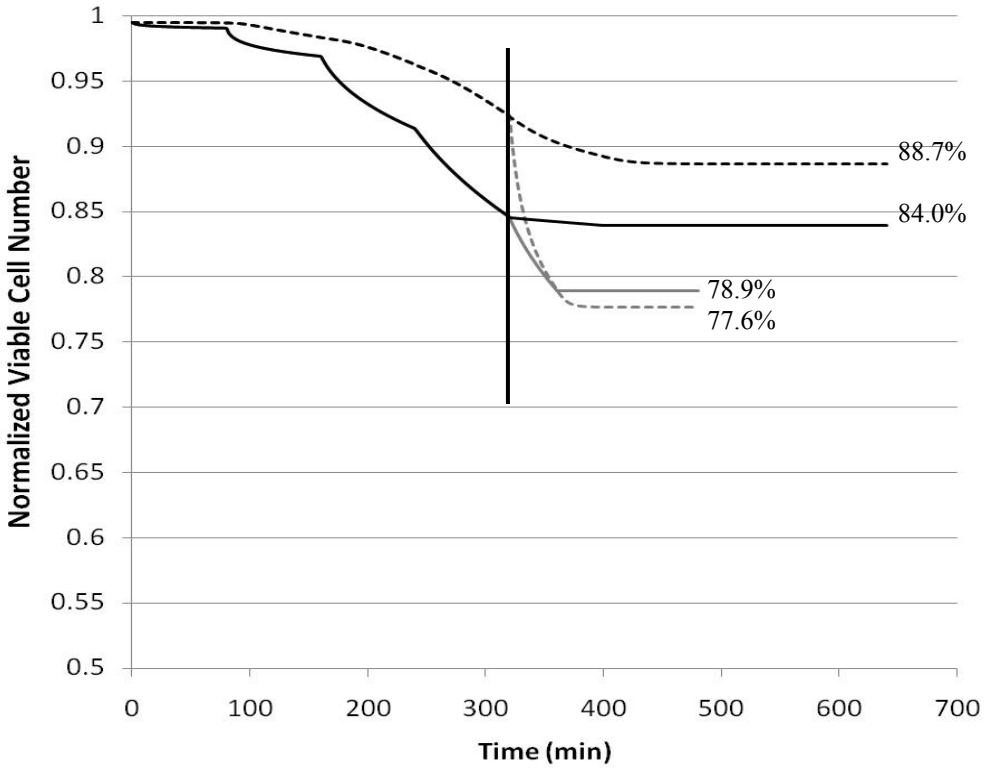

Figure 4.7. Normalized viable cell number (n/n_0) at center of slab (dashed) or edge of slab (solid) for addition steps at 4°C (80 min/step) and removal at 4°C (80 min/step, black) or 25°C (40 min/step, gray).

The previously published experimental results indicate that DMSO toxicity is much less dependent on temperature than PD (Lawson et al. 2011). Therefore, additional simulations were carried out using the cytotoxicity parameters for DMSO rather than the combined cytotoxicity that would be expected for the cocktail used in these studies. DMSO is slightly less cytotoxic than PD at low temperatures but DMSO cytotoxicity is much less sensitive to a change in temperature making it significantly less cytotoxic at higher temperatures than PD. Figure 4.8 compares the normalized viable cell number for normal parameters to the "less temperature sensitive" cytotoxicity parameters of DMSO. These results indicate that the use of a CPA that exhibits similar cytotoxicity at 4°C and 25°C will yield higher viable cell number after addition and removal than a CPA that

exhibits cytotoxicity which significantly increases with temperature. Even with addition and removal occurring at 25°C, 6M DMSO will result in less cell loss throughout the slab (92-93.2% viable cell number, Figure 4.8) than the cocktail solution including PD with all exposure carried out at 4°C (84-88.7% viable cell number, Figure 4.7). However, DMSO, even at 6M is not vitrifiable, whereas the cocktails that are vitrifiable, such as DMSO with PD, are more cytotoxic at 25°C.

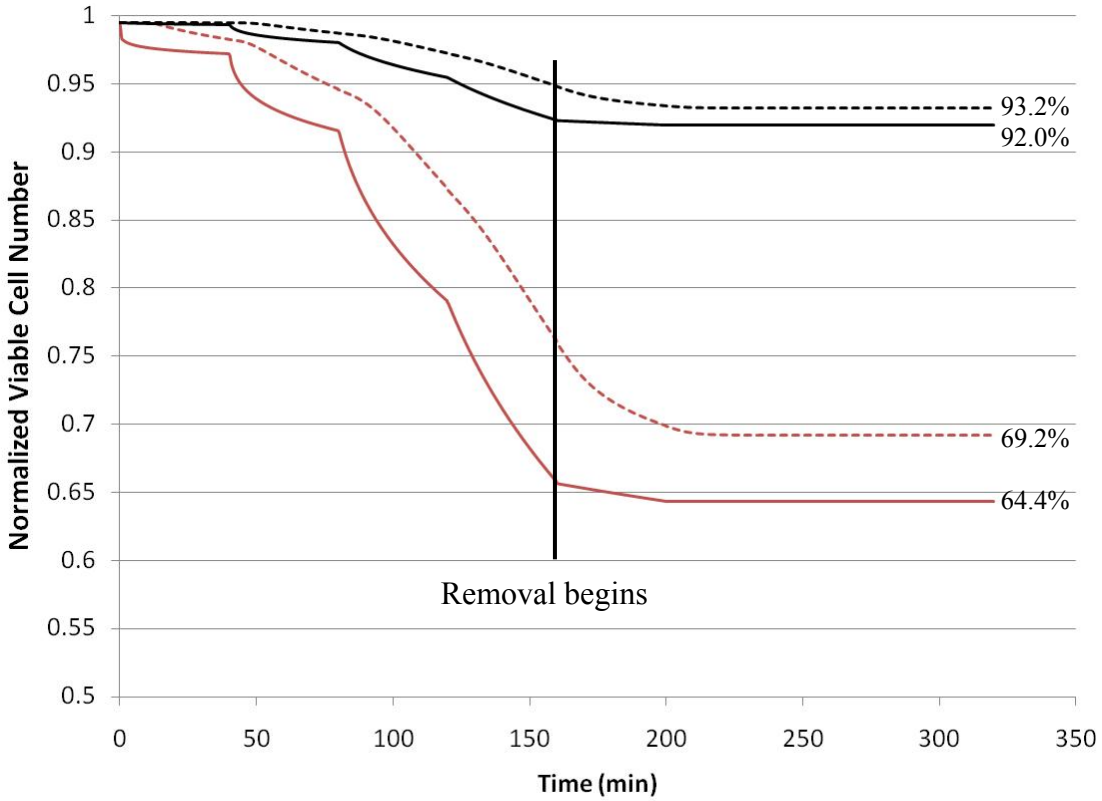

Figure 4.8. Normalized viable cell number (n/n_0) at center of slab (dashed) and at edge of slab (solid) for 25°C, 40 minute addition and removal steps for DMSO values of cytotoxicity parameters (black) vs cocktail parameters (red).

4.4. Discussion

The cryopreservation of different tissue-engineered constructs or natural tissues presents a significant challenge in bringing them to the clinic. Due to the wide array of tissues, geometries and clinically relevant sizes, it is desirable to be able to design addition and removal protocols based on the specific tissue being preserved. Significant work has been done in the area of cryopreservation to better understand the cooling and warming process, but little work has been done to better understand and design CPA addition and removal protocols. This study addresses this deficiency. Although cooling and warming rates are dictated by the vitrification solution, the proper design of addition and removal protocols can improve the success of the vitrification process. Three main concerns arise when designing addition and removal procedures: osmotic excursions, mass transfer and CPA cytotoxicity. The addition of vitrification-relevant concentrations of CPAs in a single step is generally recognized to cause excessive osmotic excursions. Previously published work from our laboratory has addressed this issue and validated the need to minimize osmotic excursions and maintain them in a tolerable normalized cell volume range (Mukherjee et al. 2007). All simulations carried out in this work maintain osmotic excursions within the tolerable range for βTC-tet murine insulinomas.

The success of vitrification is also contingent upon achieving sufficient mass transfer of the vitrifiable solution. Although recent publications utilize macroscopic observation to prove successful vitrification (Weiss et al. 2010), it is preferable to determine a solution's ability to vitrify using differential scanning calorimetry or another method of thermal analysis. Ensuring equilibration throughout the sample lends credence to the successful vitrification of macro constructs that cannot easily be tested by calorimetry. The

mathematical model allows determination of the necessary time of exposure for each CPA to achieve equilibrium throughout the construct. Although this can be determined experimentally (Mukherjee et al. 2008), the use of a mathematical model is more broadly applicable and can be applied to novel tissue-engineered constructs.

Due to the dependence of cytotoxicity on CPA concentration, exposure time and temperature, mass transfer and cytotoxicity are inextricably linked. The incorporation of a cytotoxicity equation based on experimental results for βTC-tet cells allows for insight into the importance of each of these variables in the addition and removal protocols. It is important to realize, however, that cytotoxicity parameters dictate the results and will vary with cell type. Cytotoxicity has been shown to increase with increased temperature for relatively long exposure times of ~30 minutes (Lawson et al. 2011; Tomford et al. 1984). This has led to the general assumption that CPA exposure should be carried out at low temperatures (≤ 4°C). Our results clearly indicate the importance of temperature of CPA addition and removal. The effects of temperature on cytotoxicity are clearly exacerbated for the longer exposure times necessary for larger constructs. Articular cartilage is particularly challenging due to the clinically relevant size and dense nature of the tissue. The challenge of mass transfer in articular cartilage is well known and has been investigated experimentally. Pegg's group has used the "liquidus-tracking method" in which CPAs are added as the sample is cooled. This method attempts to follow the liquidus curve of the vitrification solution's phase diagram to minimize the concentration of CPA that the cells are exposed to while ensuring that ice will not form (Pegg et al. 2006; Wang et al. 2007a). Although our cytotoxicity parameters were chosen based on experimental results with βTC-tet cells, Pegg's experiments corroborate the need for

improved mass transfer. Our simulations indicate that if the first addition step, A1, is carried out at 25°C rather than 4°C, the viable cell number will only drop by 1%. If A2 is also carried out at 25°C, the viable cell number after A1 and A2 will decrease 5%. As the concentration of the addition steps increases, the viable cell number will only decrease. While the introduction of the first two steps at room temperature may decrease the time necessary for CPA equilibration, the resulting viable cell number will be lower. Therefore, the "liquidus-tracking method" or any method that begins CPA exposure at a higher temperature and cools during the subsequent addition steps may have limited benefit, depending upon the CPA used.

The issue of overexposure is not often addressed in cryobiology although its effects can be significant. When working with a relatively simple system, such as encapsulated cells, overexposure of 1.5 minutes per step can result in additional loss in viable cell number (~3%). While this cell loss may be minimal, these effects are clearly exacerbated for larger constructs with more resistance to mass transfer. In the case of articular cartilage, chondrocyte viability is clearly critical to overall performance (Hayashi et al. 2009). Some have suggested the possibility of utilizing lower molecular weight CPAs to improve mass transfer and minimize cytotoxicity (Hayashi et al. 2009). In order to determine whether a significant increase in diffusivity, either due to a change in the matrix or the size of the CPAs, aids the addition and removal process, additional simulations were done. Mass transfer through the articular cartilage slab geometry but with mass transfer properties of alginate still requires 30 minutes/step to achieve approximately 90% equilibration, as compared to 80 minutes/step for the articular cartilage slab (4°C, results not shown). Although improvement in mass transfer

properties would slightly decrease cytotoxicity by approximately 4%, the dimension of a clinically relevant cartilage disc plays a larger role in the success or failure of vitrification. It is likely that many researchers, instead of improving diffusivity, are achieving only partial equilibration and therefore partial vitrification. While this may minimize CPA toxicity, it will increase the possibility of cryoinjury for cells in the center of the disc. This has been experimentally shown for the vitrification solution VS55, composed of DMSO, PD and formamide. Exposure to VS55 resulted in a decrease in chondrocyte viability in articular cartilage discs to 51% although rapid cooling without the solution resulted in viability of less than 5% (Guan et al. 2006). These results indicate that the cryoinjury that occurs in the absence of CPAs causes more cell death than would be seen due to CPA cytotoxicity experienced by the cells during addition and removal. Cells within the matrix that are exposed to lower concentrations of CPAs that are not vitrifiable will likely experience intracellular ice formation, which is almost always lethal (Pegg 2010).

Although experimentally determined, questions may remain about the cytotoxicity equation used in these simulations. The simulated viable cell number after addition and removal relies heavily on the parameters chosen. The cytotoxicity equation is most sensitive to a change in parameter f. When parameter f is halved, $f/2$, the viable cell number is also approximately halved. Clearly, the need to minimize cytotoxicity can be met, in part, with less toxic CPAs. The theory of cryoprotectant toxicity neutralization has been suggested by Fahy (Fahy 2010). This theory indicates that specific chemicals can neutralize the toxicity of CPAs although this has only been shown conclusively for the combination of amides with DMSO. Additionally, many have tried to minimize the

concentrations of CPAs necessary to achieve vitrification by using non-permeating solutes, such as trehalose or sucrose. Non-permeating solutes may not contribute as significantly to overall toxicity as permeating solutes (Fahy et al. 2004), but previous studies have shown that these additives are not innocuous and do contribute to toxicity (Lawson et al. 2011). Less cytotoxic CPAs may be beneficial, but these simulations indicate that it may be more critical to use CPAs that exhibit cytotoxicity that is less temperature sensitive. The previous experimental studies indicate that DMSO toxicity is less temperature sensitive than that of PD. Unfortunately, 6M DMSO is not vitrifiable in our hands. The temperature sensitivity of single-component CPAs also carry over to the cocktails that are a combination of these CPAs (Lawson et al. 2011). Nevertheless, the issue of CPA cytotoxicity remains the most critical challenge for the successful vitrification of tissues or tissue-engineered constructs (Fahy 2010).

Finally, the use of a time-dependent death rate appears to reflect the experimentally determined cytotoxicity kinetics. The value of parameter *f* indicates that βTC-tet cells become somewhat resistant to CPA cytotoxicity over time. Depending on the mechanism of resistance, it may be possible to select for CPA resistant cells and preferentially use these in tissue-engineered constructs. This phenomenon may be present in other cell types to a greater or lesser extent. It is currently unclear whether the use of discrete subpopulations would better represent the physiological phenomenon that is occurring although further experiments would be required before the subpopulations could be accurately described. It is clear that investigation into the mechanisms of cytotoxicity and resistance would provide insight and allow for better design of CPA solutions and addition/removal protocols.

4.5. Conclusions

Vitrification has been touted for use with larger tissue engineered constructs or natural tissues where ice formation can be especially detrimental (Kuleshova et al. 2007; Pegg 2010). The issue of CPA cytotoxicity is unavoidable when using the high concentrations of CPAs necessary to successfully vitrify a sample. Simulations indicate that temperature of exposure to CPAs is particularly deleterious to viable cell number. Cell death can be significantly reduced by using less cytotoxic CPAs. Additionally, the use of CPAs that exhibit less temperature sensitive cytotoxicity would allow the addition and removal steps to occur faster at a higher temperature without excessive cell death. CPA overexposure also results in significant cell loss, especially when working with larger constructs. On the other hand, CPA underexposure would achieve vitrifiable concentrations only at the outer part of a tissue. These results point to the critical need for properly designed protocols that allow for sufficient CPA equilibration while minimizing CPA cytotoxicity. This mathematical model is a useful tool in the design and optimization of such protocols for natural tissues and tissue-engineered constructs.

CHAPTER 5

EFFECTS OF CRYOPRESERVATION ON THE CELL AND BIOMATERIAL COMPONENTS OF AN ENCAPSULATED CELL SYSTEM

The use of microencapsulation to deliver secreting cells has become common in the field of Tissue Engineering. Often overlooked, the preservation of these tissue engineered constructs is critical to achieve their widespread clinical use. In this study, we investigated the effects of two types of cryopreservation, conventional freezing and vitrification, on the cellular and biomaterial components of calcium alginate/poly-L-lysine/alginate encapsulated murine insulinomas. Vitrification was carried out using two cocktails, DPS (3M dimethyl sulfoxide + 3M 1,2-propanediol + 0.5M sucrose) and P6 (1M dimethyl sulfoxide + 5M 1,2-propanediol + 0.34 M poly(ethylene)glycol with M.W. of 400). The cellular and biomaterial components were assessed *in vitro* and sub-therapeutically *in vivo*. *In vitro* assessment indicated that metabolically active cell number was similar for preserved groups and fresh. Two different insulin secretion tests were performed, which yielded similar results with few minor differences. Generally, beads vitrified with P6 performed comparably to fresh and better than those vitrified with DPS. Sub-therapeutic, week-long, *in vivo* studies in healthy mice indicated that both preserved and fresh beads fared well *in vivo* with cell growth occurring in all groups after implantation. Biomaterial assessment was done directly after preservation (*in vitro* studies) as well as after explantation. Preservation did not cause significant damage to the beads although conventionally frozen beads occasionally appeared to have ice

damage in the calcium alginate matrix. Upon explantation, biomaterial assessment revealed no systematic differences in host response or bead integrity for preserved or fresh beads. It is concluded that both conventional freezing and vitrification can be used to successfully cryopreserve encapsulated insulinomas.

5.1 Introduction

The use of microencapsulation to deliver secreting cells is one of the more promising advances in tissue engineering and cell-based therapies. Long-lasting microcapsules, such as those used for pancreatic substitutes, have been shown to increase the *in vivo* immune acceptance of a non-autologous cell implant (de Vos et al. 2006; Duvivier-Kali et al. 2001; Schmidt et al. 2008). Specifically, microencapsulation of islets or other insulin-secreting cells has been and continues to be explored for the treatment of insulin-dependent diabetes (Cheng et al. 2006; Gross et al. 2007; Safley et al. 2010). Preservation is critical in bringing any tissue-engineered construct, including encapsulated cell systems, to the clinic (Brockbank et al. 2003; Fahy et al. 2006). Cryopreservation provides long-term storage at a temperature where all metabolic, chemical and biochemical processes are suspended (Karlsson and Toner 1996). The two main types of cryopreservation being investigated are conventional freezing and vitrification. Conventional freezing utilizes low levels of cryoprotective agents (CPAs), slow cooling and rapid warming. The low concentrations of CPAs are minimally toxic but allow ice formation in the extracellular space (Karlsson and Toner 2000). Vitrification requires high concentrations of CPAs along with rapid cooling and warming to achieve a vitreous, or glassy, state (Brockbank and Taylor 2007). Step-wise addition and removal of CPAs and proper temperature control can help minimize cell death.

Despite the additional complexity, vitrification prevents ice damage and is therefore seen as a promising method of preservation for tissue-engineered substitutes (Fahy et al. 2004; Kuleshova et al. 2007).

The overarching goal for the cryopreservation of a tissue construct is to maintain both the biomaterial and cellular components; however, the importance of each component may vary from construct to construct. The performance of an encapsulated system utilizing proliferating cells may not be as affected by some loss in cell viability because the cells can regenerate. The biomaterial component, however, cannot regenerate. Previous studies indicate that the ice formed during conventional freezing may damage the alginate matrix of an encapsulated system (Heng et al. 2004; Mukherjee et al. 2005). It may also damage the semi-permeable membrane, such as that generated by poly-L-lysine treatment, often used to provide immunoprotection. Damage to either of these could compromise the immunoprotective properties and change the overall capsule morphology, possibly causing surface roughness which has been shown to affect biocompatibility (Bunger et al. 2003).

This study investigated the cryopreservation of a tissue-engineered pancreatic substitute consisting of βTC-tet murine insulinomas encapsulated in calcium-alginate/poly-L-lysine/alginate (APA) beads. Encapsulated cells were subjected to conventional freezing in 10% dimethyl sulfoxide (DMSO) or vitrification using one of two vitrification solutions. The cellular and biomaterial components of this system were evaluated after warming and compared to the unpreserved control. For the cellular component, the metabolically active cell number and insulin secretion rates were determined. The biomaterial component was assessed for overall integrity via histology

and mechanical testing and for poly-L-lysine (PLL) layer integrity by permeability studies using fluorescently-labeled dextran.

5.2 Materials and Methods

5.2.1 Cell Culture

βTC-tet cells were obtained from the laboratory of Dr. Efrat, Albert Einstein College of Medicine, Bronx, NY (Fleischer et al. 1998). Monolayer cultures were initiated from frozen stocks and propagated in T-flasks in complete growth medium consisting of Dulbecco's Modified Eagle's Medium (DMEM) (Sigma-Aldrich, St. Louis, MO) supplemented with 10% fetal bovine serum (Gemini Bioproducts, West Sacramento, CA), 1% L-glutamine (Mediatech, Inc., Manassas, VA) and 1% penicillin/streptomycin (Mediatech, Inc.). Cells were cultured in a humidified incubator at 37°C and 5% CO_2. Cells were split at a ratio of 1:5 and experiments performed with passages 38-44.

5.2.2 Encapsulation and Coating

βTC-tet cells were encapsulated using previously published protocols (Stabler et al. 2001). Briefly, cells were detached from monolayer cultures by trypsinization (0.25% Trypsin-EDTA, Mediatech Cellgro) and suspended at a density of $3.0x10^7$cells/ml in 2% sodium alginate (Pronova Ultra Pure LVM alginate NovaMatrix of FMC BioPolymer AS, Norway). Beads were formed using an electrostatic bead generator (Nisco Engineering AG, Zurich, Switzerland) that generated droplets which fell into a well-stirred 1.1% $CaCl_2$ bath. Cross-linked beads were washed and stored in complete growth medium and cultured overnight in a non-treated T-flask on a rocker plate in a 37°C and 5% CO_2, humidified incubator. Beads were coated with poly-L-lysine as previously described

(Stabler et al. 2001). In short, beads were subjected to subsequent treatments with $CaCl_2$, CHES, PLL (Sigma, MW: 19,200), and 0.2% alginate (same type as above). They were washed and stored in complete growth medium and cultured overnight as indicated above.

5.2.3 Vitrification and Conventional Freezing Protocols

Two different vitrification solutions were used, DPS (3M DMSO +3M 1,2-propanediol (PD)+0.5M sucrose) and P6 (1M DMSO+5M PD +0.34M polyethylene glycol with a molecular weight of 400). Both were prepared using a concentrated and modified version of the EuroCollins carrier solution containing 174.76 g/L dextrose, 5.6 g/L KCl, 4.2 g/L $NaHCO_3$ and 8.2 g/L NaCl. This concentrated EuroCollins solution was diluted in the final solution volume at a ratio of 1:5. All chemicals were from Sigma-Aldrich except sucrose and $NaHCO_3$ (Fisher, Fair Lawn, NJ). CPA solutions were added to encapsulated cells in a step-wise manner at 4°C as shown in Table 5.1. Rapid cooling from 4°C to -100°C at ~100°C/min was achieved by immersion in an isopentane bath held at -135°C; this was followed by slower cooling from -100°C to -135°C at ~2°C/min in the vapor phase of a mechanical freezer (Sanyo, San Diego, CA) set at -135°C. Samples were stored overnight before warming rapidly in a bath of 30% DMSO in water at room temperature. CPAs were removed in a step-wise manner at room temperature (Table 5.1). Conventionally frozen (CF) beads were exposed to 10% DMSO in complete growth medium for 10 minutes at 4°C and then transferred to cryovials (Corning Inc., Corning, NY). These were placed in an isopropyl alcohol bath (Nalgene of Thermo Fisher Scientific, Rochester, NY) in a -80°C mechanical freezer (VWR, West Chester, PA) for 90 minutes before being plunged into liquid nitrogen. Vials were stored

overnight before being rapidly warmed by agitation in a 37°C water bath until all visible ice had melted. Beads were then incubated in complete growth medium for 10 minutes at 37°C and washed with complete growth medium.

Table 5.1. Addition & removal protocols for DPS and P6. RT indicates room temperature.

	DPS				P6				Temp (°C)
Step	[DMSO]	[PD]	[Sucrose]	Time (min)	[DMSO]	[PD]	[PEG]	Time (min)	
A1	1	1	0.15	2	0.25	1	0	3	4
A2	2	2	0.3	2	0.5	2	0.1	3	4
A3	3	3	0.5	2	0.75	3.5	0.2	3	4
A4	--	--	--	--	1	5	0.338	3	4
R1	2.25	2.25	0.3	2	0.75	4	0.2	2	RT
R2	1.5	1.5	0.2	2	0.5	2	0.2	2	RT
R3	0.75	0.75	0.1	2	0.25	1	0	2	RT
R4	0	0	0	4	0	0	0	4	RT

5.2.4 Metabolically Active Cell Number and Secretory Function

Metabolically active cells and rates of insulin secretion were measured immediately post-warming. To determine the metabolic activity of cells, 100 µL of APA beads with 100 µL alamarBlue™ (Invitrogen™, Carlsbad, CA) and 1 mL complete growth medium, or only 100 µL alamarBlue™ and 1.1 mL complete growth medium for controls, were placed in each well of a 12 well plate for 3 hours in a 37°C and 5% CO_2, humidified incubator. A 100 µL supernatant volume from each well was transferred to a

black 96 well plate and read using a SPECTRAMAX Gemini Fluorescent plate reader (Molecular Devices, Sunnyvale, CA) using an excitation and an emission wavelength of 544 and 590 nm, respectively. Data were normalized to those from untreated beads. Live-Dead imaging of cells in beads was performed using the LIVE/DEAD® Viability Cytotoxicity Kit (Molecular Probes® by Invitrogen™, Carlsbad, CA). Beads were incubated for 20 minutes in 0.9% NaCl containing 2μM calcein AM and 4μM ethidium homodimer-1, and images were acquired using an LSM 510 UV confocal microscope (Carl Zeiss, Inc, Thornwood, NY) with excitation at wavelengths of 488 nm and 543 nm.

To determine high-glucose insulin secretion, 100 μL of APA beads were incubated with complete growth medium for one hour in a 37°C and 5% CO_2, humidified incubator. Samples were taken at t=0 and at t=1 hr and stored at -80°C for later assay of insulin with a Mouse Insulin ELISA (Mercodia, Uppsala, Sweden). To measure basal and stimulated insulin secretion, 100 μl of APA beads were subjected to a one hour basal period followed by a 30 minute stimulated period. Basal medium consisted of glucose- and glutamine-free DMEM (Sigma-Aldrich) supplemented with 1.31 g/L bovine serum albumin (Sigma), and stimulation medium consisted of DMEM (Sigma) with 15 mM glucose and supplemented with FBS, L-glutamine and penicillin/streptomycin at the same concentrations as in complete growth medium. Encapsulated cells were incubated in a 37°C humidified incubator with 5% CO_2 during both secretion periods. Samples were taken directly before and after the basal and stimulated periods, stored at -80°C and later analyzed with the Mouse Insulin ELISA.

5.2.5 Biomaterial Integrity

Permeability was assessed by incubating APA beads with fluorescently-labeled dextran (FITC-dextran) of 20 and 70 kDa molecular weights (Sigma). FITC-dextran was introduced at a final concentration of 0.025 mg/ml in 0.9% NaCl and images were taken at 1, 2, 3, 4, 5, 10, 15, 30 and 60 minutes using the LSM 510 UV confocal microscope. Young's moduli of preserved and fresh beads were determined using uniaxial compression. An EnduraTec ElectroForce® 3100 (Bose, Eden Prairie, MN) was used to deliver a compression rate of 0.01 mm/s with a 0.5N load cell (Interface Inc., Scottsdale, AZ). Compression was carried out to a final deformation of 10% or less. Hertz's theory was used to calculate the Young's moduli (Liu et al. 1998). For histology, APA beads were fixed in 2% glutaraldehyde (Sigma) in 0.9% NaCl and subsequently embedded using the Immunobed Embedding Kit (Electron Microscopy Sciences, Hatfield, PA). To minimize changes in bead morphology caused by the embedding process, embedding was performed with increasing concentrations of resin in double-distilled water, similar to previously reported procedures (James et al. 2004). After embedding, 5 μm sections were sliced with a Microm 355H Microtome (Thermo Fisher Scientific, Walldorf, Germany), mounted and stained with 1% Toluidine Blue (Research Organics, Cleveland, OH) to visualize the alginate matrix.

5.2.6 Statistical Analysis

Statistical calculations were performed using a one-way ANOVA and Tukey's test to determine differences between test groups. Values of $p<0.05$ were considered to indicate statistically significant differences.

5.3 Results

5.3.1 Metabolically Active Cell Number and Secretory Function

Metabolically active cell numbers for DPS, P6 and conventionally frozen (CF) samples were normalized to previous day fresh and were 0.71 ± 0.13, 0.79 ± 0.10, and 0.88 ± 0.20, respectively. No statistical differences were found among any of the fresh or cryopreserved groups ($n=5$). Results for insulin secretion measured post-warming are shown in Figure 5.1. APA beads preserved by conventional freezing had lower insulin secretion than fresh beads or beads vitrified with P6 when subjected to incubation in high-glucose medium; there were no significant differences between either of the vitrified groups and the fresh with $n=9$ (Fig. 5.1a). A somewhat different trend was observed in the stimulated insulin secretion tests, $n=4$ (Fig. 5.2b). In these, during the basal period, beads vitrified using P6 secreted more insulin than all other groups, including the fresh control. However, no significant differences were found among the stimulated secretion levels or among the stimulation indices (stimulated rate over basal secretion rate) of the groups. The stimulation indices were 1.97 ± 0.58, 2.39 ± 0.54, 1.72 ± 0.28, and 2.54 ± 0.28 for fresh, DPS, P6, and CF, respectively.

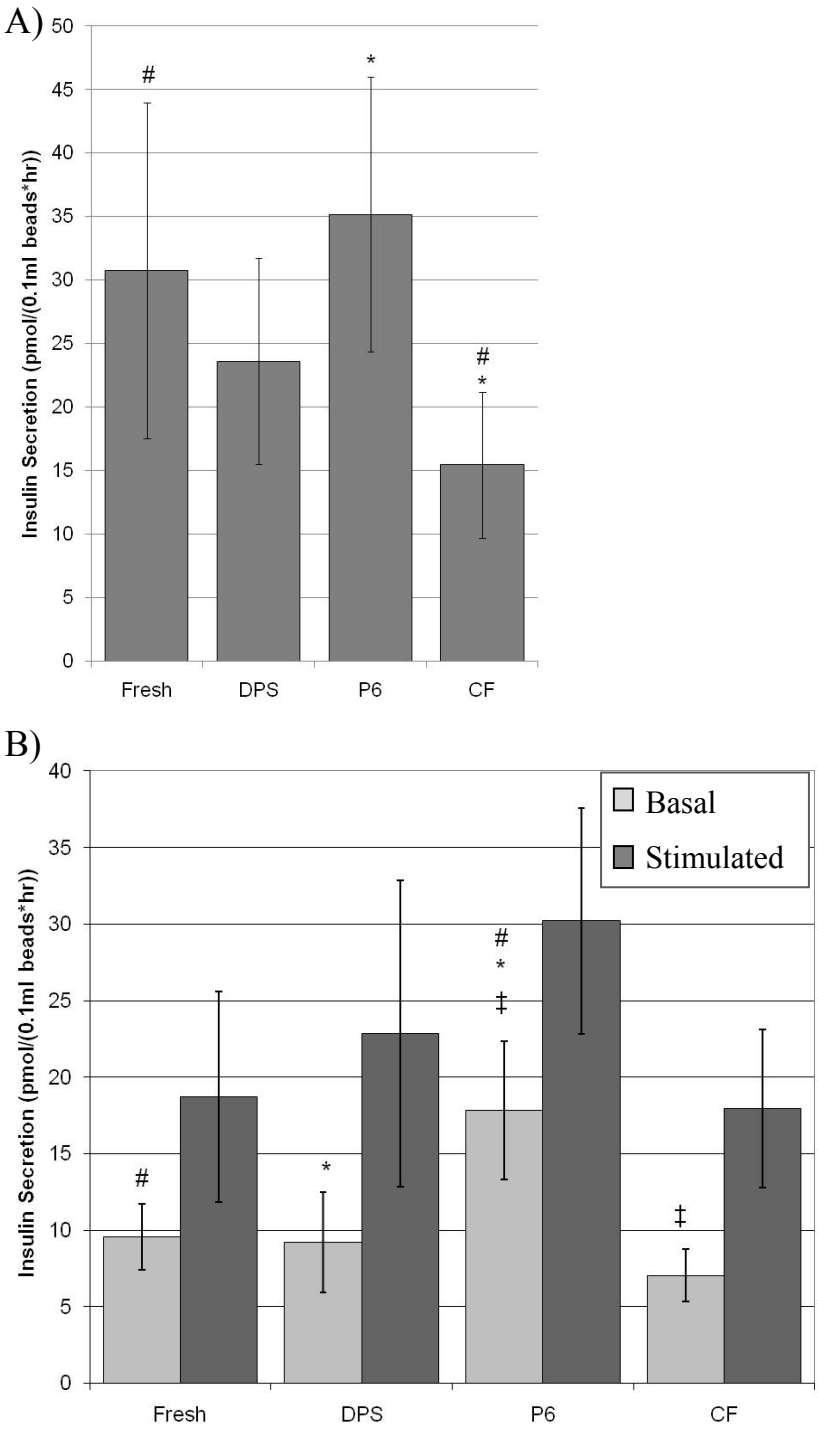

Figure 5.1. Insulin secretion for A) high-glucose exposure over 1 hr period, *n=9* and B) basal (0 mM glucose, 1 hr) and stimulated (15 mM glucose, 30 min), *n=4.*
#,*, ‡ indicate $p<0.05$ between groups.

5.3.2 Biomaterial Integrity

Assessment of permeability through the PLL layer after vitrification and conventional freezing indicated that no functional damage was done to the layer during preservation (*n=3)*. Indeed, with all groups, FITC-labeled dextran with M.W. of 20 kDa permeated almost completely within 15 minutes while FITC-dextran with M.W. of 70 kDa permeated only slightly over one hour. Results for FITC-dextran with M.W. of 70 kDa are shown in Figure 5.2. A total of 4 independent samples from each preparation were processed post-warming for histology, and representative images are shown in Figure 5.3. Images in Figure 5.3(A) show representative beads from fresh and the three cryopreservation treatments. An additional conventionally frozen sample is shown in Figure 5.3(B) as it indicates possible ice damage to the calcium alginate matrix. This image was included because similar images were seen in previous studies (Mukherjee et al. 2005), although in the present study this morphology appeared only once in the *n=4*. Figure 5.4 shows the average diameters and Young's Moduli of the fresh and cryopreserved beads, the latter immediately post-warming. No differences were found.

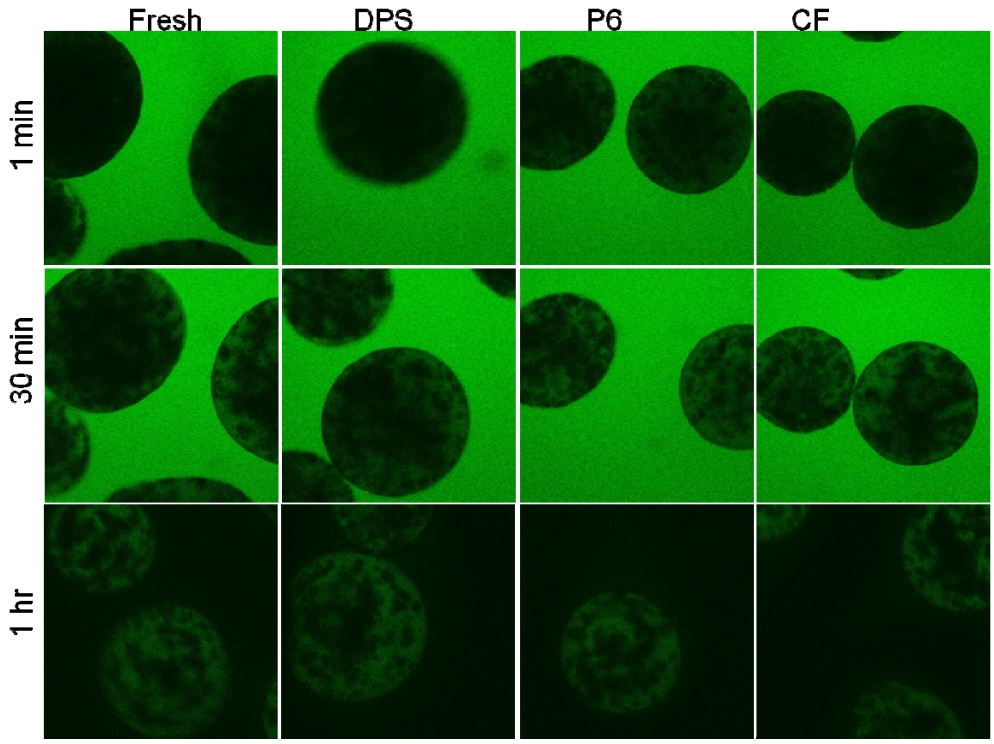

Figure 5.2. Fresh or cryopreserved beads after 1 min or 30 min incubation in FITC-labeled dextran (70 kDa) solution and at 1 hr after dextran solution was removed.

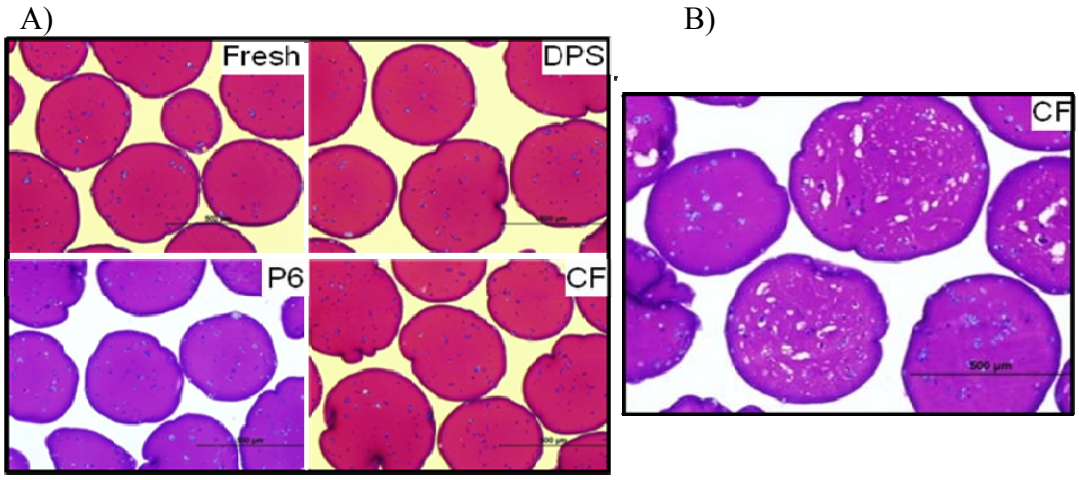

Figure 5.3. Typical histology images from a total of *n*=4 of fresh and cryopreserved beads (A). A conventionally frozen bead exhibiting what appears to be ice damage is shown in (B).

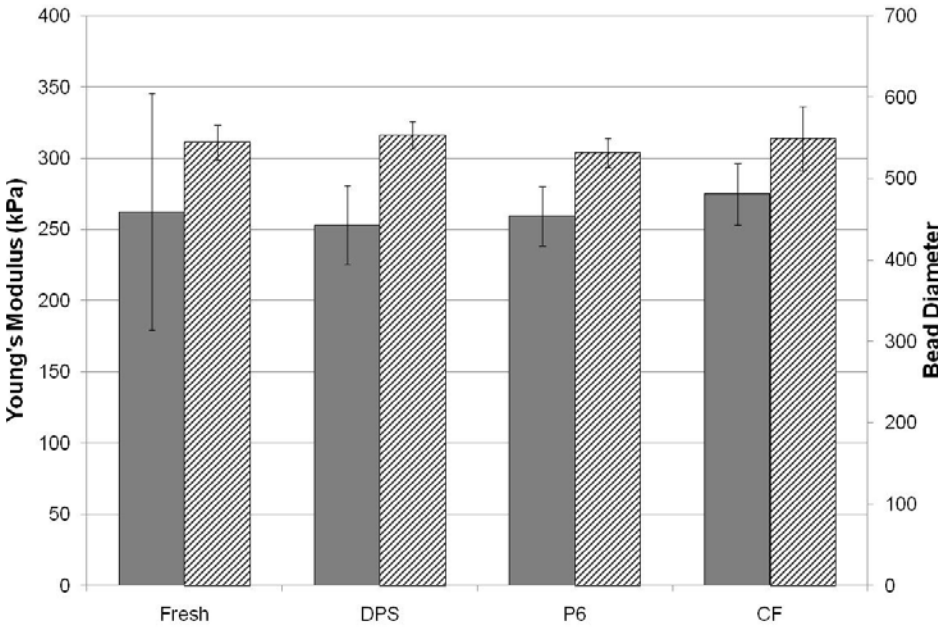

Figure 5.4. Young's moduli (solids) and bead diameters (stripes) for fresh and cryopreserved beads, *n=3*. No statistically significant differences found.

5.4 Discussion

Vitrification has been touted to be the most promising method of preservation for tissue engineered constructs due to the elimination of ice (Kuleshova et al. 2007). In our studies, we investigated the post-warming cellular viability and secretory function, as well as the biomaterial integrity, of encapsulated insulin-secreting cells that may serve as a pancreatic tissue substitute. As stated previously, the metabolically active cell number was not statistically different among any of the fresh and preserved groups. The insulin secretion results for the two different tests were not entirely consistent; however, a few general trends arose. Between the vitrified groups, P6 appeared to outperform DPS. Also, beads vitrified with P6 were generally comparable to fresh.

Although the reasons for the insulin secretion inconsistencies are unclear, one notable difference is the increased basal insulin secretion of beads vitrified with P6 (Figure 5.1B). Recent studies have shown that cryopreservation increases oxidative stress (Tatone et al. 2010) and specifically the intracellular concentration of hydrogen peroxide (Kim et al. 2010) in reproductive cells. Increased intracellular hydrogen peroxide has been shown to cause a transient increase in insulin secretion from islets (Maechler et al. 1999). It is possible that the P6 vitrification solution may cause more oxidative stress than DPS, as it has been shown to be more cytotoxic (Lawson, Ahmad et al. 2011). This may have then resulted in a transient increase in insulin secretion observed under basal conditions with P6 and may have caused insulin secretion comparable to fresh when beads were subjected to high-glucose medium (Figure 5.1A). Although the results from the two insulin secretion tests indicate small differences in secretion among groups, these differences were not reflected *in vivo*, probably due to cellular proliferation over the 7-day period of these studies.

Cell viability and function are critical for the *in vivo* success of an implant, but the biomaterial integrity also affects the performance of the construct. Previous studies indicated that ice damage occurs within the calcium alginate matrix of a conventionally frozen tissue-engineered pancreatic substitute (Mukherjee et al. 2005); however similar damage was seen only occasionally throughout our studies. Due to the low CPA concentrations used in conventional freezing, extracellular ice formation is expected to occur, although it is possible that ice crystals form in the solution in-between the cross-linked alginate chains, thus not damaging the matrix. Furthermore, any ice formation that

may have occurred in conventional freezing did not appear to affect the integrity of the poly-L-lysine layer or the stiffness of the beads.

5.5 Conclusions

Although literature touts the use of vitrification to preserve tissue-engineered constructs, it appears that APA-encapsulated cells may be successfully preserved using either vitrification or conventional freezing. *In vitro* studies indicated some differences in the performance of the conventionally frozen and vitrified beads as assessed by insulin secretion and metabolic activity. However, there were no significant differences in the biomaterial component. It remains unclear whether ice formation may affect the *in vivo* performance of this tissue-engineered pancreatic substitute.

CHAPTER 6

THE EFFECTS OF CRYOPRESERVATION ON THE *IN VIVO* EFFICACY OF AN ENCAPSULATED CELL SYSTEM

Cryopreservation is a critical step in bringing any tissue-engineered system from the benchtop to the clinic. There are two main types of cryopreservation: conventional freezing and vitrification. Conventional freezing uses low concentrations of cryoprotective agents (CPAs) and allows ice formation while vitrification utilizes high concentrations of CPAs to eliminate ice formation. In this study, we investigated the effects of these methods of cryopreservation on the *in vivo* performance of calcium alginate/poly-L-lysine/alginate encapsulated murine insulinomas. Vitrification was carried out using two cocktails, DPS (3M dimethyl sulfoxide + 3M 1,2-propanediol + 0.5M sucrose) and P6 (1M dimethyl sulfoxide + 5M 1,2-propanediol + 0.34M poly(ethylene)glycol with M.W. of 400). Conventional freezing was done using 10% dimethyl sulfoxide in complete growth medium. Sub-therapeutic studies were done with healthy mice receiving a small volume of fresh or preserved beads. Beads were explanted on days 2 and 7. Biomaterial assessment indicates possible ice damage in some conventionally frozen explants. Insulin secretion results indicate that beads vitrified with DPS perform worse within the first two days but that all cells exhibit growth during the sub-therapeutic *in vivo* period. For therapeutic studies, diabetic mice were implanted with fresh or preserved beads. Mice were sacrificed upon construct failure or at 2 weeks and beads were explanted for analysis. *In vivo* performance of conventionally frozen beads was comparable to fresh beads with both groups achieving

normoglycemia (50-250 mg/dl) relatively quickly and maintaining normoglycemia for the majority of the experiment. Vitrified groups performed worse with beads vitrified with DPS or P6 reverting only 3 of 8 mice or 5 of 8 mice, respectively. Beads vitrified with DPS also took significantly longer to revert than fresh or conventionally frozen. Biomaterial assessment of the explants indicated that all groups experienced similar host-cell attachment and damage *in vivo.* The ice formation that occurs during conventional freezing did not significantly damage the encapsulated cell system or its *in vivo* performance. Insulin secretion results for the explanted beads indicated that all preserved groups secreted significantly less insulin than fresh. Although ice has been shown to be detrimental to some biomaterials, our *in vivo* results indicate that conventional freezing is the better method for preservation of an encapsulated cell system.

6.1 Introduction

Although often overlooked, cryopreservation is considered by many to be critical in bringing tissue engineered constructs from the benchtop to the clinic with off-the-shelf availability (Pancrazio et al. 2007; Sambanis 2000). Two main methods of cryopreservation are currently being investigated for the preservation of constructs: conventional freezing and vitrification. In conventional freezing, a low level of cryoprotective agent (CPA) is added and the sample is slowly cooled, stored and thawed by rapid warming. Vitrification is more complex and requires multi-step addition of high concentrations of CPAs and rapid cooling and warming. Both methods have disadvantages. The conventional freezing method allows ice formation (Brockbank and Taylor 2007; Karlsson and Toner 1996) while the solutions used in vitrification are more cytotoxic due to the higher concentrations of CPAs (Saragusty et al. 2009). However,

aside from these disadvantages it is difficult to confidently determine which preservation method may be preferable for a specific tissue-engineered construct due to the high variability of results reported in literature.

An example of this is the preservation of encapsulated cell systems which are widely used in the field of Tissue Engineering to deliver cells and are broadly applicable. The preservation of microencapsulated insulin-secreting cells in particular has been widely investigated although the results have been highly variable. Conventional freezing has been shown to be successful in maintaining encapsulated islets (Schneider and Klein 2011; Stiegler et al. 2006) and myoblasts (Murua et al. 2009) as well as their function when implanted. Alginate encapsulation has been shown to benefit conventional freezing, as encapsulated cells fare better during conventional freezing than free cells or cell clusters do (Malpique et al. 2010). However, other groups have reported that conventional freezing leads to damage in the alginate or agarose matrix of an encapsulated system (Agudelo and Iwata 2008; Hang et al. 2010; Heng et al. 2004; Mukherjee et al. 2005). The ice formation that occurs in conventional freezing is clearly detrimental for constructs that serve a biomechanical function, such as heart valves (Schenke-Layland et al. 2007). Ice formation may also detrimentally affect the performance of an encapsulated system by changing the mechanical strength or overall morphology of the encapsulation material. Surface roughness has been shown to affect the *in vivo* inflammatory response (Bunger et al. 2003; Lanza et al. 1991). The ice-free method of preservation, vitrification, has been used to successfully cryopreserve encapsulated cells and islets, although none of these studies have compared the performance of conventional freezing to vitrification within the context of *in vivo*

efficacy (Agudelo et al. 2009; Wu et al. 2007). Additionally, alginate encapsulation appears to aid in the thermal transition of the sample to the vitreous state by causing preferential vitrification of water in the alginate bead compared to the bulk water (Zhang et al. 2010).

This study was designed to directly compare the two cryopreservation methods, vitrification and conventional freezing, and determine their effects on the *in vivo* performance of an encapsulated cell system. Insulin-secreting βTC-tet murine insulinomas were encapsulated in calcium-alginate/poly-L-lysine/alginate (APA) beads and were subjected to conventional freezing in 10% dimethyl sulfoxide (DMSO) or vitrification using one of two vitrification solutions. In sub-therapeutic studies, fresh or cryopreserved beads were implanted in healthy mice and were explanted on days 2 and 7 for assessment of the biomaterial and cell function. For therapeutic studies, streptozotocin-induced diabetic mice were implanted with fresh or cryopreserved beads and the *in vivo* performance and *ex vivo* cell function and biomaterial component of the implants were assessed.

6.2 Materials & Methods

6.2.1 Cell Culture

βTC-tet cells were obtained from the laboratory of Dr. Efrat at the Albert Einstein College of Medicine, Bronx, NY (Fleischer et al. 1998). Monolayer cultures were initiated from frozen stocks and propagated in T-flasks in complete growth medium consisting of Dulbecco's Modified Eagle's Medium (DMEM) (Sigma-Aldrich, St. Louis, MO) supplemented with 10% fetal bovine serum (Gemini Bioproducts, West Sacramento, CA), 1% L-glutamine (Mediatech, Inc., Manassas, VA) and 1%

penicillin/streptomycin (Mediatech, Inc.). Cells were incubated in a humidified incubator at 37°C and 5% CO_2. Cells were split at a ratio of 1:5 and experiments performed with passages 38-44.

6.2.2 Encapsulation and Coating

βTC-tet cells were encapsulated using previously published protocols (Stabler et al. 2001). Briefly, cells were detached from monolayer cultures by trypsinization (0.25% Trypsin-EDTA, Mediatech Cellgro) and suspended at a density of $6.0x10^6$ cells/ml (sub-therapeutic) or $1.0x10^7$cells/ml (therapeutic) in 2% sodium alginate (Pronova Ultra Pure LVM alginate NovaMatrix of FMC BioPolymer AS, Norway). Beads were formed using an electrostatic bead generator (Nisco Engineering AG, Zurich, Switzerland) that generated droplets which fell into a well-stirred 1.1% $CaCl_2$ bath. Cross-linked beads were washed and stored in complete growth medium and cultured overnight (sub-therapeutic) or for 4-6 hours (therapeutic) in a non-treated T-flask on a rocker plate in a 37°C and 5% CO_2, humidified incubator. Beads were coated with poly-L-lysine (PLL) as previously described (Stabler et al. 2001). In short, beads were subjected to subsequent treatments with $CaCl_2$, 2-(Cyclohexylamino) ethanesulfonic acid, PLL (Sigma, MW: 19,200), and 0.2% alginate (same type as above). They were washed and stored in complete growth medium and cultured overnight as indicated above.

6.2.3 Vitrification and Conventional Freezing Protocols

Two different vitrification solutions were used, DPS (3M DMSO +3M 1,2-propanediol (PD)+0.5M sucrose) and P6 (1M DMSO+5M PD +0.34M polyethylene glycol with a molecular weight of 400). Both were prepared using a concentrated and modified version of the EuroCollins carrier solution containing 174.76 g/L dextrose, 5.6

g/L KCl, 4.2 g/L $NaHCO_3$ and 8.2 g/L NaCl. This concentrated EuroCollins solution was diluted in the final solution volume at a ratio of 1:5. All chemicals were from Sigma-Aldrich except sucrose and $NaHCO_3$ (Fisher, Fair Lawn, NJ). Solutions were added to encapsulated cells in a step-wise manner at 4°C as shown in Table 5.1. Rapid cooling from 4°C to -100°C at 100°C/min was achieved by immersion in an isopentane bath held at -135°C; this was followed by slower cooling from -100°C to -135°C at 2°C/min in the vapor phase of a mechanical freezer (Sanyo, San Diego, CA) set at -135°C. A dummy vial with a thermocouple in the final vitrification solution was used to measure cooling rates. Samples were stored overnight before warming rapidly in a bath of 30% DMSO in water at room temperature. CPAs were removed in a step-wise manner at room temperature (Table 5.1). Conventionally frozen (CF) beads were exposed to 10% DMSO in complete growth medium for 10 minutes at 4°C and then transferred to cryovials (Corning Inc., Corning, NY). These were placed in an isopropyl alcohol bath (Nalgene of Thermo Fisher Scientific, Rochester, NY) in a -80°C mechanical freezer (VWR, West Chester, PA) for 90 minutes before being plunged into liquid nitrogen (-196°C). Vials were stored overnight before being warmed by agitation in a 37°C water bath until all visible ice had melted. Beads were then incubated in complete growth medium for 10 minutes at 37°C and washed with complete growth medium.

6.2.4 Sub-therapeutic *in vivo* Techniques

All *in vivo* procedures were done in compliance with the Georgia Tech Institutional Animal Care and Use Committee. Sub-therapeutic studies were carried out in 5-week old, healthy Balb/c mice (The Jackson Laboratory, Bar Harbor, ME). Prior to implantation, preserved or fresh beads were washed three times with unsupplemented 25

mM glucose DMEM (Sigma-Aldrich). Briefly, mice were anesthetized to a surgical plane with 1.5% isoflurane in oxygen. Hair was removed from the surgical site, which was prepped with chlorhexadine and isopropyl alcohol. A small midline abdominal incision was made through the skin and a 16 gauge needle was inserted to deliver 0.2 ml fresh or preserved beads. The muscle layer was closed with sutures and the skin layer with wound clips. Mice were allowed to recover until ambulatory before subcutaneous administration of 0.05 mg/kg buprenorphine. Blood glucose levels were monitored daily throughout the experiment using the Truetrack Blood Glucose Monitoring System (CVS/pharmacy, Woonsocket, RI). Mice with blood glucose less than 100 mg/dL were given 1 mg/ml tetracycline (Sigma-Aldrich) in 2.5% sucrose (Fisher) solution as a replacement for water to regulate growth of the encapsulated βTC-tet cells (Black et al. 2006; Simpson et al. 2005). Mice were euthanized by asphyxiation on Days 2 and 7 post-implantation.

6.2.5 Therapeutic *in vivo* Techniques

For therapeutic studies, 10-week old male Balb/c mice (The Jackson Laboratory) were injected with repeated doses of streptozotocin (Sigma) in 0.09M citrate buffer solution (Sigma) at a dosage of 210 mg/kg. Mice were considered diabetic after two consecutive non-fasting blood glucose levels of 350 mg/dL or higher. Blood glucose levels were monitored using the Truetrack Blood Glucose Monitoring System (CVS/pharmacy). After confirmation of a diabetic state, mice were implanted with 0.3 ml of fresh or preserved alginate/poly-L-lysine/alginate (APA) beads. Surgery procedures were the same as for sub-therapeutic studies. Immediately post-implantation, the implant was considered to have failed if blood glucose levels did not fall within the

defined normoglycemic range (50-250 mg/dL) within four days. Thereafter, constructs were considered to have failed when two consecutive blood glucose readings were above 250 mg/dL. Mice with blood glucose less than 100 mg/dL were given 4 mg/ml tetracycline (Sigma-Aldrich) in 2.5% sucrose (Fisher) solution as described above. Mice were sacrificed and explants retrieved upon construct failure or 14 days after implantation. Mice were euthanized by CO_2 asphyxiation.

6.2.6 Post-Explantation Assessment

To determine high-glucose insulin secretion, 100 µL of APA beads were incubated with complete growth medium for one hour in a 37°C and 5% CO_2, humidified incubator. Samples were taken at t=0 and at t=1 hour and were analyzed with a Mouse Insulin ELISA (Mercodia, Uppsala, Sweden).

Live-Dead imaging of cells in beads was performed using the LIVE/DEAD® Viability Cytotoxicity Kit (Molecular Probes® by Invitrogen™, Carlsbad, CA). Beads were incubated for 20 minutes in 0.9% NaCl containing 2µM calcein AM and 4µM ethidium homodimer-1, and images were acquired using an LSM 510 UV confocal microscope (Carl Zeiss) with excitation at 488 nm and 543 nm. Histological images were obtained as follows. APA beads were fixed in 2% glutaraldehyde (Sigma) in 0.9% NaCl and subsequently embedded using the Immunobed Embedding Kit (Electron Microscopy Sciences, Hatfield, PA). To minimize changes in morphology caused by the embedding process, embedding was performed with increasing concentrations of resin in double-distilled water similarly to previously reported procedures (James et al. 2004). After embedding, 5 µm sections were sliced with a Microm 355H Microtome (Thermo Fisher

Scientific, Walldorf, Germany), mounted and stained with 1% Toluidine Blue (Research Organics, Cleveland, OH) to visualize the alginate matrix.

6.2.7 Statistical Analysis

Statistical calculations were performed using a one-way ANOVA and Tukey's test to determine differences between test groups. Values of $p<0.05$ were considered to indicate statistically significant differences.

6.3 Results

6.3.1 Sub-therapeutic *in vivo* Studies

Results for high-glucose insulin secretion from beads before implantation and from beads explanted from mice on Days 2 and 7 are shown in Figure 6.1. Although there were no differences between groups pre-implantation, beads vitrified with DPS performed significantly worse than fresh and the other preserved groups after two days *in vivo*. By day 7, the performance of the beads became highly variable and any differences were masked. Several mice from each group received tetracycline to arrest cell growth due to lower blood glucose levels. In spite of this, insulin secretion appeared to increase with time for all groups, indicating cell growth in the implanted beads.

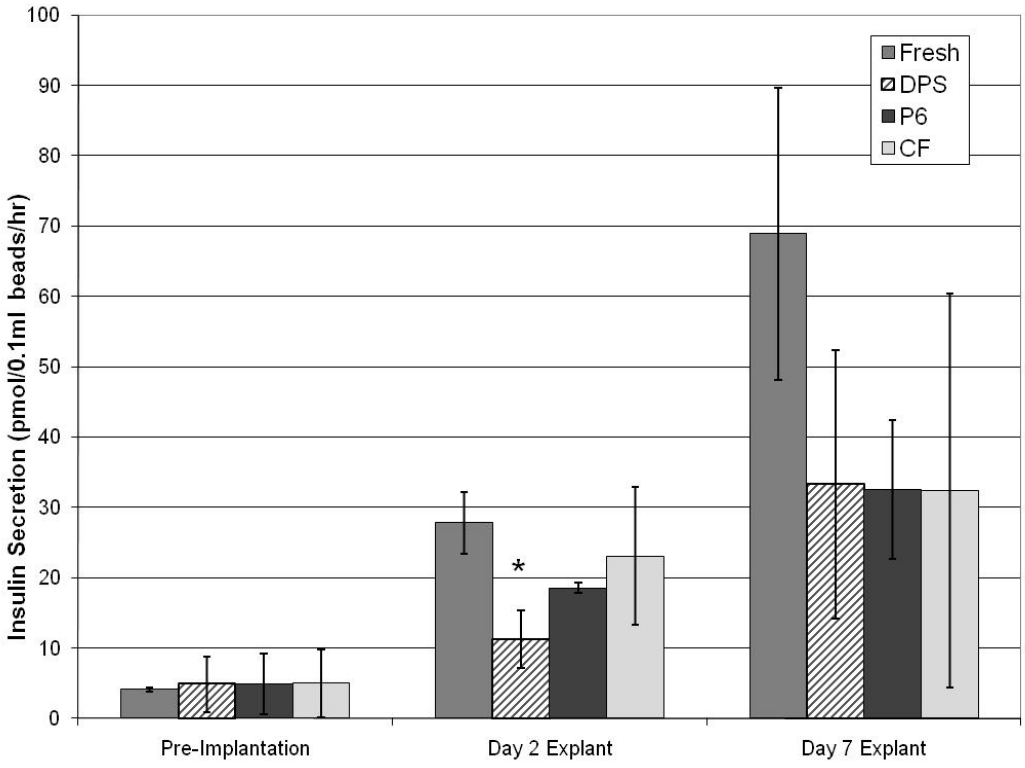

Figure 6.1. Sub-therapeutic high-glucose insulin secretion for fresh and preserved groups pre-implantation and at 2 and 7 days post-explantation, *n=3*. * indicates $p<0.05$ when compared to same day fresh. CF indicates conventionally frozen.

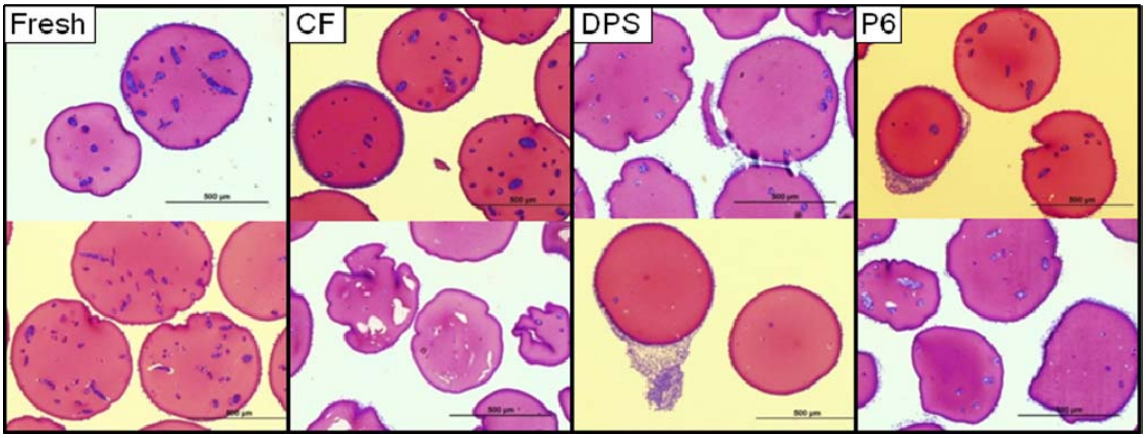

Figure 6.2. Sub-therapeutic histology for explanted beads, day 7. Images representative of *n=3.*

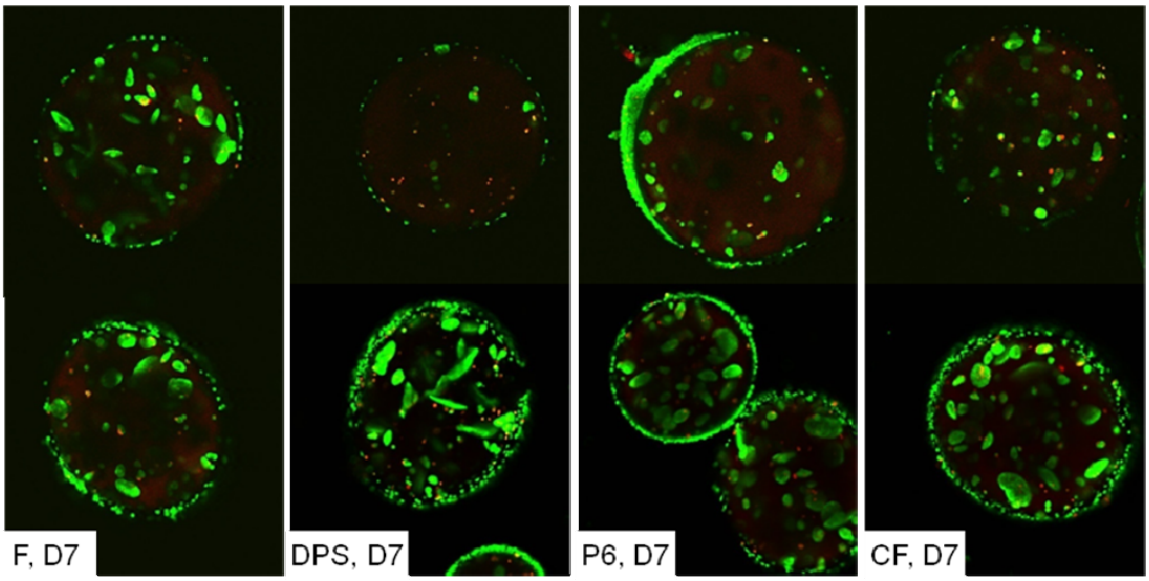

Figure 6.3. Sub-therapeutic Live-Dead imaging for explanted beads, day 7. Images representative of *n=3.*

Histological images of beads explanted on day 7 are shown in Figure 6.2. The levels of host-cell attachment were highly variable and there were no noticeable trends across groups. The alginate matrix appeared to be damaged in some conventionally frozen explants. Live-Dead imaging (Figure 6.3) revealed no correlation between host-cell attachment and cell viability within the constructs. In most of the explanted beads, the majority of the cells were alive, and images indicated significant cell growth by day 7. However, upon explantation, beads vitrified using DPS exhibited greater variability than the other groups, with several explants yielding DPS beads with high viability as well as beads with only dead cells. Generally, these images revealed single dead cells or larger clusters of mostly living cells.

6.3.2 Therapeutic *in vivo* Studies

Overall *in vivo* performance of preserved and fresh beads is shown in Figure 6.4A. Average blood glucose levels for mice are given in Figure 6.4B. Fresh and conventionally frozen beads performed comparably, with both groups lowering blood glucose levels to less than 250 mg/dl relatively quickly and maintaining blood glucose within the defined range (50-250 mg/dl) for the majority of the experiment. Mice implanted with either of the vitrified groups did not perform as well as those given fresh beads. Of the two vitrified groups, beads vitrified with DPS did not appear to perform as well as those vitrified with P6. Mice implanted with DPS-vitrified beads took significantly longer to revert to the defined normoglycemic range than fresh or conventionally frozen. Table 6.1 shows the number of implants from each group that was able to revert mice to the normoglycemic range for more than two days. Three implants vitrified with DPS were unable to revert mice to normoglycemia within four days and 2

additional implants were only able to revert mice for one or two days. Of the 8 mice implanted with DPS-vitrified beads, only 3 mice achieved and maintained blood glucose levels within the defined normoglycemic range. Beads vitrified with P6 were slightly more efficacious with only 3 of 8 implants failing and the rest maintaining normoglycemia throughout the experiment.

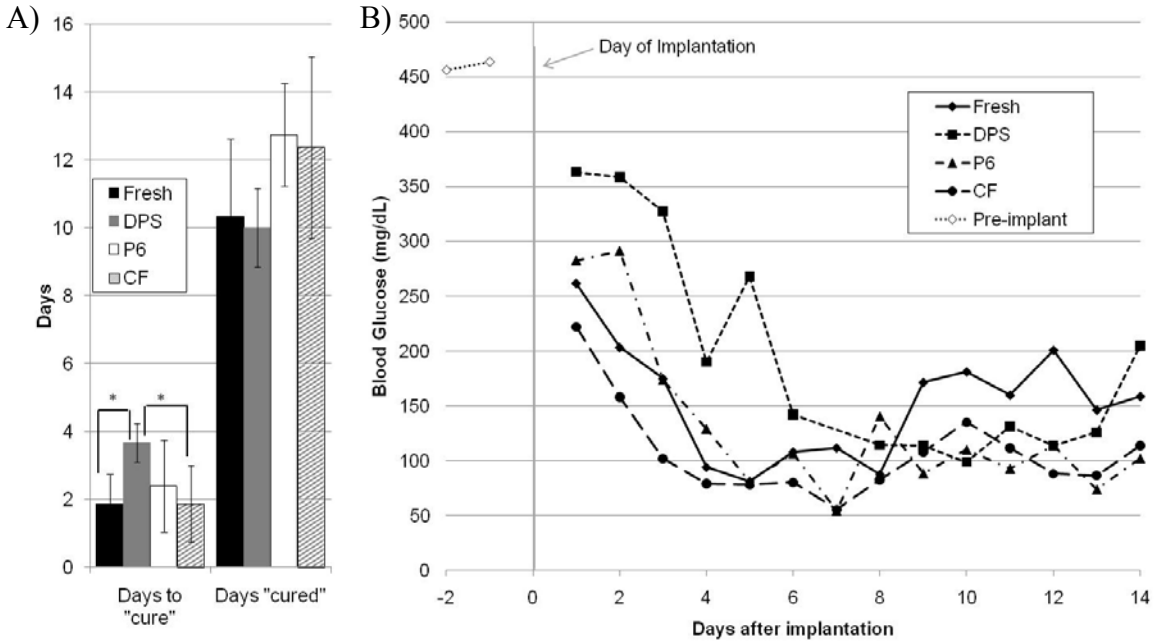

Figure 6.4. A) Days post-implantation to revert mice to normoglycemia and total days of normoglycemia B) Average blood glucose levels. *n=3-9: n-value decreased as mice were sacrificed.* * indicates $p<0.05$.

Table 6.1. *In vivo* efficacy of implants in streptozotocin-induced Balb/c mice.

Number of constructs maintaining normoglycemia in mice for more than two days	
Fresh	7 out of 8
Conventionally Frozen	8 out of 8
Vitrified (DPS)	3 out of 8
Vitrified (P6)	5 out of 8

Mice were explanted upon failure or after 14 days. Post-explantation insulin secretion is shown in Figure 6.5. These results include explants that failed although trends were similar when the failed explants were excluded (data not shown). All preserved groups secreted significantly less insulin than fresh. Biomaterial assessment of explanted beads is shown in Figures 6.6-6.8. Pre-implantation microscopy of fresh and preserved groups is also shown in Figure 6.6 for comparison. Explanted beads exhibited variability between mice and between beads from a single explant. Microscopy images reveal cell growth, host-cell attachment and occasional damage to the beads. This damage appears to have occurred during the *in vivo* period and occurred to some extent in all groups. Live-Dead Imaging (Figure 6.7) reveals similar trends but also shows single dead cells in premature explants and living cell clusters in successful implants. Histological images (Figure 6.8) show cell growth and *in vivo* damage to the beads.

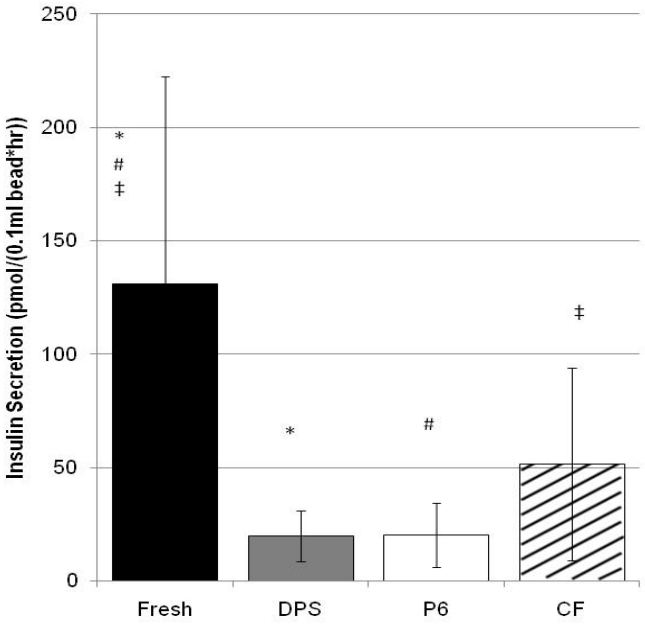

Figure 6.5. Post-explantation insulin secretion including "failed" explants. #,*,‡ indicates $p<0.05$ when comparing groups. *n=8* for CF, DPS, P6, *n=5* for fresh.

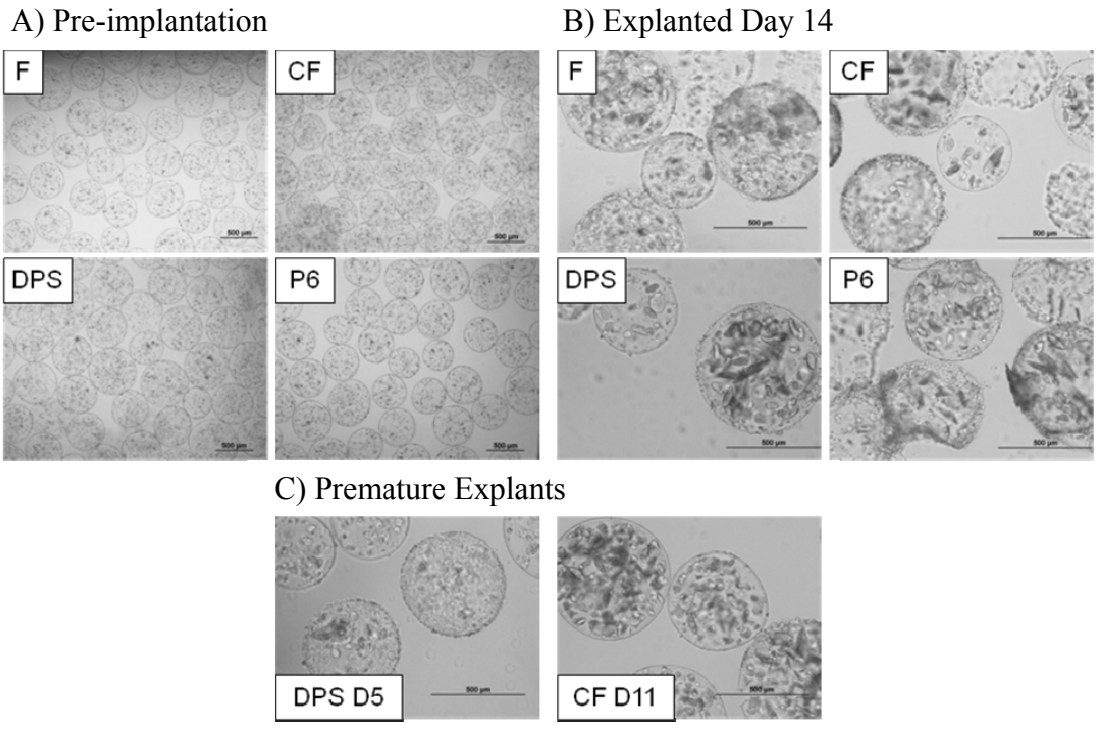

Figure 6.6. Microscopy of fresh and cryopreserved beads A) before implantation, B) explanted after 14 days *in vivo* and C) prematurely explanted due to "failure", scale bar indicates 500 µm. D5 and D11 indicate days of explants, day 5 and day 11, respectively.

A) Explanted Day 14

B) Premature Explants

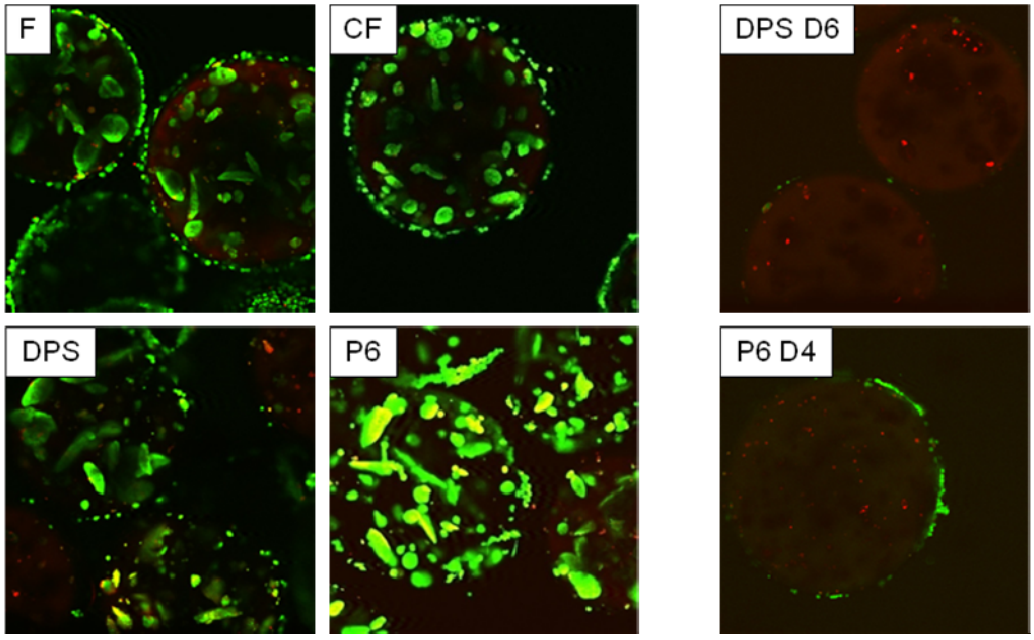

Figure 6.7. Live-Dead imaging of beads A) explanted after 14 days *in vivo* and B) prematurely explanted due to "failure". D6 and D4 indicate days of explants, day 6 and day 4, respectively.

A) Explanted Day 14

B) Premature Explants

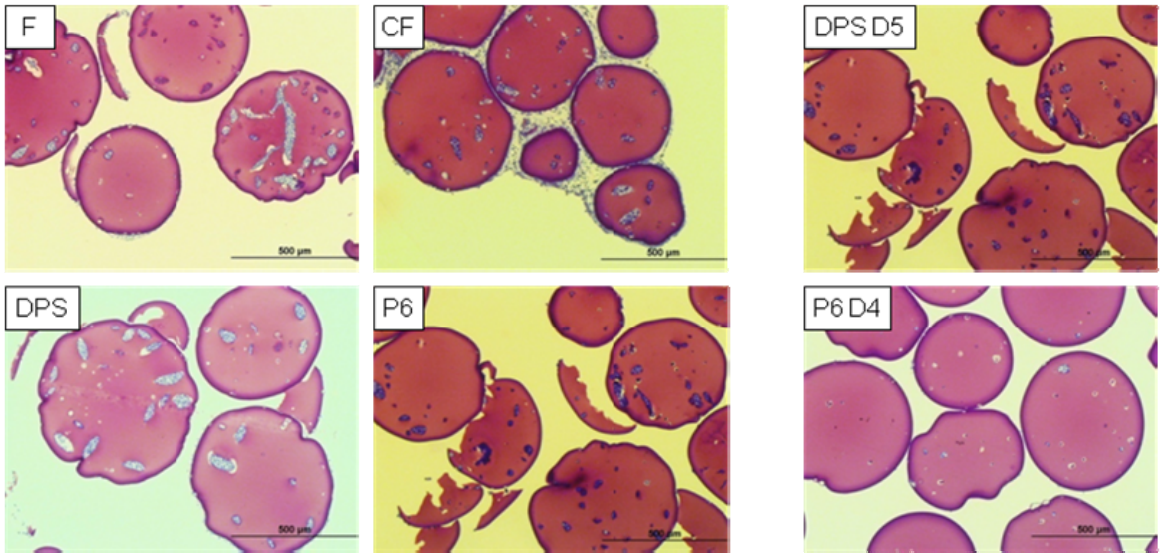

Figure 6.8. Histological images of beads A) explanted after 14 days *in vivo* and B) prematurely explanted due to "failure".

6.4 Discussion

6.4.1 Sub-therapeutic *in vivo* Studies

To determine the best method of preservation for a tissue-engineered construct, it is critical to compare the *in vivo* performance of both vitrified and conventionally frozen constructs as well as the fresh or unpreserved control. Although significant research has been done to determine the efficacy of vitrification, little of this work has compared vitrified to conventionally frozen or investigated the *in vivo* performance. Sub-therapeutic studies were done to allow for direct comparison of biomaterial and cellular function at two time points: days 2 and 7. These studies revealed that beads vitrified using DPS secreted significantly less insulin than all other groups after explantation on day 2. However, all groups fared well *in vivo* and insulin secretion studies paired with Live-Dead imaging indicate that the cellular component does regenerate *in vivo*. Biomaterial assessment indicated that both fresh and preserved beads experienced minimal host response within the seven days of the experiment. These results suggest that preserved groups may perform comparably to fresh although it was unclear whether beads vitrified with DPS would recover quickly enough to have a therapeutic effect *in vivo.* The *in vivo* therapeutic efficacy of a tissue-engineered construct remains the ultimate assessment of success.

6.4.2 Therapeutic *in vivo* Studies

In therapeutic studies, conventionally frozen beads were found to perform comparably to fresh, both in the time necessary to revert diabetes and in the number of mice maintained in the normoglycemic range throughout the experiment. The success of conventional freezing in the preservation of alginate-encapsulated cells is not

unprecedented (Malpique et al. 2010; Stiegler et al. 2006) and is likely due to the nature of the encapsulation. Cells were suspended in alginate without adhesive motifs resulting in an environment similar to a cell suspension. Ice forms preferentially in the extracellular matrix of the alginate (Karlsson and Toner 2000) which may not detrimentally affect the cells suspended in the alginate.

Vitrified beads did not perform as well as conventionally frozen or fresh beads. Beads vitrified using P6 or DPS reverted diabetes in only 5 of 8 or 3 of 8 mice, respectively. Additionally, beads vitrified with DPS took significantly longer to revert diabetes than either fresh or conventionally frozen (Figure 6.4). These results corroborate the sub-therapeutic performance of beads vitrified with DPS and indicate that the cellular component may not have had sufficient time to regenerate and have a therapeutic effect. Previous studies from our laboratory indicate comparable or better *in vitro* performance of vitrified alginate beads when compared to conventionally frozen beads (Mukherjee et al. 2005). It is not entirely clear why vitrification resulted in such poor *in vivo* performance in these studies. The high concentrations of CPAs present in the vitrification solutions are cytotoxic and cause a loss of cell viability (Lawson 2011). These effects may be amplified in the current studies due to the low cell density. A low dose was necessary in sub-therapeutic studies to minimize the therapeutic effect. Additionally, therapeutic studies required a low cell density due to the implant volume, therapeutic dose of cells and need to retrieve beads after euthanization. Post-explantation assessment required a minimum measurable volume of 0.05 ml beads. An implant volume of 0.3 ml was chosen to increase the probability of retrieving this volume. Preliminary *in vivo* studies determined the approximate cell number necessary to have a

therapeutic effect within one or two days of implantation, leading to an encapsulation density of $1.0x10^7$ cells/ml. The lower cell density of either study was likely exacerbated *in vivo* due to the dispersion of microencapsulated beads within the intraperitoneal cavity. High cell densities have been shown to significantly increase insulin secretion in beta cell lines, relative to low cell densities, due to the change in cell-cell signaling (La Flamme et al. 2007; Luther et al. 2005). Higher cell density encapsulations have also been shown to retain cell viability and function better during conventional freezing (Murua et al. 2009). This may also be the case for vitrification. Vitrification of a low cell density encapsulation may result in a low viable cell density that is slow to recover and is too low to have a therapeutic effect, especially when implanted in the intraperitoneal cavity.

Upon explantation, biomaterial assessment revealed that APA beads incurred damage and host-cell attachment while *in vivo*. Neither of these phenomena appear to correlate to the test group, whether preserved or fresh. Additionally, cell death does not appear to be due to host-cell attachment or compromised bead integrity. This is likely due to the short time frame of the experiment. The host-cell attachment that is seen may be truncated due to the time *in vivo* and would likely increase if the experiment was lengthened. Bead integrity is critical to the long-term success of an implant as it provides a level of immunoprotection. However, unencapsulated allogeneic islets can last eight days *in vivo* (Vergani et al. 2010). As it is clear that the matrix damage occurred during the *in vivo* period, it is reasonable that the damaged beads maintained viability comparable to that of intact beads upon explantation. The *in vivo* use of APA beads is widespread and has resulted in conflicting reports, specifically regarding the immune response to the beads and specific encapsulation parameters (Orive et al. 2006). Despite

the variability in the explanted biomaterial, which has also been noted by other groups (Safley et al. 2008), it is clear that the ice formation that occurs during conventional freezing does not compromise the biomaterial integrity enough to result in poor *in vivo* performance. The ice damage that the alginate matrix incurs during conventional freezing (Mukherjee et al. 2005) may not compromise the semi-permeable membrane, overall morphology or strength of the bead (Murua et al. 2009).

The insulin secretory function of explanted beads was also variable, especially for the fresh and conventionally frozen beads, but still revealed statistical differences. All preserved beads secreted significantly less than fresh on an explanted volume basis. Although not statistically significant, this also appeared to be the trend in sub-therapeutic studies. This would be expected for the poor-performing vitrified groups. The reason for the poor performance of explanted conventionally frozen beads is more difficult to ascertain. Although many mice with conventionally frozen implants received tetracycline, further review of the data reveals that many of the explants that were exposed to tetracycline also secreted more insulin upon explantation than those that did not. Tetracycline was also administered to several mice implanted with fresh beads. It is unlikely that tetracycline is the cause of the lower insulin secretion seen for explanted conventionally frozen beads. In spite of the lower insulin secretion post-explantation, conventionally frozen beads exhibit *in vivo* efficacy comparable to fresh beads. This suggests that there is a range of viable implanted cell number that will have a therapeutic effect *in vivo.* Conventionally frozen beads may be on the lower end of this range. All of these results were calculated on a per volume basis as the beads cannot easily be dissolved. To measure volumes as accurately as possible, an attempt was made to use

beads with minimal or no host-cell attachment. This may have contributed to the variations in insulin secretion results.

6.5 Conclusions

Preservation is a critical step in bringing a tissue-engineered construct from the benchtop to the clinic. Of the two main types of cryopreservation, vitrification is often considered to be the most promising due to the elimination of ice formation. These studies investigated the cryopreservation of a widely used encapsulated cell system. Although previous studies indicate that ice damage may occur in the alginate matrix during conventional freezing, this damage appears to be negligible in the experimental, therapeutic *in vivo* system. Conventionally frozen APA beads perform comparably to fresh while vitrified beads perform significantly worse. Additionally, biomaterial assessment upon explantation indicates that all groups experience similar damage and host-cell attachment during two weeks *in vivo*. It has been shown that ice damage is detrimental when considering constructs or natural tissues that serve an important mechanical function (Schenke-Layland et al. 2007), but this does not appear to be the case for an encapsulated cell system that primarily serves as a physical barrier for immune cells.

CHAPTER 7

CONCLUSIONS AND FUTURE DIRECTIONS

7.1 Conclusions

The field of Tissue Engineering continues to grow rapidly through the use of novel biomaterials and the incorporation of a variety of cell types, including stem cells. Unfortunately, there remains a gap in the knowledge of preservation techniques for most of these constructs. In this thesis, we have approached the preservation of one of the most commonly used tissue-engineered constructs, encapsulated cells. CPA addition and removal protocols for vitrification were rationally designed using an expanded mathematical model. In order to better understand the effects of cryopreservation on an encapsulated cell system, the biomaterial and cellular function were evaluated *in vitro* and *in vivo* for the two main types of cryopreservation: conventional freezing and vitrification. This thesis has contributed to the field of cryopreservation and tissue engineering by systematically comparing the effects of these two types of preservation on one of the most commonly used technologies, cell encapsulation.

In the first part of the thesis, the previously described mathematical model (Mukherjee et al. 2008) was expanded to incorporate heat transfer as well as cytotoxicity due to CPA exposure. Cytotoxicity kinetics were determined experimentally and are reported in Chapter 3. These results indicate that for the βTC-tet cell line, the CPA toxicity is contingent upon the time and temperature of exposure, CPA identity and concentration as well as the cell type and, more specifically, the metabolic activity of the

cells. Additionally, the use of CPA cocktails to minimize the toxicity of the overall solution may not be as effective as previously thought. Our results indicate that the addition of non-permeating solutes may serve to increase the intracellular concentration of permeating CPAs which increases the toxicity experienced by the cells. These cytotoxicity results were incorporated into the expanded mathematical model for the design of CPA addition and removal protocols (Chapter 4).

The previously described mathematical model described the mass transfer of CPAs through the matrix of the bead and the subsequent permeability of these CPAs through the cell membrane. This allowed the design of addition and removal protocols that maintained cell osmotic excursions within a tolerable range. This has been validated experimentally (Mukherjee et al. 2007). The incorporation of heat transfer and a cytotoxicity equation based on experiment allowed for more insight into the design of addition and removal protocols. Simulations indicate that, for the βTC-tet cell line, the temperature of CPA exposure is the most critical parameter. Mathematical simulations were also done for a more recalcitrant tissue, articular cartilage. These simulations also indicate that the most critical parameter for successful vitrification of a tissue is the temperature of exposure. For this large construct, temperature of removal is also critical. Overexposure also leads to a decrease in viable cell number. For successful vitrification, it is critical to ensure full equilibration throughout the sample while minimizing the cells' overexposure to CPAs. A mathematical model, such as this one, is widely applicable for the design of appropriate addition and removal protocols.

The second part of the thesis was designed to address the two types of cryopreservation and their effects on an encapsulated cell system. Chapter 5 focuses on

the *in vitro* evaluation of the biomaterial component and cellular component after preservation. The function of the alginate/poly-L-lysine/alginate (APA) bead is to provide a physical barrier between the implanted cells and the host cells that play a role in the immune protection of the implant. *In vitro* results revealed no significant differences in the biomaterial although occasional instances of damage to the alginate matrix, likely due to ice formation, were seen for conventionally frozen beads. Additionally, post-thaw viability and insulin secretion were similar for all groups, preserved or fresh. A transient increase in basal insulin secretion was seen for beads vitrified using P6 although this difference may not affect the *in vivo* performance. *In vitro* studies indicated that APA beads can be successfully preserved by conventional freezing or vitrification. These results also suggested that preserved beads would perform similarly to fresh beads when implanted *in vivo*. It remained unclear whether possible ice damage to the alginate matrix, seen occasionally in conventionally frozen beads, would affect the inflammatory immune response towards implanted beads. Despite the similarities seen *in vitro*, the *in vivo* results, as reported in Chapter 6, indicate significant differences in the performance of conventionally frozen and vitrified beads. Both vitrified groups showed less success in reverting streptozotocin-induced diabetic mice to a normoglycemic range. Additionally, one of the vitrified groups took significantly longer to revert diabetes than fresh or conventionally frozen. Explant assessment indicated that the ice formation that occurs in conventional freezing does not have a noticeable effect on the *in vivo* response to an APA bead. The encapsulated APA system is very similar to a cell suspension and, likely due to this, it appears that conventional freezing is the better method of preservation for this system.

This thesis utilized rational design of CPA addition and removal for an encapsulated cell system and determined the effects of both vitrification, or ice-free cryopreservation, and conventional freezing on the *in vitro* and *in vivo* performance of the system. The described mathematical model can be used to design addition and removal protocols and can be used for a range of natural tissues or tissue-engineered constructs. More generally, this thesis indicates the need for systematic assessment of conventional freezing and vitrification for the preservation of each tissue or tissue-engineered construct. Although vitrification is often used specifically to eliminate ice formation and ice damage, it can be more technically complex than conventional freezing. Therefore, with the long-term goal of clinical relevance, it is important to determine whether any benefits of vitrification outweigh the difficulties associated with its complexity. For the investigated system, conventional freezing appears to be sufficient and requires less technical expertise.

7.2 Future Directions

7.2.1 Fundamental Cryopreservation Work

In the field of cryobiology, significant work has been done to address the fundamental understanding of conventional freezing. This understanding has been critical to the progress that has been made in the conventional freezing of different cell types and systems. Currently, most vitrification literature focuses on the application of vitrification in the preservation of larger tissues or constructs. Different groups have proposed the use of novel CPA cocktails (Agudelo et al. 2009), but there does not appear to be a systematic method that is used in the design of these cocktails. To systematically assess and then design CPA cocktails, two properties must be determined: the glass-

forming ability of the solution and the cytotoxicity. CPA cytotoxicity is currently one of the most critical challenges for successful vitrification (Fahy 2010). The CPA concentration necessary is determined based on its glass-forming ability. Differential scanning calorimetry (DSC) can be used to determine the glass-transition temperature as well as the critical cooling and warming rates for a solution. The use of different additives or non-permeating CPAs and different mixtures of permeating CPAs can be systematically evaluated for glass-forming ability and cytotoxicity. This will allow for a better understanding of the different CPAs and their use in cocktails. It is currently unclear how CPAs may interact with each other and how this will affect the glass-forming ability of the solution and its overall cytotoxicity. The issue of cryoprotectant toxicity neutralization is clearly important (Fahy 2010), and these studies would add significant insight to this theory. They may also lead to better design of CPA cocktails for the vitrification of recalcitrant tissues.

7.2.2 Mathematical Modeling

A previously described mathematical model has been expanded in this thesis so that vitrification CPA addition and removal protocols can be systematically designed and better understood. This model focuses on a relatively simple geometry with homogeneous cell distribution and biomaterial properties. As the field of Tissue Engineering continues to grow, the constructs that are developed will become more complex. This has already occurred for the tissue-engineered pancreatic substitute. Researchers are investigating the use of prevascularized beds (Pileggi et al. 2006), seeded endothelial cells (Jay et al. 2010) or novel heterogeneous biomaterials (Mason and Mahoney 2010) to address the issue of vascularization which is critical for encapsulated

islets. Newly developed constructs will require cryopreservation. The current mathematical model could easily be changed to reflect some of the complexities that may be incorporated in new constructs. The use of anisotropic materials would affect the mass transfer through the matrix. Anisotropy occurs in natural tissues also, such as mature bovine articular cartilage where cell density and distribution vary throughout (Jadin et al. 2005). More complex constructs may also incorporate different cell types which exhibit different permeability constants and different levels of tolerance for osmotic excursions. The modeling of cell-clusters, such as islets, would require additional considerations. In a cell cluster, such as an islet, the mechanism of CPA mass transfer would likely be different. Mass transfer could occur through microvasculature. Additionally, if no vasculature is present, mass transfer could occur through direct contact of cell membranes and would rely upon the permeability of these membranes. Incorporation of any of these complexities in the mathematical model would also make it more easily applicable to natural tissues.

7.2.3 Cryopreservation of Tissue-Engineered Constructs

The main advantage of vitrification is that it eliminates ice formation. Ice formation may not be critical for the preservation of an encapsulated cell system due to its size, high diffusivity and the suspended nature of the cells. It has been suggested that vitrification and conventional freezing may perform comparably when working with small tissue structures (Brockbank and Taylor 2007). Due to the complexity of the vitrification process, it is important to ensure that vitrification is necessary by comparing the effects of both types of cryopreservation on a specific construct. Encapsulated islets have been used increasingly in the laboratory setting for the treatment of diabetes.

Determining the best method of cryopreservation of this system would be the most direct extension of this thesis. Iwata's research group in Japan has utilized a new vitrification solution for the vitrification of encapsulated islets. They indicate that vitrified islets were able to revert diabetes in mice, although this required twice the number of encapsulated islets as compared to unpreserved islets (Agudelo et al. 2009). This indicates that these islets may have incurred damage during the vitrification process, possibly due to unsuccessful vitrification at the core of the islets. The cryosubstitution technique, in which an organic solvent is introduced at the temperature of storage and dissolves any ice that has formed, can be used to visualize ice formation. This method could be used to corroborate the successful vitrification of the islets. The mathematical model, as explained above, could be changed to reflect the mass transfer of CPAs through the islets. Properly designed protocols would minimize the chance of ice formation. Although the cryopreservation of free and encapsulated islets has been shown in literature, a systematic comparison of the two methods is necessary. It remains to be seen whether conventional freezing will be sufficient for the preservation of most encapsulated systems.

Within the context of a load-bearing construct or a construct that primarily serves a mechanical function, the elimination of ice may be critical to the performance of the construct. Ice formation can lead to a loss of mechanical integrity and important physiological properties, such as viscoelasticity (Thakrar et al. 2006) or contractility (Dahl et al. 2006). Future studies of the effects of cryopreservation should focus on more complex tissues or tissue-engineered constructs. Adherent cells seeded into a hydroxyapatite matrix require that these cells remain attached for proper function, but conventional freezing has been shown to cause detachment (Liu et al. 2006). It is

systems such as these, where ice formation is particularly damaging, that should be investigated.

Additionally, it is critical that studies on the effects of cryopreservation look deeper into the mechanisms of damage. Many studies have addressed the preservation of hepatocytes, a commonly used cell type, but few have investigated the reason for nonattachment after conventional freezing (Terry et al. 2007). Understanding of the molecular mechanisms behind different types of cryodamage will allow better design of procedures and will lead to more successful cryopreservation methods.

APPENDIX A

SUPPLEMENTARY DATA OF CYTOTOXICITY EFFECTS OF CRYOPROTECTANTS AS SINGLE-COMPONENT AND COCKTAIL VITRIFICATION SOLUTIONS

This appendix presents supplementary data for CHAPTER 3. The data presented here exhibit the same trends as those shown in CHAPTER 3. Viable cell number was determined using alamarBlue™ which measures the metabolic activity of the cells. Cell viability as determined by Trypan Blue was shown in Chapter 3 as this is a more direct measure of cell toxicity. The trends for alamarBlue™ results are very similar to those obtained by the Trypan Blue dye exclusion assay (CHAPTER 3).

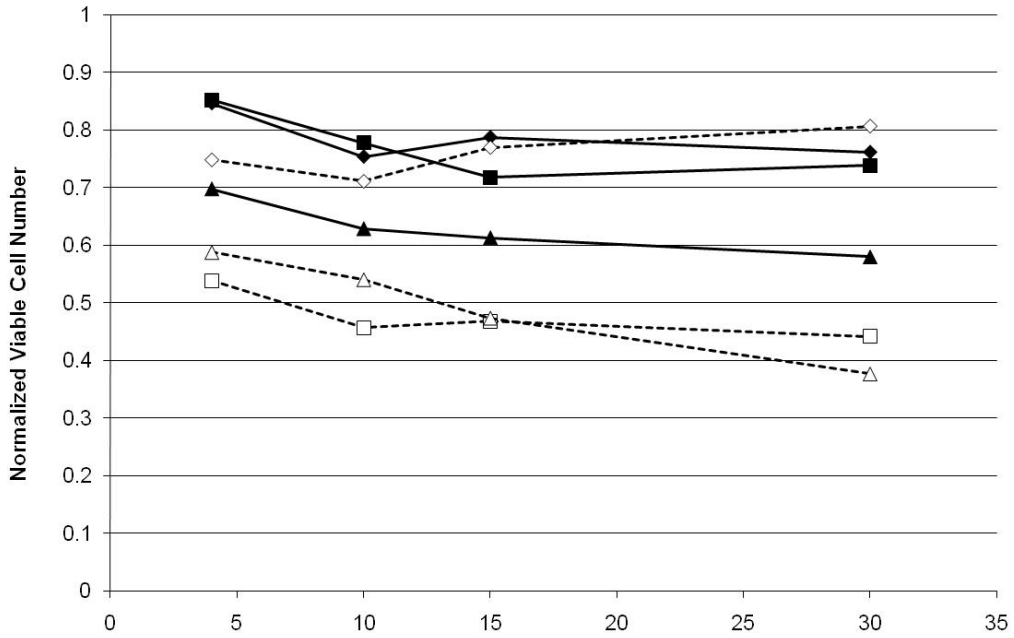

Figure A.1. Viable Cell Number vs. time for DMSO for 2M (—◆—), 4M (—■—) and 6M (—▲—) at 4°C or room temperature (empty) for encapsulated βTC-tet cells. Viable cell number determined by alamarBlue™, normalized to untreated control. Error bars not shown for clarity. Statistical significance shown in Table A.1, *n=3*.

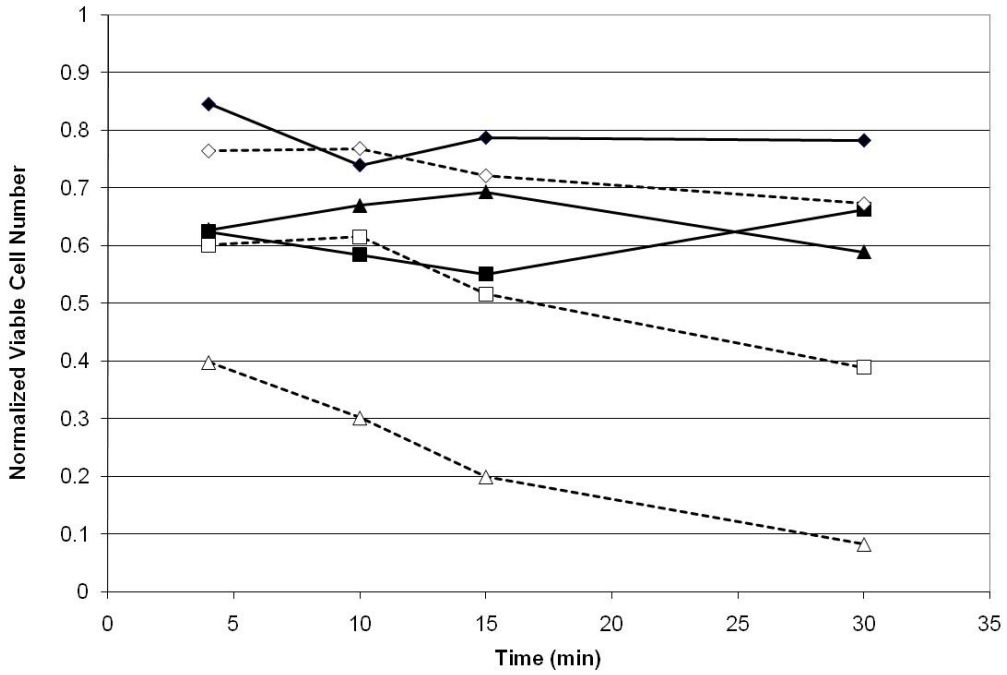

Figure A.2. Viable Cell Number vs. time for PD for 2M (—◆—), 4M (—■—) and 6M (—▲—) at 4°C or room temperature (empty) for encapsulated βTC-tet cells. Viable cell number determined by alamarBlue™, normalized to untreated control. Error bars not shown for clarity. Statistical significance shown in Table A.1, *n=3*.

Table A.1. Pairwise Comparison of Single-Component Cytotoxicity Kinetics. $p<0.05$ for corresponding letters (e.g. $p<0.05$ when comparing 4M and 6M DMSO at 30 minutes at 4°C, letter M)

Viable Cell Number	Incubation at 4°C				Incubation at 25°C			
	4 min	10 min	15 min	30 min	4 min	10 min	15 min	30 min
2M DMSO	O	-	N	L	-	K	I,J	G,H
4M DMSO	A,P	B	C	D,M	A	B,K	C,I	D,G
6M DMSO	E,O,P,Q		F,N	L,M,Q	E	-	F,J	H
2M PD	R,q,r,s	s	p	S,n,o	R,f	d	b,c	S,Y,Z
4M PD	U,q	V	W,p	T,X,n	U,g,i,j	V,e,k,l	W,b,i,k, m	T,X,Y,a, j,l,m
6M PD	r	-	-	o	f,g,h	d,e	b,c	Z,a,h

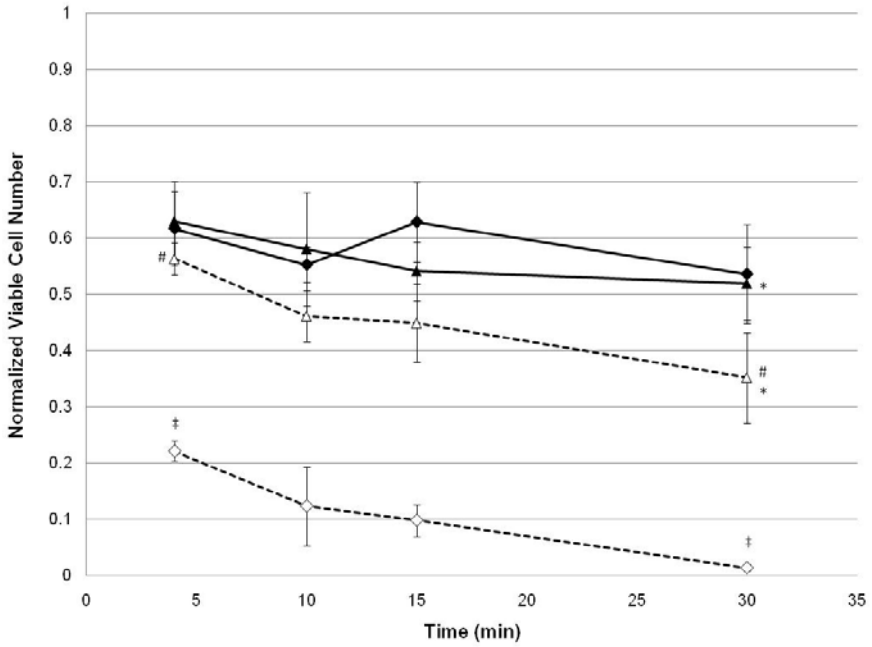

Figure A.3. Viable Cell Number vs. time for P6 (–◆–) and DPS (–▲–) at 4°C or room temperature (empty) for encapsulated βTC-tet cells. Viable cell number normalized to untreated control. Error bars indicate standard deviations, *n=3*. #, *,† indicate $p<0.05$ when comparing groups. Also, $p<0.05$ comparing P6 at RT to all other groups at each time point.

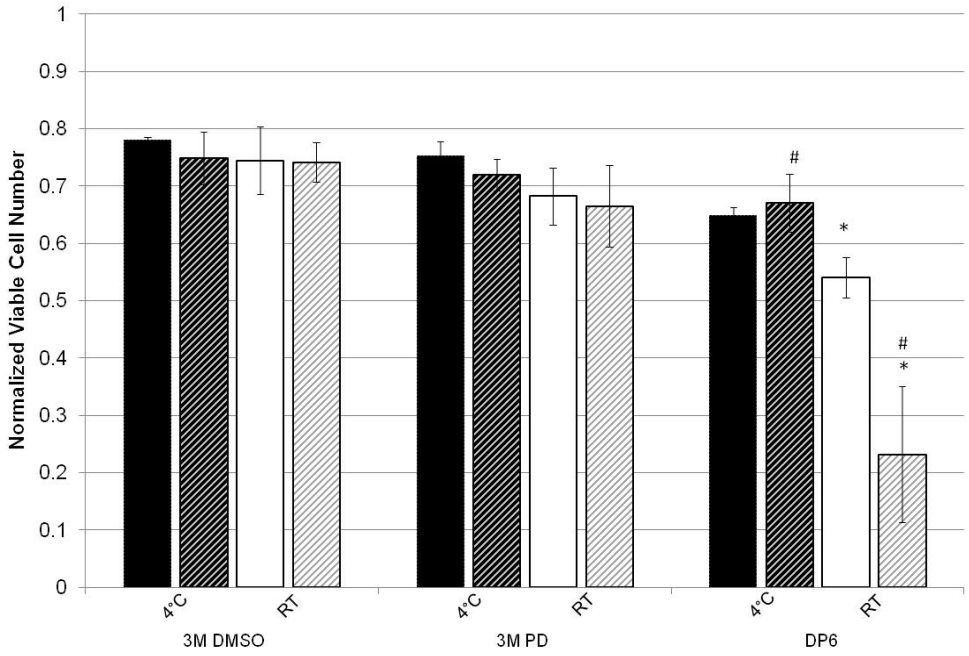

Figure A.4. Viable Cell Number for 3M DMSO, 3M PD and DP6 for encapsulated βTC-tet cells (solids) compared to encapsulated HepG2 cells (stripes) for an incubation period of 15 minutes. Viable cell number normalized to untreated control. Error bars indicate standard deviations, *n=3*. *,# indicates $p<0.05$

APPENDIX B

MATLAB® CODE FOR MATHEMATICAL MODEL

B.1 Introduction

This appendix provides the Matlab® code that makes up the entirety of the mathematical model described in CHAPTER 4. It is shown for the alginate bead. The model consists of a main program which passes variables to sub-programs. The sub-programs calculate the concentration and temperature profiles, convert concentration from molarity to osmolarity, calculate the water volume and solutes within cells at different positions throughout the bead and calculate cytotoxicity as a function of time for cells at different positions throughout the bead.

B.2 Main Program

```
%*********************************************************************
% Institution:        Georgia Institute of Technology
% Dept:        School of Chemical & Biomolecular Engineering
% PI:          A. Sambanis
% Title:       Developing Cryoprotectant Addition-Removal Protocols Using a
%              2-parameter Model for βTC-tet cells
% Authors:     Alison Lawson, Indra Neil Mukherjee and Yang Li
%*********************************************************************
% Clear all global variables needed for simulations
clear;
   global timestep; global Ra; global rstep; global R;
```

```
%CPA information
mwdmso=78.13;          % molecular weight DMSO [g/mol]
ddmso=1.11;            % density DMSO [g/cm^3]
mwpd=76.09;            % molecular weight Propanediol [g/mol]
dpd=1.04;              % density Propanediol [g/cm^3] (PD)
mwfm=45.04;            % molecular weight formamide [g/mol]
dfm=1.133;             % density of formamide [g/cm^3] (FM)
mwsucrose=342.3;       % molecular weight of sucrose [g/mol]

% Experimentally determined density of final solutions for conversion
% between osmolality and osmolarity
dDPSA3=1.098;          %density of final solution of DPS
dP4A4=1.027;           %density of final solution of P6
dsoln=dP4A4;           %!!!Define Solution

% CELLS = βTC tet cells
% Volume information: Vo, Vb determined experimentally by Dr. Mukherjee
Vo=750;                % isotonic cell volume [um^3]
vs=mwdmso/ddmso*1e12;  % partial molar solute volume [um^3/mol]
Vb=0.184*Vo;           % inactive cell volume [um^3]
Vwo=Vo-Vb;             % initial vol. of intracellular H2O [um^3]
A = 4.836*Vo^(2/3);    % surface area of cell [um^2]
Mino=0.3;              % initial intracellular non-perm solute C [osmolarity]
```

```
% Universal gas constant values
    R = 8.21e13;            % universal gas constant [um^3*atm/mol*K]
    Rcal = 1.98721;         % universal gas constant [cal/mol*K]
% Miscellaneous Definitions
  C_EC=0.3*ones(100,1);     % Account for extracellular osmolality
                            % due to EuroCollins [osmolality]
  n = 2;                    % specify the number of CPAs in solution
  Ra =250;                  % Radius of the construct (um)
  rstep=100;                % Number of different radial positions, with lower
                            % number indicating position toward center of bead
  B_CPA{1,1} = 0.0843;      % DMSO virial coefficient
  B_CPA{1,2} = 0.0576;      % PD virial coefficient
  B_CPA{1,3} = -0.0306;     % FM virial coefficient
% Diffusivity data
  alpha=1.4586e11;          % thermal diffusivity of water [um^2/s]
% Assume Arrhenius Equation for Diffusivity dependence on T
  Ao = [0.593e3 0.293e3 0.893e3]; % Pre-exponential Factor for DMSO, PD &
                                  % FM [um^2/s]
  Ao_S = 0.178e3;                 % Pre-exponential Factor for sucrose [um^2/s]
  Eact = [1.895e17 3.67e17 1.359e17];
                                  % Activation Energy for DMSO, PD &
                                  % FM [um^3*atm/mol]
  Ea_S = 4.198e17;                % Act. Energy for Sucrose [um^3*atm/mol]
```

```
% Define CPA Addition protocol
tinitial = 298;                          % Initial temperature of bead (K)
addsteps=4;                              % Number of addition steps
cpaconcadd=zeros(3,addsteps);            % Create array
cpaconcadd(1,:) = [0.5 1 1 1];           % Conc. of DMSO for each step [M]
cpaconcadd(2,:) = [1 2 4 5];             % Conc. of PD for each step [M]
cpaconcadd(3,:) = [0 0 0 0];             % Conc. of FM for each step [M]
tExtAdd = [298 298 298 298];
 Addition_sucrose = [0 0 0 0.3384];      % Conc. of sucrose for each step [M]
timeadd=[60*3 60*3 60*3 60*3];           % exposure time for each step [s]

% Define CPA Removal protocol
removesteps = 4;                         % Number of removal steps
cpaconcremove=zeros(3,removesteps);      % Create array
cpaconcremove(1,:)= [0.75 0.5 0.25 0];   % Conc. of DMSO for each step [M]
cpaconcremove(2,:)= [4 2 1 0];           % Conc. of PD for each step [M]
cpaconcremove(3,:)= [0 0 0 0];           % Conc. of FM for each step [M]
tExtRem = [298 298 298 298];             % External T for each step [K]
removal_sucrose = [0.2 0.2 0 0];         % Conc. of sucrose for each step [M]
timeremoval=[60*2 60*2 60*2 60*5];       % exposure time for each step [s]
```

```
% Compile Addition & Removal
 steps = addsteps + removesteps;
 cpaconc = [cpaconcadd cpaconcremove];
 sucroseconc= [Addition_sucrose removal_sucrose];
 tExt = [tExtAdd tExtRem];                    %  External T [K]
 Time_All =[timeadd timeremoval];
 sumsteps = steps * 100;
 sumTime =sum(Time_All);
 timestep=100;                                % Number of points for each step
 Conc = zeros(1, rstep);                      % Create array
 Temp = ones(1, rstep)*tinitial;              % Create array
 t2 = zeros(sumsteps,1);
 maxrows = 100*steps;                         % Pre-allocate Profile arrays
 cols = 10;
 Profileat50 = zeros(maxrows, cols);
 Profileat0 = zeros(maxrows, cols);
 ProfileatR = zeros(maxrows, cols);
 loc = [1 100; 101 200; 201 300; 301 400; 401 500; 501 600; 601
                                                  700; 701 800; 801 900; 901 1000];
      % matrix to define elements to store in Profileat0 for each step
```

```
% CPA ADDITION
  for j=1:steps;                    % For loop of addition steps
        tfinal=sum(Time_All(1:j));
        tstart=sum(Time_All(1:(j-1)));
% First determine conc. and T profiles in bead
        if j==1                     % 1st step utilizes initial values
          Ci1 = zeros(1,100);
          Ci2 = zeros(1,100);
          Ci3 = zeros(1,100);
          CiS = zeros(1,100);       % Initially no CPAs present in bead
          ti = ones(1,100);         % Initially no T-gradient in bead
          Ti = tinitial*ti;
          cext = cpaconc(:,j);
          cextS = sucroseconc(j);
          text = tExt(j);
          addtime = Time_All(j);
          [Conc_1 Conc_2 Conc_3 Conc_S Temp] = pdenewmh_total(alpha, Ti, Ci1,
            Ci2, Ci3, CiS, cext, cextS, text, Ao, Eact, Ao_S, Ea_S, addtime);
% Pass diffusivity info, C &T profile in bead & external C to mass/heat pde: p.142
% Return concentration profile of CPAs and temperature profile in bead
        % Input conc. and T profile into cell perm. Eqns at r=0, 50, 100
        y0 = [Vwo; 0; 0; 0];        % Define initial values: Vw=Vwo, Ns=0
          tspan = linspace(tstart, tfinal, timestep);
```

```
    t2(loc(j,1):loc(j,2)) = tspan;
% At r=0
    C_1 = Conc_1(:,1);
    C_2 = Conc_2(:,1);
    C_3 = Conc_3(:,1);
    C_S = Conc_S(:,1);
    C_tot = C_1+C_2+C_3+C_S+C_EC;
    T = Temp(:,1);
% Convert Molarity to Osmolarity: p. 144
    [Osm_1 Osm_2 Osm_3 Osm_S] = conversion (C_1,C_2,
        C_3,C_S,mwdmso,mwpd,mwfm,mwsucrose,dsoln);
    Osm_tot = Osm_1+Osm_2+Osm_3+Osm_S+.3;
% Pass osmolarities to permeability equations: p.146
    [t,y] =ode15s(@(t,y) Perm(t,y,tspan,A,R,T,Osm_tot,...
        Osm_1,Osm_2,Osm_3,Mino,Rcal), tspan, y0);
    Ntot = y(:,2)+y(:,3)+y(:,4);
    Vnorm = 1/Vwo*(y(:,1)+Vb);                    % Normalized cell volume
    yconv = [y(:,2)*1e15./y(:,1) y(:,3)*1e15./y(:,1) y(:,4)*1e15/y(:,1)];
                                                  % Convert from moles/um^3 to M
% Store all profiles
    Profileat0(loc(j,1):loc(j,2),1) = Conc_1(:,1);
    Profileat0(loc(j,1):loc(j,2),2) = Conc_2(:,1);
    Profileat0(loc(j,1):loc(j,2),3) = Conc_3(:,1);
```

```
Profileat0(loc(j,1):loc(j,2),4) = Conc_S(:,1);

Profileat0(loc(j,1):loc(j,2),5) = Temp(:,1);

Profileat0(loc(j,1):loc(j,2),6) = Vnorm;

Profileat0(loc(j,1):loc(j,2),7) = yconv(:,1);

Profileat0(loc(j,1):loc(j,2),8) = yconv(:,2);

Profileat0(loc(j,1):loc(j,2),9) = yconv(:,3);

Profileat0(loc(j,1):loc(j,2),10) = Ntot;

y0at0 = [y(100,1); y(100,2); y(100,3); y(100,4)];
```

% REPEAT FOR DIFFERENT POSITIONS

% At r approx = 125 um from center (123.7)

```
C_1 = Conc_1(:,50);

C_2 = Conc_2(:,50);

C_3 = Conc_3(:,50);

C_S = Conc_S(:,50);

C_tot = C_1+C_2+C_3+C_S+C_EC;

T = Temp(:,50);
```

% Convert Molarity to Osmolarity: p. 144

```
[Osm_1 Osm_2 Osm_3 Osm_S] = conversion (C_1,C_2,...
        C_3,C_S,mwdmso,mwpd,mwfm,mwsucrose,dsoln);

Osm_tot = Osm_1+Osm_2+Osm_3+Osm_S+.3;
```

% Pass osmolarities to permeability equations: p. 146

```
[t,y] =ode15s(@(t,y)Perm(t,y,tspan,A,R,T,Osm_tot,...
        Osm_1,Osm_2,Osm_3,Mino,Rcal), tspan, y0);
```

```
Ntot = y(:,2)+y(:,3)+y(:,4);
Vnorm = 1/Vwo*y(:,1);                    % Normalized cell volume
yconv = [y(:,2)*1e15./y(:,1) y(:,3)*1e15./y(:,1) y(:,4)*1e15/y(:,1)];
                                         % Convert from moles/um^3 to M
% Store all profiles
Profileat50(loc(j,1):loc(j,2),1) = Conc_1(:,50);
Profileat50(loc(j,1):loc(j,2),2) = Conc_2(:,50);
Profileat50(loc(j,1):loc(j,2),3) = Conc_3(:,50);
Profileat50(loc(j,1):loc(j,2),4) = Conc_S(:,50);
Profileat50(loc(j,1):loc(j,2),5) = Temp(:,50);
Profileat50(loc(j,1):loc(j,2),6) = Vnorm;
Profileat50(loc(j,1):loc(j,2),7) = yconv(:,1);
Profileat50(loc(j,1):loc(j,2),8) = yconv(:,2);
Profileat50(loc(j,1):loc(j,2),9) = yconv(:,3);
Profileat50(loc(j,1):loc(j,2),10) = Ntot;
y0at50 = [y(100,1); y(100,2); y(100,3); y(100,4)];
% At r=R
C_1 = Conc_1(:,100);
C_2 = Conc_2(:,100);
C_3 = Conc_3(:,100);
C_S = Conc_S(:,100);
C_tot = C_1+C_2+C_3+C_S+C_EC;
T = Temp(:,100);
```

```
% Convert Molarity to Osmolarity: p. 144
    [Osm_1 Osm_2 Osm_3 Osm_S] = conversion (C_1,C_2,...
            C_3,C_S,mwdmso,mwpd,mwfm,mwsucrose,dsoln);
    Osm_tot = Osm_1+Osm_2+Osm_3+Osm_S+.3;
% Pass osmolarities to permeability equations: p. 146
    [t,y] =ode15s(@(t,y)Perm(t,y,tspan,A,R,T,Osm_tot,...
            Osm_1,Osm_2,Osm_3,Mino,Rcal), tspan, y0);
    Ntot = y(:,2)+y(:,3)+y(:,4);
    Vnorm = 1/Vwo*(y(:,1)+Vb);                    % Normalized cell volume
    yconv = [y(:,2)*1e15./y(:,1) y(:,3)*1e15./y(:,1) y(:,4)*1e15/y(:,1)];
                                                  % Convert from moles/um^3 to M
% Store all profiles
    ProfileatR(loc(j,1):loc(j,2),1) = Conc_1(:,99);
    ProfileatR(loc(j,1):loc(j,2),2) = Conc_2(:,99);
    ProfileatR(loc(j,1):loc(j,2),3) = Conc_3(:,99);
    ProfileatR(loc(j,1):loc(j,2),4) = Conc_S(:,99);
    ProfileatR(loc(j,1):loc(j,2),5) = Temp(:,99);
    ProfileatR(loc(j,1):loc(j,2),6) = Vnorm;
    ProfileatR(loc(j,1):loc(j,2),7) = yconv(:,1);
    ProfileatR(loc(j,1):loc(j,2),8) = yconv(:,2);
    ProfileatR(loc(j,1):loc(j,2),9) = yconv(:,3);
    ProfileatR(loc(j,1):loc(j,2),10) = Ntot;
    y0atR = [y(100,1); y(100,2); y(100,3); y(100,4)];
```

```
else                    % other steps utilize C & T profile from previous step
    r = linspace(0, Ra, rstep);
    Ci1 = Conc_1(100,:)';
    Ci2 = Conc_2(100,:);
    Ci3 = Conc_3(100,:);
    CiS = Conc_S(100,:);
    Ti = Temp(100,:);
    cext = cpaconc(:,j);
    cextS = sucroseconc(j);
    text = tExt(j);
    addtime = Time_All(j);
        [Conc_1 Conc_2 Conc_3 Conc_S Temp] =
    pdenewmh_total(alpha, Ti, Ci1, Ci2, Ci3, CiS, cext,
    cextS, text, Ao, Eact, Ao_S, Ea_S, addtime);
% Pass diffusivity info, C &T profile in bead & external C to mass/heat pde: p. 142
    tspan = linspace(tstart, tfinal, timestep);
    t2(loc(j,1):loc(j,2)) = tspan;
% At r=0
    C_1 = Conc_1(:,1);
    C_2 = Conc_2(:,1);
    C_3 = Conc_3(:,1);
    C_S = Conc_S(:,1);
```

```
C_tot = C_1+C_2+C_3+C_S+C_EC;

T = Temp(:,1);

y0 = y0at0;
```

% Convert Molarity to Osmolarity: p. 144

```
[Osm_1 Osm_2 Osm_3 Osm_S] = conversion (C_1,C_2,...
        C_3,C_S,mwdmso,mwpd,mwfm,mwsucrose,dsoln);

Osm_tot = Osm_1+Osm_2+Osm_3+Osm_S+.3;
```

% Pass osmolarities to permeability equations: p. 146

```
[t,y] =ode15s(@(t,y) Perm(t,y,tspan,A,R,T,Osm_tot,...
      Osm_1,Osm_2,Osm_3,Mino,Rcal), tspan, y0);

Ntot = y(:,2)+y(:,3)+y(:,4);

Vnorm = 1/Vwo*(y(:,1)+Vb);                    % Normalized cell volume

yconv = [y(:,2)*1e15./y(:,1) y(:,3)*1e15./y(:,1) y(:,4)*1e15/y(:,1)];

                                  % Convert from moles/um^3 to M
```

% Store all profiles

```
Profileat0(loc(j,1):loc(j,2),1) = Conc_1(:,1);

Profileat0(loc(j,1):loc(j,2),2) = Conc_2(:,1);

Profileat0(loc(j,1):loc(j,2),3) = Conc_3(:,1);

Profileat0(loc(j,1):loc(j,2),4) = Conc_S(:,1);

Profileat0(loc(j,1):loc(j,2),5) = Temp(:,1);

Profileat0(loc(j,1):loc(j,2),6) = Vnorm;

Profileat0(loc(j,1):loc(j,2),7) = yconv(:,1);

Profileat0(loc(j,1):loc(j,2),8) = yconv(:,2);
```

```
        Profileat0(loc(j,1):loc(j,2),9) = yconv(:,3);

        Profileat0(loc(j,1):loc(j,2),10) = Ntot;

        y0at0 = [y(100,1); y(100,2); y(100,3); y(100,4)];
% At r approx = 125 um from center (123.7)

        C_1 = Conc_1(:,50);

        C_2 = Conc_2(:,50);

        C_3 = Conc_3(:,50);

        C_S = Conc_S(:,50);

        C_tot = C_1+C_2+C_3+C_S+C_EC;

        T = Temp(:,50);

        y0 = y0at50;
% Convert Molarity to Osmolarity: p. 144

        [Osm_1 Osm_2 Osm_3 Osm_S] = conversion (C_1,C_2,...

                C_3,C_S,mwdmso,mwpd,mwfm,mwsucrose,dsoln);

        Osm_tot = Osm_1+Osm_2+Osm_3+Osm_S+.3;
% Pass osmolarities to permeability equations: p. 146

        [t,y] =ode15s(@(t,y) Perm(t,y,tspan,A,R,T,Osm_tot,...

                Osm_1,Osm_2,Osm_3,Mino,Rcal), tspan, y0);

        Ntot = y(:,2)+y(:,3)+y(:,4);

        Vnorm = 1/Vwo*(y(:,1)+Vb);                    % Normalized cell volume

        yconv = [y(:,2)*1e15./y(:,1) y(:,3)*1e15./y(:,1) y(:,4)*1e15/y(:,1)];

                                                % Convert from moles/um^3 to M
```

```
% Store all profiles
        Profileat50(loc(j,1):loc(j,2),1) = Conc_1(:,50);
        Profileat50(loc(j,1):loc(j,2),2) = Conc_2(:,50);
        Profileat50(loc(j,1):loc(j,2),3) = Conc_3(:,50);
        Profileat50(loc(j,1):loc(j,2),4) = Conc_S(:,50);
        Profileat50(loc(j,1):loc(j,2),5) = Temp(:,50);
        Profileat50(loc(j,1):loc(j,2),6) = Vnorm;
        Profileat50(loc(j,1):loc(j,2),7) = yconv(:,1);
        Profileat50(loc(j,1):loc(j,2),8) = yconv(:,2);
        Profileat50(loc(j,1):loc(j,2),9) = yconv(:,3);
        Profileat50(loc(j,1):loc(j,2),10) = Ntot;
        y0at50 = [y(100,1); y(100,2); y(100,3); y(100,4)];
    % At r=R
        C_1 = Conc_1(:,99);
        C_2 = Conc_2(:,99);
        C_3 = Conc_3(:,99);
        C_S = Conc_S(:,99);
        C_tot = C_1+C_2+C_3+C_S+C_EC;
        T = Temp(:,99);
        y0 = y0atR;
    % Convert Molarity to Osmolarity: p. 144
        [Osm_1 Osm_2 Osm_3 Osm_S] = conversion (C_1,C_2,...
            C_3,C_S,mwdmso,mwpd,mwfm,mwsucrose,dsoln);
```

```
% Pass osmolarities to permeability equations: p. 146
        Osm_tot = Osm_1+Osm_2+Osm_3+Osm_S+.3;
        [t,y] =ode15s(@(t,y) Perm(t,y,tspan,A,R,T,Osm_tot,...
            Osm_1,Osm_2,Osm_3,Mino,Rcal), tspan, y0);
        Ntot = y(:,2)+y(:,3)+y(:,4);
        Vnorm = 1/Vwo*(y(:,1)+Vb);                    % Normalized cell volume
        yconv = [y(:,2)*1e15./y(:,1) y(:,3)*1e15./y(:,1) y(:,4)*1e15/y(:,1)];
                                                % Convert from moles/um^3 to M
% Store all profiles
        ProfileatR(loc(j,1):loc(j,2),1) = Conc_1(:,99);
        ProfileatR(loc(j,1):loc(j,2),2) = Conc_2(:,99);
        ProfileatR(loc(j,1):loc(j,2),3) = Conc_3(:,99);
        ProfileatR(loc(j,1):loc(j,2),4) = Conc_S(:,99);
        ProfileatR(loc(j,1):loc(j,2),5) = Temp(:,99);
        ProfileatR(loc(j,1):loc(j,2),6) = Vnorm;
        ProfileatR(loc(j,1):loc(j,2),7) = yconv(:,1);
        ProfileatR(loc(j,1):loc(j,2),8) = yconv(:,2);
        ProfileatR(loc(j,1):loc(j,2),9) = yconv(:,3);
        ProfileatR(loc(j,1):loc(j,2),10) = Ntot;
        y0atR = [y(100,1); y(100,2); y(100,3); y(100,4)];


    end
end
```

```
% Pass profiles to cytotoxicity equation: p. 145
        Profile=Profileat0;
        [viability rate] = cytotoxicity(Profile,t2,sumsteps);
        viabilityat0=viability;
        rateat0=rate;

        Profile=Profileat50;
        [viability rate] = cytotoxicity(Profile,t2,sumsteps);
        viabilityat50=viability;
        rateat50=rate;

        Profile=ProfileatR;
        [viability rate] = cytotoxicity(Profile,t2,sumsteps);
        viabilityatR=viability;
        rateatR=rate;
% Output profiles and cytotoxicity to Excel Spreadsheet
        xlswrite('Output.xls', Profileat0, 'Profile0', 'A1');
        xlswrite('Output.xls', Profileat50, 'Profile50', 'A1');
        xlswrite('Output.xls', ProfileatR, 'ProfileR', 'A1');
        xlswrite('Output.xls', t2, 'time', 'A1');
        xlswrite('Output.xls', viabilityat0, 'viability', 'A1');
        xlswrite('Output.xls', viabilityat50, 'viability', 'B1');
        xlswrite('Output.xls', viabilityatR, 'viability', 'C1');
```

B.3 Mass & Heat Transfer Program

```
m = 2;                                          % spherical geometry

r = linspace(0, Ra, rstep);                     % create a row of radius values

t = linspace(0, addtime, timestep);             % create a row of time values

options = [];                % use of options allows passing of additional variables

 % Pass variables from main program

sol = depe(m,@pdenewmhSpde,@pdenewmhSic,@pdenewmhSbc,r,t,options,alpha,Ti,...

          Ci1,Ci2,Ci3,CiS,cext,cextS,text,Ao,Eact,Ao_S,Ea_S,addtime);

Conc_1 = sol(:,:,1);

Conc_2 = sol(:,:,2);

Conc_3 = sol(:,:,3);

Conc_S = sol(:,:,4);

Temp = sol(:,:,5);

 % Use pde solver to determine all concentration profiles and temperature profile

function [c,f,s] = pdenewmhSpde(r,t,u,DuDx,alpha,Ti,Ci1,Ci2,Ci3,CiS,cext,...

              cextS,text,Ao,Eact,Ao_S,Ea_S,addtime)

D_1 = 0.8*Ao(1)*exp(Eact(1)/R*(1/277-1/u(5)));

D_2 = 0.8*Ao(2)*exp(Eact(2)/R*(1/277-1/u(5)));

D_3 = 0.8*Ao(3)*exp(Eact(3)/R*(1/277-1/u(5)));

D_S = 0.8*Ao_S*exp(Ea_S/R*(1/277-1/u(5)));

c = [1/D_1; 1/D_2; 1/D_3; 1/D_S; 1/alpha];

f = [1; 1; 1; 1; 1] .* DuDx;

s = [0; 0; 0; 0; 0];
```

```
% Initial Conditions
function u0 = pdenewmhSic(r,alpha,Ti,Ci1,Ci2,Ci3,CiS,cext,cextS,...
    text,Ao,Eact,Ao_S,Ea_S,addtime)
global Ra; global rstep;
rspan = linspace(0, Ra, rstep);
% Use interpolate to describe conc. and T profile.  For first step, all coeff = 0.
C01 = interp1(rspan,Ci1,r);
C02 = interp1(rspan,Ci2,r);
C03 = interp1(rspan,Ci3,r);
C0S = interp1(rspan,CiS,r);
T0 = interp1(rspan,Ti,r);
u0 = [C01; C02; C03; C0S; T0];
% Boundary Conditions
function [pl,ql,pr,qr] = pdenewmhSbc(xl,ul,xr,ur,t,alpha,Ti,Ci1,Ci2,Ci3,...
                        CiS,cext,cextS,text,Ao,Eact,Ao_S,Ea_S,addtime)
pl = [0; 0; 0; 0; 0];
ql=[1;1;1;1;1];
pr=[ur(1)-cext(1); ur(2)-cext(2); ur(3)-cext(3); ur(4)-cextS; ur(5)-text];
qr=[0;0;0;0;0];
```

B.4 Convert Molarity to Osmolarity

```
function [Osm_1 Osm_2 Osm_3 Osm_S] = conversion(C_1,C_2,C_3,C_S,...
    mwdmso,mwpd,mwfm,mwsucrose,dsoln)
% Virial coefficients for CPAs [molal]^-1
B_dmso = 0.108;
B_pd = 0.039;
B_fm = 0.108;                    % use DMSO value
B_sucrose = 0.125;

% Determine ratio of L solution/kg solvent assuming volume additivity
ratio_1 = 1./(dsoln-C_1.*mwdmso./1000);
ratio_2 = 1./(dsoln-C_2.*mwpd./1000);
ratio_3 = 1./(dsoln-C_3.*mwfm./1000);
ratio_S = 1./(dsoln-C_S.*mwsucrose./1000);

% Determine  L soln:kg solvent assuming mass additivity & density of final soln

% Convert to Molality
Mol_1 = C_1.*ratio_1;
Mol_2 = C_2.*ratio_2;
Mol_3 = C_3.*ratio_3;
Mol_S = C_S.*ratio_S;
```

```
% Convert to Osmolality (osmol/kg solvent)
Osmol_1 = Mol_1+B_dmso.*Mol_1.*Mol_1;
Osmol_2 = Mol_2+B_pd.*Mol_2.*Mol_2;
Osmol_3 = Mol_3+B_fm.*Mol_3.*Mol_3;
Osmol_S = Mol_S+B_sucrose.*Mol_S.*Mol_S;

% Convert to Osmolarity (osmol/L solution) using ratio
Osm_1 = Osmol_1./ratio_1;
Osm_2 = Osmol_2./ratio_2;
Osm_3 = Osmol_3./ratio_3;
Osm_S = Osmol_S./ratio_S;
```

B.5 Cell Permeability Program

```
function dydt = Perm(t,y,tspan,A,R,T,Osm_tot,Osm_1,Osm_2,Osm_3,Mino,Rcal)

 dydt = zeros(4,1);

 T = interp1(tspan,T,t);                          % Interpolate temperature profile

Osm_tot = interp1(tspan,Osm_tot,t);          % Interpolate all osmolarity profiles

Osm_1 = interp1(tspan,Osm_1,t);

Osm_2 = interp1(tspan,Osm_2,t);

Osm_3 = interp1(tspan,Osm_3,t);

Ps1=4.73e-2*exp(14100/Rcal*(1/277-1./T));                % DMSO

Ps2=5.81e-2*exp(14600/Rcal*(1/277-1./T));                % PD

Ps3=5.27e-2*exp(14350/Rcal*(1/277-1./T));                % FM: avg of PD & DMSO

Lp=6.67e-4*exp(15400/Rcal*(1/277-1./T));


dydt(1) = -Lp.*A*R.*T.*(Osm_tot/1e15-(Mino*612e-15+y(2)+y(3)+y(4))/y(1));

                                          % Water flux into the cell: y(1)= Vw

dydt(2) = A.*Ps1.*(Osm_1/1e15-y(2)/y(1));  % Solute flux into cell: y(2) = Ns DMSO

dydt(3) = A.*Ps2.*(Osm_2/1e15-y(3)/y(1));  % Solute flux into cell for PD

dydt(4) = A.*Ps3.*(Osm_3/1e15-y(4)/y(1));  % Solute flux into cell for FM

 %Assumptions:

% 1. Water and solutes do not interact with each other

%  2. Ns for each component is unaffected by others (Each solute flux is only

% affected by its own previous solute concentration: Mint or Cint(1) = Ns(1)/Vw

% 3. Conc. of nonpermeating solute only effects external conc. for water flux
```

B.6 Cytotoxicity Program

```
function [viability rate] = cytotoxicity(Profile,t2,sumsteps)
% This version accounts for two CPAs: DMSO & PD
parameters = [20000 124000; 4270 4930; 0.08 0.17];
                                % parameters(i,1) for DMSO, parameters(i,2) for PD
Totprof=Profile(:,1)+Profile(:,2)+Profile(:,3);
% Determine parameters of solution
avgparb=parameters(1,1).*Profile(:,1)./(Totprof)+parameters(1,2).*Profile(:,2)./(Totprof)
avgpard=parameters(2,1).*Profile(:,1)./(Totprof)+parameters(2,2).*Profile(:,2)./(Totprof)
avgparf=parameters(3,1).*Profile(:,1)./(Totprof)+parameters(3,2).*Profile(:,2)./(Totprof)
A=avgparb.*(Totprof).*exp(-avgpard./Profile(:,5));
m=avgparf.*Totprof;
viab=zeros(sumsteps,1);         % Create matrix
rates=zeros(sumsteps,1);
feval=zeros(sumsteps,1);

 Sknot=.995;                    % Initial guess for viable cell number
 S0=Sknot;
 x0=1;
% Incrementally solve cytotoxicity equation for each time step using fzero function:
   for n = 1:sumsteps;
      if n==1;
         bigA = 0;
```

```
        bigm = 0;
        delt = t2(2)/60;
    else
        bigA = abs((A(n)+A(n-1))/2);
        bigm = abs((m(n)+m(n-1))/2);
        delt=(t2(n)-t2(n-1))/60;
    end
    [x,fval]= fzero(@(x)cytosolve(x,bigA,bigm,delt,S0),x0);          % Send to solver
    feval(n)=fval;
    viab(n)=x;
    rates(n)=(x-x0)/delt;
    S0 = x;
    x0 = x;
  end
viability=viab;
rate=rates;
```

B.7 Cytotoxicity Equation Solver

```
function F = cytosolve(x,bigA,bigm,delt,S0)
% Solve incremental equation where x = n/n0, bigA = (An-An-1)/2, A=b*C*exp(-d/T),
% bigm = (mn-mn-1)/2, m = f*C and delt = tn-tn-1 so cytotoxicity eqn (from
% CHAPTER 4) is x = exp(-A*t^m)
F=-(log(x)-log(S0))/(delt)-bigA*bigm*(-(log(x)+log(S0))/(bigA*2))^((bigm-1)/bigm);
```

REFERENCES

Agudelo, C. A., Iwata, H., 2008. The development of alternative vitrification solutions for microencapsulated islets. Biomaterials 29, 1167-76.

Agudelo, C. A., Teramura, Y., Iwata, H., 2009. Cryopreserved agarose-encapsulated islets as bioartificial pancreas: a feasibility study. Transplantation 87, 29-34.

Alipio, Z., Liao, W., Roemer, E. J., Waner, M., Fink, L. M., Ward, D. C., Ma, Y., 2010. Reversal of hyperglycemia in diabetic mouse models using induced-pluripotent stem (iPS)-derived pancreatic beta-like cells. Proc. Natl. Acad. Sci. U S A 107, 13426-31.

Alsaleh, F. M., Smith, F. J., Keady, S., Taylor, K. M., 2010. Insulin pumps: from inception to the present and toward the future. J. Clin. Pharm. Ther. 35, 127-38.

Bara, H., Sambanis, A., 2009. Development and characterization of a tissue engineered pancreatic substitute based on recombinant intestinal endocrine L-cells. Biotechnol. Bioeng. 103, 828-34.

Bara, H., Thule, P. M., Sambanis, A., 2009. A cell-based approach for diabetes treatment using engineered non-beta cells. J. Diabetes Sci. Technol. 3, 555-61.

Baust, J. M., Van Buskirk, R., Baust, J. G., 2000. Cell viability improves following inhibition of cryopreservation-induced apoptosis. In Vitro Cell Dev.-An. 36, 262-270.

Beattie, G. M., Crowe, J. H., Lopez, A. D., Cirulli, V., Ricordi, C., Hayek, A., 1997. Trehalose: A cryoprotectant that enhances recovery and preserves function of human pancreatic islets after long-term storage. Diabetes 46, 519-523.

Belzer, F. O., 1988. Principles of Organ Preservation. Transplant P 20, 925-927.

Belzer, F. O., Southard, J. H., 1988. Principles of solid-organ preservation by cold storage. Transplantation 45, 673-6.

Benson, J. P., Papas, K. K., Constantinidis, I., Sambanis, A., 1997. Towards the development of a bioartificial pancreas: effects of poly-L-lysine on alginate beads with BTC3 cells. Cell Transplant. 6, 395-402.

Bird, R. B., Stewart, W. E., Lightfoot, E. N., 2002. Transport Phenomena. John Wiley & Sons, Inc., New York, NY.

Black, S. P., Constantinidis, I., Cui, H., Tucker-Burden, C., Weber, C. J., Safley, S. A., 2006. Immune responses to an encapsulated allogeneic islet beta-cell line in diabetic NOD mice. Biochem. Bioph. Res. Co. 340, 236-243.

Brockbank, K. G., Chen, Z. Z., Song, Y. C., 2010. Vitrification of porcine articular cartilage. Cryobiology 60, 217-21.

Brockbank, K. G. M., Taylor, M. J., 2007. Tissue Preservation. In: Baust, J. G., Baust, J. M., (Eds.), Advances in Biopreservation. CRC Press, Taylor & Francis Group, Boca Raton, FL, pp. 157-196.

Brockbank, K. G. M., Walsh, J. R., Song, Y. C., Taylor, M. J., 2003. Vitrification: Preservation of Cellular Implants. In: Ashammakhi, N., Ferretti, P., (Eds.), Topics in Tissue Engineering. University of Oulu, Oulu, FI, pp. 1-26.

Bunger, C. M., Gerlach, C., Freier, T., Schmitz, K. P., Pilz, M., Werner, C., Jonas, L., Schareck, W., Hopt, U. T., de Vos, P., 2003. Biocompatibility and surface structure of chemically modified immunoisolating alginate-PLL capsules. J. Biomed. Mater. Res. A 67A, 1219-1227.

Char, C. D., Guerrero, S. N., Alzamora, S. M., 2010. Mild Thermal Process Combined with Vanillin Plus Citral to Help Shorten the Inactivation Time for Listeria innocua in Orange Juice. Food Bioprocess Tech. 3, 752-761.

Cheng, S. Y., Constantinidis, I., Sambanis, A., 2006. Insulin secretion dynamics of free and alginate-encapsulated insulinoma cells. Cytotechnology 51, 159-170.

Chin, K., Khattak, S. F., Bhatia, S. R., Roberts, S. C., 2008. Hydrogel-perfluorocarbon composite scaffold promotes oxygen transport to immobilized cells. Biotechnol. Progr. 24, 358-366.

Choi, K., Kim, Y. B., 2010. Molecular mechanism of insulin resistance in obesity and type 2 diabetes. Korean J Intern Med 25, 119-29.

Constantinidis, I., Rask, I., Long, R. C., Jr., Sambanis, A., 1999. Effects of alginate composition on the metabolic, secretory, and growth characteristics of entrapped beta TC3 mouse insulinoma cells. Biomaterials 20, 2019-27.

Cornolti, R., Figliuzzi, M., Remuzzi, A., 2009. Effect of micro- and macroencapsulation on oxygen consumption by pancreatic islets. Cell Transplant. 18, 195-201.

Csorba, T. R., Lyon, A. W., Hollenberg, M. D., 2010. Autoimmunity and the pathogenesis of type 1 diabetes. Crit. Rev. Clin. Lab. Sci. 47, 51-71.

Cui, Z. F., Dykhuizen, R. C., Nerem, R. M., Sembanis, A., 2002. Modeling of cryopreservation of engineered tissues with one-dimensional geometry. Biotechnol. Progr. 18, 354-361.

Dahl, S. L., Chen, Z., Solan, A. K., Brockbank, K. G., Niklason, L. E., Song, Y. C., 2006. Feasibility of vitrification as a storage method for tissue-engineered blood vessels. Tissue Eng. 12, 291-300.

de Groot, M., Schuurs, T. A., van Schilfgaarde, R., 2004. Causes of limited survival of microencapsulated pancreatic islet grafts. J. Surg. Res. 121, 141-50.

de Vos, P., Faas, M. M., Strand, B., Calafiore, R., 2006. Alginate-based microcapsules for immunoisolation of pancreatic islets. Biomaterials 27, 5603-5617.

Delaunay, C., Darquy, S., Honiger, J., Capron, F., Rouault, C., Reach, G., 1998. Glucose-insulin kinetics of a bioartificial pancreas made of an AN69 hydrogel hollow fiber containing porcine islets and implanted in diabetic mice. Artif. Organs 22, 291-9.

Dragomir, C. T., Pausescu, E., 1974. Theoretical considerations regarding the cell membrane function during cold-induced preservation of tissues and organs: new possibilities for optimizing the process. J. Theor. Biol. 47, 281-93.

Dusseault, J., Leblond, F. A., Robitaille, R., Jourdan, G., Tessier, J., Menard, M., Henley, N., Halle, J. P., 2005. Microencapsulation of living cells in semi-permeable membranes with covalently cross-linked layers. Biomaterials 26, 1515-22.

Duvivier-Kali, V. F., Omer, A., Parent, R. J., O'Neil, J. J., Weir, G. C., 2001. Complete protection of islets against allorejection and autoimmunity by a simple barium-alginate membrane. Diabetes 50, 1698-1705.

Efrat, S., Linde, S., Kofod, H., Spector, D., Delannoy, M., Grant, S., Hanahan, D., Baekkeskov, S., 1988. Beta-cell lines derived from transgenic mice expressing a hybrid insulin gene-oncogene. Proc. Natl. Acad. Sci. U S A 85, 9037-41.

Elmoazzen, H., Poovadan, A., Law, G. K., Elliott, J. A. W., McGann, L. E., Jomha, N. M., 2007. Dimethyl sulfoxide toxicity kinetics in intact articular cartilage Cell Tissue Banking 8, 125-133.

Emamaullee, J. A., Shapiro, A. M., 2007. Factors influencing the loss of beta-cell mass in islet transplantation. Cell Transplant. 16, 1-8.

Fahy, G. M., 2010. Cryoprotectant toxicity neutralization. Cryobiology 60, S45-S53.

Fahy, G. M., Levy, D. I., Ali, S. E., 1987. Some Emerging Principles Underlying the Physical-Properties, Biological Actions, and Utility of Vitrification Solutions. Cryobiology 24, 196-213.

Fahy, G. M., Wowk, B., Wu, J., 2006. Cryopreservation of complex systems: The missing link in the regenerative medicine supply chain. Rejuv. Res. 9, 279-293.

Fahy, G. M., Wowk, B., Wu, J., Paynter, S., 2004a. Improved vitrification solutions based on the predictability of vitrification solution toxicity. Cryobiology 48, 22-35.

Fahy, G. M., Wowk, B., Wu, J., Phan, J., Rasch, C., Chang, A., Zendejas, E., 2004b. Cryopreservation of organs by vitrification: perspectives and recent advances. Cryobiology 48, 157-178.

Fan, G. J., Choo, H., Liaw, P. K., 2007. A new criterion for the glass-forming ability of liquids. J. Non-Cryst. Solids 353, 102-107.

Fleischer, N., Chen, C., Surana, M., Leiser, M., Rossetti, L., Pralong, W., Efrat, S., 1998. Functional analysis of a conditionally transformed pancreatic beta-cell line. Diabetes 47, 1419-25.

Frid, A., Hirsch, L., Gaspar, R., Hicks, D., Kreugel, G., Liersch, J., Letondeur, C., Sauvanet, J. P., Tubiana-Rufi, N., Strauss, K., 2010. New injection recommendations for patients with diabetes. Diabetes Metab. 36 Suppl 1, S3-18.

Fuller, B. J., 2004. Cryoprotectants: the essential antifreezes to protect life in the frozen state. Cryo Letters 25, 375-88.

Fuller, B. J., Lee, C. Y., 2007. Hypothermic perfusion preservation: the future of organ preservation revisited? Cryobiology 54, 129-45.

Gardner, C. M., Burke, N. A., Chu, T., Shen, F., Potter, M. A., Stover, H. D., 2010. Poly(methyl vinyl ether-alt-maleic acid) Polymers for Cell Encapsulation. J. Biomater. Sci. Polym. Ed.

Grant, G. T., Morris, E. R., Rees, D. A., Smith, P. J. C., Thom, D., 1973. Biological Interactions between Polysaccharides and Divalent Cations: The Egg-Box Model. Febs Lett. 32, 195-198.

Grondin, M., Hamel, F., Averill-Bates, D. A., Sarhan, F., 2009. Wheat proteins enhance stability and function of adhesion molecules in cryopreserved hepatocytes. Cell Transplant 18, 79-88.

Gross, J. D., Long, R. C., Constantinidis, I., Sambanis, A., 2007. Monitoring of dissolved oxygen and cellular bioenergetics within a pancreatic substitute. Biotechnol. Bioeng. 98, 261-270.

Guan, J., Urban, J. P., Li, Z. H., Ferguson, D. J., Gong, C. Y., Cui, Z. F., 2006. Effects of rapid cooling on articular cartilage. Cryobiology 52, 430-9.

Gugerli, R., Cantana, E., Heinzen, C., von Stockar, U., Marison, I. W., 2002. Quantitative study of the production and properties of alginate/poly-L-lysine microcapsules. J. Microencapsul. 19, 571-90.

Guo, T., Hebrok, M., 2009. Stem cells to pancreatic beta-cells: new sources for diabetes cell therapy. Endocr. Rev. 30, 214-27.

Han, J., Lee, H. H., Kwon, H., Shin, S., Yoon, J. W., Jun, H. S., 2007. Engineered enteroendocrine cells secrete insulin in response to glucose and reverse hyperglycemia in diabetic mice. Mol. Ther. 15, 1195-202.

Han, X., Liu, Y., Critser, J. K., 2010. Determination of the quaternary phase diagram of the water-ethylene glycol-sucrose-NaCl system and a comparison between two theoretical methods for synthetic phase diagrams. Cryobiology 61, 52-7.

Hang, H., Shi, X., Gu, G., Wu, Y., Gu, J., Ding, Y., 2010. In vitro analysis of cryopreserved alginate-poly-L-lysine-alginate-microencapsulated human hepatocytes. Liver Int. 30, 611-22.

Hayashi, M., Tsuchiya, H., Otoi, T., Agung, B., Yamamoto, N., Tomita, K., 2009. Influence of freezing with liquid nitrogen on whole-knee joint grafts and protection of cartilage from cryoinjury in rabbits. Cryobiology 59, 28-35.

He, S. Y., Woods, C., 2004. Effects of dimethyl sulfoxide and glycine on cryopreservation induced damage of plasma membranes and mitochondria to striped bass (Morone saxatilis) sperm. Cryobiology 48, 254-262.

Heng, B. C., Ye, C. P., Liu, H., Toh, W. S., Rufaihah, A. J., Yang, Z., Bay, B. H., Ge, Z., Ouyang, H. W., Lee, E. H., Cao, T., 2006. Loss of viability during freeze-thaw of intact and adherent human embryonic stem cells with conventional slow-cooling protocols is predominantly due to apoptosis rather than cellular necrosis. J. Biomed. Sci. 13, 433-445.

Heng, B. C., Yu, Y. J. H., Ng, S. C., 2004. Slow-cooling protocols for microcapsule cryopreservation. J. Microencapsul. 21, 455-467.

Hering, B. J., Walawalkar, N., 2009. Pig-to-nonhuman primate islet xenotransplantation. Transpl. Immunol. 21, 81-6.

Hoesli, C. A., Luu, M., Piret, J. M., 2009. A novel alginate hollow fiber bioreactor process for cellular therapy applications. Biotechnol. Prog. 25, 1740-51.

Ito, M., Bujo, H., Takahashi, K., Arai, T., Tanaka, I., Saito, Y., 2005. Implantation of primary cultured adipocytes that secrete insulin modifies blood glucose levels in diabetic mice. Diabetologia 48, 1614-20.

Jadin, K. D., Wong, B. L., Bae, W. C., Li, K. W., Williamson, A. K., Schumacher, B. L., Price, J. H., Sah, R. L., 2005. Depth-varying density and organization of chondrocytes in immature and mature bovine articular cartilage assessed by 3d imaging and analysis. J. Histochem. Cytochem. 53, 1109-19.

James, R., Jenkins, L., Ellis, S. E., Burg, K. J. L., 2004. Histological processing of hydrogel scaffolds for tissue-engineering applications. J. Histotechnol. 27, 133-139.

Jay, S. M., Shepherd, B. R., Andrejecsk, J. W., Kyriakides, T. R., Pober, J. S., Saltzman, W. M., 2010. Dual delivery of VEGF and MCP-1 to support endothelial cell transplantation for therapeutic vascularization. Biomaterials 31, 3054-62.

Jeon, O., Bouhadir, K. H., Mansour, J. M., Alsberg, E., 2009. Photocrosslinked alginate hydrogels with tunable biodegradation rates and mechanical properties. Biomaterials 30, 2724-34.

Jomha, N. M., Lavoie, G., Muldrew, K., Schachar, N. S., McGann, L. E., 2002. Cryopreservation of intact human articular cartilage. J. Orthop. Res. 20, 1253-5.

Judas, F., Rosa, S., Teixeira, L., Lopes, C., Ferreira Mendes, A., 2007. Chondrocyte viability in fresh and frozen large human osteochondral allografts: effect of cryoprotective agents. Transplant Proc 39, 2531-4.

Juste, S., Lessard, M., Henley, N., Menard, M., Halle, J. P., 2005. Effect of poly-L-lysine coating on macrophage activation by alginate-based microcapsules: assessment using a new in vitro method. J Biomed Mater Res A 72, 389-98.

Karlsson, J. O. M., Toner, M., 2000. Cryopreservation. In: Lanza, R. P., et al., (Eds.), Principles of Tissue Engineering. Academic Press, San Diego, CA, pp. 293-305.

Karlsson, J. O. M., Toner, M., 1996. Long-term storage of tissues by cryopreservation: Critical issues. Biomaterials 17, 243-256.

Katenz, E., Vondran, F. W., Schwartlander, R., Pless, G., Gong, X., Cheng, X., Neuhaus, P., Sauer, I. M., 2007. Cryopreservation of primary human hepatocytes: the benefit of trehalose as an additional cryoprotective agent. Liver Transpl.13, 38-45.

Kim, S. H., Yu, D. H., Kim, Y. J., 2010. Effects of cryopreservation on phosphatidylserine translocation, intracellular hydrogen peroxide, and DNA integrity in canine sperm. Theriogenology 73, 282-292.

Kleinhans, F. W., 1998. Membrane permeability modeling: Kedem-Katchalsky vs a two-parameter formalism. Cryobiology 37, 271-289.

Kleinhans, F. W., Mazur, P., 2007. Comparison of actual vs. synthesized ternary phase diagrams for solutes of cryobiological interest. Cryobiology 54, 212-22.

Kozlowski, M., Olson, D. E., Rubin, J., Lyszkowicz, D., Campbell, A., Thule, P. M., 2007. Adeno-associated viral delivery of a metabolically regulated insulin transgene to hepatocytes. Mol. Cell. Endocrinol. 273, 6-15.

Kuleshova, L. L., Gouk, S. S., Hutmacher, D. W., 2007. Vitrification as a prospect for cryopreservation of tissue-engineered constructs. Biomaterials 28, 1585-1596.

Kuleshova, L. L., MacFarlane, D. R., Trounson, A. O., Shaw, J. M., 1999. Sugars exert a major influence on the vitrification properties of ethylene glycol based solutions and have low toxicity to embryos and oocytes. Cryobiology 38, 119-130.

Kulseng, B., Thu, B., Espevik, T., Skjak-Braek, G., 1997. Alginate polylysine microcapsules as immune barrier: permeability of cytokines and immunoglobulins over the capsule membrane. Cell Transplant. 6, 387-94.

Kumachev, A., Greener, J., Tumarkin, E., Eiser, E., Zandstra, P. W., Kumacheva, E., 2011. High-throughput generation of hydrogel microbeads with varying elasticity for cell encapsulation. Biomaterials 32, 1477-83.

Kyrychenko, A., Dyubko, T. S., 2008. Molecular dynamics simulations of microstructure and mixing dynamics of cryoprotective solvents in water and in the presence of a lipid membrane. Biophys. Chem. 136, 23-31.

La Flamme, K. E., LaTempa, T. J., Grimes, C. A., Desai, T. A., 2007. The effects of cell density and device arrangement on the behavior of macroencapsulated beta-cells. Cell Transplant 16, 765-74.

Lam, V. W., Pleass, H. C., Hawthorne, W., Allen, R. D., 2010. Evolution of pancreas transplant surgery. Anz. J. Surg. 80, 411-8.

Langer, R. M., 2010. Islet transplantation: lessons learned since the Edmonton breakthrough. Transplant. Proc. 42, 1421-4.

Lanza, R. P., Butler, D. H., Borland, K. M., Staruk, J. E., Faustman, D. L., Solomon, B. A., Muller, T. E., Rupp, R. G., Maki, T., Monaco, A. P., et al., 1991.

Xenotransplantation of canine, bovine, and porcine islets in diabetic rats without immunosuppression. Proc. Natl. Acad. Sci. U S A 88, 11100-4.

Lawson, A., Ahmad, H., Sambanis, A., 2011. Cytotoxicity effects of cryoprotectants as single-component and cocktail vitrification solutions. Cryobiology IN PRESS.

Lee, J. I., Nishimura, R., Sakai, H., Sasaki, N., Kenmochi, T., 2008. A newly developed immunoisolated bioartificial pancreas with cell sheet engineering. Cell Transplant. 17, 51-9.

Li, F.-F., Liu, J., 2010. Characterization of Micro-/Nano-Scale Ice Crystal Formation in Cryo-Biomedical Engineering: A Review. J. Comput. Theor. Nanosci. 7, 85-96.

Li, H. B., Jiang, H., Wang, C. Y., Duan, C. M., Ye, Y., Su, X. P., Kong, Q. X., Wu, J. F., Guo, X. M., 2006a. Comparison of two types of alginate microcapsules on stability and biocompatibility in vitro and in vivo. Biomed. Mater. 1, 42-7.

Li, Y., Lu, R. H., Luo, G. F., Pang, W. J., Yang, G. S., 2006b. Effects of different cryoprotectants on the viability and biological characteristics of porcine preadipocyte. Cryobiology 53, 240-247.

Liu, B. L., Mcgrath, J., Mccabe, L., Baumann, M., 2006. Cellular response of Murine Osteoblasts to Cryopreservation: the influence of attachment to Hydroxyapatite (HA) scaffolds. Afr. J. Biotechnol. 5, 2014-2019.

Liu, K. K., Williams, D. R., Briscoe, B. J., 1998. The large deformation of a single micro-elastomeric sphere. J. Phys. D Appl. Phys. 31, 294-303.

Luther, M. J., Davies, E., Muller, D., Harrison, M., Bone, A. J., Persaud, S. J., Jones, P. M., 2005. Cell-to-cell contact influences proliferative marker expression and apoptosis in MIN6 cells grown in islet-like structures. Am. J. Physiol. Endocrinol. Metab. 288, E502-9.

Maechler, P., Jornot, L., Wollheim, C. B., 1999. Hydrogen peroxide alters mitochondrial activation and insulin secretion in pancreatic beta cells. J. Biol. Chem. 274, 27905-27913.

Malpique, R., Osorio, L. M., Ferreira, D. S., Ehrhart, F., Brito, C., Zimmermann, H., Alves, P. M., 2010. Alginate encapsulation as a novel strategy for the cryopreservation of neurospheres. Tissue Eng. Part C Methods 16, 965-77.

Mason, M. N., Mahoney, M. J., 2010. A novel composite construct increases the vascularization potential of PEG hydrogels through the incorporation of large fibrin ribbons. J. Biomed. Mater. Res. A 95, 283-93.

Matsumura, K., Bae, J. Y., Hyon, S. H., 2010. Polyampholytes as cryoprotective agents for mammalian cell cryopreservation. Cell Transplant. 19, 691-9.

McCarthy, M. I., 2010. Genomics, type 2 diabetes, and obesity. N. Engl. J. Med. 363, 2339-50.

Morimoto, S., Mendoza-Rodriguez, C. A., Hiriart, M., Larrieta, M. E., Vital, P., Cerbon, M. A., 2005. Protective effect of testosterone on early apoptotic damage induced by streptozotocin in rat pancreas. J. Endocrinol. 187, 217-24.

Mueller-Klieser, W., Freyer, J. P., Sutherland, R. M., 1986. Influence of glucose and oxygen supply conditions on the oxygenation of multicellular spheroids. Br. J. Cancer 53, 345-53.

Mukaida, T., Wada, S., Takahashi, K., Pedro, P. B., An, T. Z., Kasai, M., 1998. Vitrification of human embryos based on the assessment of suitable conditions for 8-cell mouse embryos. Hum. Reprod. 13, 2874-2879.

Mukherjee, I. N., 2008. A Rational Design Approach for the Cryopreservation of Natural and Engineered Tissues. Chemical & Biomolecular Engineering, Ph.D. Georgia Institute of Technology, Atlanta, GA, pp. 219.

Mukherjee, I. N., Li, Y., Song, Y. C., Long, R. C., Sambanis, A., 2008. Cryoprotectant transport through articular cartilage for long-term storage: experimental and modeling studies. Osteoarthr. Cartilage 16, 1379-1386.

Mukherjee, I. N., Song, Y. C., Sambanis, A., 2007. Cryoprotectant delivery and removal from murine insulinomas at vitrification-relevant concentrations. Cryobiology 55, 10-18.

Mukherjee, N., Chen, Z., Sambanis, A., Song, Y., 2005. Effects of cryopreservation on cell viability and insulin secretion in a model tissue-engineered pancreatic substitute (TEPS). Cell Transplant. 14, 449-56.

Murua, A., Orive, G., Hernandez, R. M., Pedraz, J. L., 2009. Cryopreservation based on freezing protocols for the long-term storage of microencapsulated myoblasts. Biomaterials 30, 3495-501.

Nathan, D. M., 1993. Long-term complications of diabetes mellitus. N. Engl. J. Med. 328, 1676-85.

Orive, G., Tam, S. K., Pedraz, J. L., Halle, J. P., 2006. Biocompatibility of alginate-poly-L-lysine microcapsules for cell therapy. Biomaterials 27, 3691-700.

Pancrazio, J. J., Wang, F., Kelley, C. A., 2007. Enabling tools for tissue engineering. Biosens. Bioelectron. 22, 2803-11.

Pegg, D. E., 2010. The relevance of ice crystal formation for the cryopreservation of tissues and organs. Cryobiology 60, S36-44.

Pegg, D. E., Wang, L., Vaughan, D., 2006. Cryopreservation of articular cartilage. Part 3: the liquidus-tracking method. Cryobiology 52, 360-8.

Peleg, M., Normand, M. D., 2004. Calculating microbial survival parameters and predicting survival curves from non-isothermal inactivation data. Crit. Rev. Food Sci. Nutr. 44, 409-18.

Petrenko, Y. A., Jones, D. R., Petrenko, A. Y., 2008. Cryopreservation of human fetal liver hematopoietic stem/progenitor cells using sucrose as an additive to the cryoprotective medium. Cryobiology 57, 195-200.

Pileggi, A., Molano, R. D., Ricordi, C., Zahr, E., Collins, J., Valdes, R., Inverardi, L., 2006. Reversal of diabetes by pancreatic islet transplantation into a subcutaneous, neovascularized device. Transplantation 81, 1318-24.

Ponce, S., Orive, G., Hernandez, R., Gascon, A. R., Pedraz, J. L., de Haan, B. J., Faas, M. M., Mathieu, H. J., de Vos, P., 2006. Chemistry and the biological response against immunoisolating alginate-polycation capsules of different composition. Biomaterials 27, 4831-9.

Prickett, R. C., Elliott, J. A., McGann, L. E., 2010. Application of the osmotic virial equation in cryobiology. Cryobiology 60, 30-42.

Rahimi, G., Isachenko, V., Todorov, P., Tawadros, S., Mallmann, P., Nawroth, F., Isachenko, E., 2009. Apoptosis in Human Ovarian Tissue after Conventional Freezing or Vitrification and Xenotransplantation. Cryoletters 30, 300-309.

Rajaei, F., Karja, N. W. K., Agung, B., Wongsrikeao, P., Taniguchi, M., Murakami, M., Sambuu, R., Nii, M., Otoi, T., 2005. Analysis of DNA fragmentation of porcine embryos exposed to cryoprotectants. Reprod. Domest. Anim. 40, 429-432.

Rees, D. A., Alcolado, J. C., 2005. Animal models of diabetes mellitus. Diabet. Med. 22, 359-70.

Ricordi, C., Finke, E. H., Lacy, P. E., 1986. A method for the mass isolation of islets from the adult pig pancreas. Diabetes 35, 649-53.

Robertson, R. P., 2010. Islet transplantation a decade later and strategies for filling a half-full glass. Diabetes 59, 1285-91.

Robitaille, R., Dusseault, J., Henley, N., Desbiens, K., Labrecque, N., Halle, J. P., 2005. Inflammatory response to peritoneal implantation of alginate-poly-L-lysine microcapsules. Biomaterials 26, 4119-27.

Rodrigues, J. P., Paraguassu-Braga, F. H., Carvalho, L., Abdelhay, E., Bouzas, L. F., Porto, L. C., 2008. Evaluation of trehalose and sucrose as cryoprotectants for hematopoietic stem cells of umbilical cord blood. Cryobiology 56, 144-151.

Ross-Rodriguez, L. U., Elliott, J. A., McGann, L. E., 2010. Investigating cryoinjury using simulations and experiments. 1: TF-1 cells during two-step freezing (rapid cooling interrupted with a hold time). Cryobiology 61, 38-45.

Rudolph, A. S., Crowe, J. H., 1985. Membrane Stabilization during Freezing - the Role of 2 Natural Cryoprotectants, Trehalose and Proline. Cryobiology 22, 367-377.

Russell-Minda, E., Jutai, J., Speechley, M., Bradley, K., Chudyk, A., Petrella, R., 2009. Health technologies for monitoring and managing diabetes: a systematic review. J. Diabetes. Sci. Technol. 3, 1460-71.

Safley, S. A., Cui, H., Cauffiel, S., Tucker-Burden, C., Weber, C. J., 2008. Biocompatibility and immune acceptance of adult porcine islets transplanted intraperitoneally in diabetic NOD mice in calcium alginate poly-L-lysine microcapsules versus barium alginate microcapsules without poly-L-lysine. J. Diabetes Sci. Technol. 2, 760-7.

Safley, S. A., Cui, H., Gordon, K. B., Weber, C. J., 2010. Microencapsulation Prevents Allo- and Autoimmune Destruction of Donor Islets in NOD Mice. Am. J. Transplant. 10, 229-229.

Safley, S. A., Kapp, L. M., Tucker-Burden, C., Hering, B., Kapp, J. A., Weber, C. J., 2005. Inhibition of cellular immune responses to encapsulated porcine islet xenografts by simultaneous blockade of two different costimulatory pathways. Transplantation 79, 409-18.

Sambanis, A., 2000. Engineering challenges in the development of an encapsulated cell system for treatment of type 1 diabetes. Diabetes Technol. Ther. 2, 81-9.

Saragusty, J., Gacitua, H., Rozenboim, I., Arav, A., 2009. Do physical forces contribute to cryodamage? Biotechnol Bioeng 104, 719-28.

Schenke-Layland, K., Xie, J., Heydarkhan-Hagvall, S., Hamm-Alvarez, S. F., Stock, U. A., Brockbank, K. G., MacLellan, W. R., 2007. Optimized preservation of extracellular matrix in cardiac tissues: implications for long-term graft durability. Ann Thorac Surg 83, 1641-50.

Schmidt, J. J., Rowley, J., Kong, H. J., 2008. Hydrogels used for cell-based drug delivery. J Biomed Mater Res A 87A, 1113-1122.

Schneider, S., Klein, H. H., 2011. Preserved insulin secretion capacity and graft function of cryostored encapsulated rat islets. Regul Pept 166, 135-8.

Shapiro, A. M., Lakey, J. R., 2000. Future trends in islet cell transplantation. Diabetes Technol. Ther. 2, 449-52.

Shapiro, A. M., Lakey, J. R., Ryan, E. A., Korbutt, G. S., Toth, E., Warnock, G. L., Kneteman, N. M., Rajotte, R. V., 2000. Islet transplantation in seven patients with

type 1 diabetes mellitus using a glucocorticoid-free immunosuppressive regimen. N. Engl. J. Med. 343, 230-8.

Shaw, J. M., Kuleshova, L. L., MacFarlane, D. R., Trounson, A. O., 1997. Vitrification properties of solutions of ethylene glycol in saline containing PVP, Ficoll, or dextran. Cryobiology 35, 219-229.

Simpson, N. E., Grant, S. C., Gustavsson, L., Peltonen, V. M., Blackband, S. J., Constantinidis, I., 2006. Biochemical consequences of alginate encapsulation: A NMR study of insulin-secreting cells. Biomaterials 27, 2577-2586.

Simpson, N. E., Khokhlova, N., Oca-Cossio, J. A., McFarlane, S. S., Simpson, C. P., Constantinidis, I., 2005. Effects of growth regulation on conditionally-transformed alginate-entrapped insulin secreting cell lines in vitro. Biomaterials 26, 4633-4641.

Skelin, M., Rupnik, M., Cencic, A., 2010. Pancreatic beta cell lines and their applications in diabetes mellitus research. ALTEX 27, 105-13.

Soon-Shiong, P., 1999. Treatment of type I diabetes using encapsulated islets. Adv. Drug Deliv. Rev. 35, 259-270.

Stabler, C., Wilks, K., Sambanis, A., Constantinidis, I., 2001. The effects of alginate composition on encapsulated beta TC3 cells. Biomaterials 22, 1301-1310.

Stephenne, X., Najimi, M., Ngoc, D. K., Smets, F., Hue, L., Guigas, B., Sokal, E. M., 2007. Cryopreservation of human hepatocytes alters the mitochondrial respiratory chain complex I. Cell Transplant. 16, 409-419.

Stiegler, P. B., Stadlbauer, V., Schaffellner, S., Halwachs, G., Lackner, C., Hauser, O., Iberer, F., Tscheliessnigg, K., 2006. Cryopreservation of insulin-producing cells microencapsulated in sodium cellulose sulfate. Transplant. Proc. 38, 3026-30.

Stolar, M., 2010. Glycemic control and complications in type 2 diabetes mellitus. Am. J. Med. 123, S3-11.

Strand, B. L., Ryan, T. L., In't Veld, P., Kulseng, B., Rokstad, A. M., Skjak-Brek, G., Espevik, T., 2001. Poly-L-Lysine induces fibrosis on alginate microcapsules via the induction of cytokines. Cell Transplant. 10, 263-75.

Sutton, R. L., 1992. Critical Cooling Rates for Aqueous Cryoprotectants in the Presence of Sugars and Polysaccharides. Cryobiology 29, 585-598.

Szarko, M., Muldrew, K., Bertram, J. E., 2010. Freeze-thaw treatment effects on the dynamic mechanical properties of articular cartilage. BMC Musculoskelet. Disord. 11, 231.

Tatone, C., Di Emidio, G., Vento, M., Ciriminna, R., Artini, P. G., 2010. Cryopreservation and oxidative stress in reproductive cells. Gynecol. Endocrinol. 26, 563-567.

Terry, C., Hughes, R. D., Mitry, R. R., Lehec, S. C., Dhawan, A., 2007. Cryopreservation-induced nonattachment of human hepatocytes: role of adhesion molecules. Cell Transplant. 16, 639-47.

Tesfaye, N., Seaquist, E. R., 2010. Neuroendocrine responses to hypoglycemia. Ann. NY Acad. Sci. 1212, 12-28.

Thakrar, R. R., Patel, V. P., Hamilton, G., Fuller, B. J., Seifalian, A. M., 2006. Vitreous cryopreservation maintains the viscoelastic property of human vascular grafts. Faseb J. 20, 874-81.

Thule, P. M., Liu, J., Phillips, L. S., 2000. Glucose regulated production of human insulin in rat hepatocytes. Gene Ther 7, 205-14.

Todd, J. A., 2010. Etiology of type 1 diabetes. Immunity 32, 457-67.

Tomford, W. W., Fredericks, G. R., Mankin, H. J., 1984. Studies on cryopreservation of articular cartilage chondrocytes. J. Bone Joint Surg. Am. 66, 253-9.

Tripathy, D., Chavez, A. O., 2010. Defects in insulin secretion and action in the pathogenesis of type 2 diabetes mellitus. Curr. Diab. Rep. 10, 184-91.

Tsai, S., Rawson, D. M., Zhang, T., 2008. Studies on Cryoprotectant Toxicity to Early Stage Zebrafish (Danio Rerio) Ovarian Follicles. Cryoletters 29, 477-483.

Van Buskirk, R. G., Snyder, K. K., Baust, J. M., Mathew, A. J., Baust, J. G., 2004. Hypothermic storage and cryopreservation- The issues of successful short-term and long-term preservation of cells and tissues. BioProcess International 2, 42-49.

Vergani, A., D'Addio, F., Jurewicz, M., Petrelli, A., Watanabe, T., Liu, K., Law, K., Schuetz, C., Carvello, M., Orsenigo, E., Deng, S., Rodig, S. J., Ansari, J. M., Staudacher, C., Abdi, R., Williams, J., Markmann, J., Atkinson, M., Sayegh, M. H., Fiorina, P., 2010. A novel clinically relevant strategy to abrogate autoimmunity and regulate alloimmunity in NOD mice. Diabetes 59, 2253-64.

Vijan, S., 2010. Type 2 diabetes. Ann. Intern. Med. 152, ITC31-15; quiz ITC316.

Wang, H. Y., Inada, T., Funakoshi, K., Lu, S. S., 2009. Inhibition of nucleation and growth of ice by poly(vinyl alcohol) in vitrification solution. Cryobiology 59, 83-89.

Wang, L. H., Pegg, D. E., Lorrison, J., Vaughan, D., Rooney, P., 2007a. Further work on the cryopreservation of articular cartilage with particular reference to the liquidus tracking (LT) method. Cryobiology 55, 138-147.

Wang, M. S., Childs, R. F., Chang, P. L., 2005. A novel method to enhance the stability of alginate-poly-L-lysine-alginate microcapsules. J Biomater Sci Polym Ed 16, 91-113.

Wang, X., Hua, T. C., Sun, D. W., Liu, B. L., Yang, G. H., Cao, Y. L., 2007b. Cryopreservation of tissue-engineered dermal replacement in Me2SO: Toxicity study and effects of concentration and cooling rates on cell viability. Cryobiology 55, 60-65.

Weber, L. M., He, J., Bradley, B., Haskins, K., Anseth, K. S., 2006. PEG-based hydrogels as an in vitro encapsulation platform for testing controlled beta-cell microenvironments. Acta Biomater. 2, 1-8.

Weiss, A. D., Forbes, J. F., Scheuerman, A., Law, G. K., Elliott, J. A., McGann, L. E., Jomha, N. M., 2010. Statistical prediction of the vitrifiability and glass stability of multi-component cryoprotective agent solutions. Cryobiology 61, 123-7.

Wu, Y., Yu, H., Chang, S., Magalhaes, R., Kuleshova, L. L., 2007. Vitreous cryopreservation of cell-biomaterial constructs involving encapsulated hepatocytes. Tissue Eng. 13, 649-58.

Wusteman, M., Rauen, U., Simmonds, J., Hunds, N., Pegg, D. E., 2008a. Reduction of cryoprotectant toxicity in cells in suspension by use of a sodium-free vehicle solution. Cryobiology 56, 72-9.

Wusteman, M. C., Pegg, D. E., Robinson, M. P., Wang, L. H., Fitch, P., 2002. Vitrification media: toxicity, permeability, and dielectric properties. Cryobiology 44, 24-37.

Wusteman, M. C., Simmonds, J., Vaughan, D., Pegg, D. E., 2008b. Vitrification of rabbit tissues with propylene glycol and trehalose. Cryobiology 56, 62-71.

Yang, H., Iwata, H., Shimizu, H., Takagi, T., Tsuji, T., Ito, F., 1994. Comparative studies of in vitro and in vivo function of three different shaped bioartificial pancreases made of agarose hydrogel. Biomaterials 15, 113-20.

Yin, H. Y., Cui, L., Liu, G. P., Cen, L., Cao, Y. L., 2009. Vitreous cryopreservation of tissue engineered bone composed of bone marrow mesenchymal stem cells and partially demineralized bone matrix. Cryobiology 59, 180-187.

Youn, J. I., Telenkov, S. A., Kim, E., Bhavaraju, N. C., Wong, B. J., Valvano, J. W., Milner, T. E., 2000. Optical and thermal properties of nasal septal cartilage. Lasers Surg. Med. 27, 119-28.

Zhang, W., Yang, G., Zhang, A., Xu, L. X., He, X., 2010. Preferential vitrification of water in small alginate microcapsules significantly augments cell cryopreservation by vitrification. Biomed. Microdevices 12, 89-96.

Zimmermann, H., Zimmermann, D., Reuss, R., Feilen, P. J., Manz, B., Katsen, A., Weber, M., Ihmig, F. R., Ehrhart, F., Gessner, P., Behringer, M., Steinbach, A., Wegner, L. H., Sukhorukov, V. L., Vasquez, J. A., Schneider, S., Weber, M. M., Volke, F., Wolf, R., Zimmermann, U., 2005. Towards a medically approved technology for alginate-based microcapsules allowing long-term immunoisolated transplantation. J. Mater. Sci. Mater. Med. 16, 491-501.

Zoungas, S., Patel, A., 2010. Cardiovascular outcomes in type 2 diabetes: the impact of preventative therapies. Ann. NY Acad. Sci. 1212, 29-40.